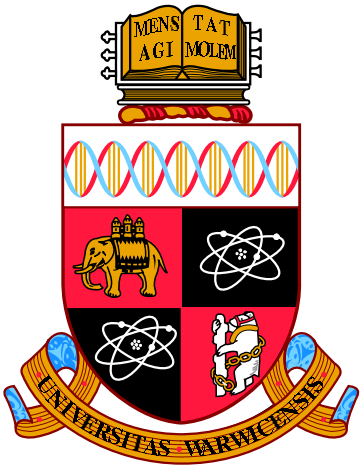

Veering triangulations and polynomial invariants of three-manifolds

by

Anna Barbara Parlak

Thesis

Submitted to the University of Warwick

for the degree of

Doctor of Philosophy

Warwick Mathematics Institute

July 2021

Contents

List of Tables

List of Figures

List of Algorithms

Dependencies between algorithms

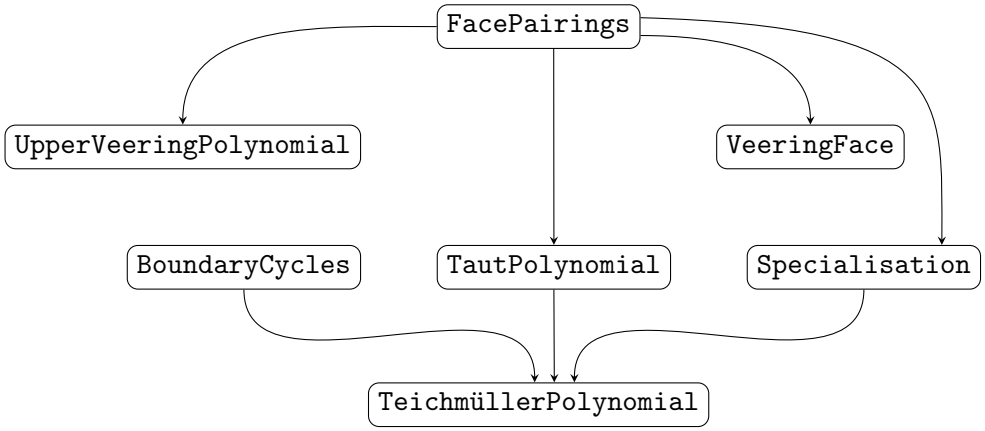

Acknowledgements

Firstly, I would like to thank my supervisor Saul Schleimer for his advice and guidance throughout my PhD. I am also thankful to him for encouraging me to learn a little bit of programming which turned out to be surprisingly useful in my research.

I owe special thanks to Sam Taylor for explaining to me his work (joint with Michael Landry and Yair Minsky) on the polynomial invariants of veering triangulations, answering my numerous questions and sharing with me their early drafts. Since these polynomial invariants became the core of my thesis, all of this was invaluably helpful. I also thank Dave Futer who after chatting with me about my research suggested that I reach out to Sam. He is probably unaware that by doing that he accidentally changed the course of my PhD.

I am grateful to the organisers of the "Perspectives on Dehn surgery" workshop held at ICERM in July 2019. Without their travel funding my trip to the United States would not have been possible, and this thesis would not exist in its present form.

I am indebted to Henry Segerman and Saul Schleimer for their generous help in implementing the algorithms given in this thesis. This implementation is based on their Veering Census and accompanying tools for computing with veering triangulations. I also thank them for permitting me to reuse some of their figures.

I thank Damiano Testa for being my stand-in supervisor while Saul was away in the autumn term of 2019, and Mark Bell for answering my questions about `flipper`. I also thank Joe Scull for always being happy to discuss whatever math question I came up with, and for giving feedback on Chapter 1 of this thesis.

Finally, I am grateful to the Engineering and Physical Sciences Research Council for funding my studies, and to the Warwick Mathematics Institute for providing a stimulating research environment.

Declarations

This thesis is submitted to the University of Warwick in support of my application for the degree of Doctor of Philosophy. It has been composed by myself and has not been submitted in any previous application for any degree. I declare that the presented material is, to the best of my knowledge, my own work except where otherwise indicated in the text, or where the material is widely known.

In the thesis I give algorithms that were implemented in collaboration with Saul Schleimer and Henry Segerman [48]. The implementations rely on the Veering Census [26] and accompanying tools for computing with veering triangulations previously devised by Schleimer and Segerman. The implementations do not consitute a part of the thesis, but were used to compute examples and to experimentally test various hypotheses.

Large parts of this thesis appeared in the following preprints posted on arXiv, an open-access repository of electronic preprints.

- *The taut polynomial and the Alexander polynomial*
  `arXiv:2101.12162 [math.GT]`. Submitted.
- *Computation of the taut, the veering and the Teichmüller polynomials*
  `arXiv:2009.13558 [math.GT]`. Submitted.

All figures, except Figure 3.6 and Figure 12.1, were created by me using Inkscape. Figure 3.6 uses Figure 6.2(B) of [51] as a template. Figure 12.1 is taken from [26]. Both figures were modified by me with Inkscape.

This thesis was typeset in LaTeX2e using the style package *warwickthesis*.

Abstract

In this thesis we study the taut polynomial of a veering triangulation, defined by Landry, Minsky and Taylor [LMT]. We introduce the notion of edge-orientability and prove that when a veering triangulation is edge-orientable then its taut polynomial is equal to the Alexander polynomial of the underlying manifold. For triangulations that are not edge-orientable, we give a sufficient condition for equality between the support of the taut polynomial and that of the Alexander polynomial.

We also consider 3-manifolds obtained by Dehn filling a veering triangulation. In this case, we give a formula that relates the specialisation of the taut polynomial under the Dehn filling and the Alexander polynomial of the Dehn-filled manifold.

Using the results of [LMT] we extend the theorem of McMullen which relates the Alexander polynomial of a manifold and the Teichmüller polynomial of a fibred face of its Thurston norm ball. We interpret the obtained result in terms of existence of orientable fibred classes in the corresponding fibred cone.

The computational part of the thesis includes algorithms to compute the taut polynomial, the upper veering polynomial, and their specialisations. Using this and the results of [LMT] we give an algorithm to compute the Teichmüller polynomial of any fibred face of the Thurston norm ball. We also present an algorithm to find the face of the Thurston norm ball determined by a veering triangulation. We use implementations of these algorithms to compute examples illustrating the theoretical results of the thesis.

Notation

Symbol	Description	Page
M	an oriented 3-manifold with torus cusps	13
$\mathcal{T} = (T, F, E)$	an ideal triangulation with the set T of tetrahedra, the set F of faces and the set E of edges	13
$(\mathcal{T}, \pm\alpha)$	a transverse taut triangulation	14
$\mathcal{V} = (\mathcal{T}, \pm\alpha, \pm\nu)$	a (transverse taut) veering triangulation	15
$\mathcal{T}^{(k)}$	the k-skeleton of $\mathcal{T}$	16
$\mathscr{B}$	the horizontal branched surface of $(\mathcal{T}, \alpha)$	16
B	the branch equations matrix of $(\mathcal{T}, \alpha)$	16
w	a nonzero, nonnegative, integral solution to the system of branch equations of $(\mathcal{T}, \alpha)$	17
S^w	the surface carried by $\mathscr{B}$ with weights w	17
β	the boundary track of $(\mathcal{T}, \alpha)$	18
$T_1, \ldots, T_b$	boundary tori of the truncated model of M	18
β_j	$\beta \cap T_j$	18
τ	a dual train track in $\mathscr{B}$	20
τ_f	the restriction of a dual train track $\tau \subset \mathscr{B}$ to $f \in F$	20
$\tau^\uparrow$, $\tau^\downarrow$	the upper/lower tracks of $(\mathcal{T}, \alpha)$	20
ψ	a pseudo-Anosov homeomorphism (of a surface)	28
$\mathscr{F}^s$, $\mathscr{F}^u$	the stable and unstable foliations of a pseudo-Anosov homeomorphism or a pseudo-Anosov flow	28
$\mathscr{L}^s$, $\mathscr{L}^u$	the stable and unstable laminations of a pseudo-Anosov homeomorphism or a pseudo-Anosov flow	28

Ψ	a pseudo-Anosov flow (on a 3-manifold)	30
$\mathrm{sing}(\Psi)$	the singular orbits of Ψ	30
$\mathscr{B}^{\uparrow}$, $\mathscr{B}^{\downarrow}$	the upper/lower branched surfaces of a veering triangulation	34
M^{ab}	the maximal free abelian cover of M	36
H	$H_1(M;\mathbb{Z})/_{\text{torsion}}$ (used in Chapters 4 – 9 and Chapter 15)	36
H_M	$H_1(M;\mathbb{Z})/_{\text{torsion}}$ (used in Chapters 10 – 14)	75
H'	a free abelian quotient of $H_1(M;\mathbb{Z})$	36
$\mathbb{Z}[H']$	the integral group ring on H'	36
$\mathcal{T}'$	the triangulation induced by $\mathcal{T}$ on the free abelian cover with the deck group H'	36
$H' \cdot X$	the set of $h \cdot x$, $h \in H'$, $x \in X$, $X \in \{T, F, E\}$	37
$\mathcal{F}$	a fundamental domain for the action of H' on $\mathcal{T}'$	37
$\mathcal{D}$	the 2-complex dual to $\mathcal{T}$	38
Γ	the dual graph of $\mathcal{T}$ (the 1-skeleton of $\mathcal{D}$)	38
Υ	a spanning tree of Γ	38
C	a collection of simplicial 1-cycles in $\mathcal{D}$	39
H^C	the free abelian quotient of $H_1(M;\mathbb{Z})$ determined by C	39
F_Υ	the subset of F consisting of faces dual to the edges of Γ which are *not* in Υ	39
B_Υ	the matrix obtained from $B : \mathbb{Z}^E \to \mathbb{Z}^F$ by deleting its rows corresponding to the edges of Υ	39
$\mathcal{D}_\Upsilon$	the 2-complex obtained from $\mathcal{D}$ by contracting Υ to a point	39
$(B\|C)$	the augmentation of B by C	40
$\zeta(f)$	the non-tree cycle associated to a non-tree edge f	40
$\mathrm{Fit}_i(\mathcal{M})$	the i-th Fitting ideal of a module $\mathcal{M}$	42
$\mathcal{V}^{ab}$	the triangulation of M^{ab} induced by $\mathcal{V}$	44

$\mathcal{E}^{\uparrow}_{\alpha}(\mathcal{V})$, $\mathcal{E}^{\downarrow}_{\alpha}(\mathcal{V})$, $\mathcal{E}_{\alpha}(\mathcal{V})$	the taut module of $\mathcal{V}$	44
$D^{\uparrow}$, $D^{\downarrow}$	a presentation matrix for $\mathcal{E}^{\uparrow}_{\alpha}(\mathcal{V})$, $\mathcal{E}^{\downarrow}_{\alpha}(\mathcal{V})$	44
$\Theta^{\uparrow}_{\mathcal{V}}$, $\Theta^{\downarrow}_{\mathcal{V}}$, $\Theta_{\mathcal{V}}$	the taut polynomial of $\mathcal{V}$	45
$D^{\uparrow}_{\Upsilon}$	the restriction of $D^{\uparrow}$ to $\mathbb{Z}[H]^{F_{\Upsilon}} \to \mathbb{Z}[H]^{E}$	47
$\Phi^{\uparrow}_{\mathcal{V}}$, $\Phi^{\downarrow}_{\mathcal{V}}$	the upper/lower flow graph	50
$\mathcal{E}^{\uparrow}_{\alpha,\nu}(\mathcal{V})$, $\mathcal{E}^{\downarrow}_{\alpha,\nu}(\mathcal{V})$	the upper/lower veering module of $\mathcal{V}$	52
$K^{\uparrow}$, $K^{\downarrow}$	a presentation matrix for $\mathcal{E}^{\uparrow}_{\alpha,\nu}(\mathcal{V})$, $\mathcal{E}^{\downarrow}_{\alpha,\nu}(\mathcal{V})$	52
$V^{\uparrow}_{\mathcal{V}}$, $V^{\downarrow}_{\mathcal{V}}$	the upper/lower veering polynomial of $\mathcal{V}$	52
$\mathcal{V}^{or}$	the edge-orientation double cover of $\mathcal{V}$	65
τ_t	the restriction of τ to the four faces of $t \in T$	65
ω	the edge-orientation homomorphism	66
Δ_M	the Alexander polynomial of M	68
$\mathcal{D}^{ab}_{\Upsilon}$	the maximal free abelian cover of $\mathcal{D}_{\Upsilon}$	69
d^{Υ}_1, d^{Υ}_2	the boundary maps of $\mathcal{D}^{ab}_{\Upsilon}$	69
$\Delta_{(M,\partial M)}$	the zeroth Fitting invariant of $H_1(M^{ab}, \partial M^{ab}; \mathbb{Z})$	69
∂^{Υ}_3, ∂^{Υ}_2	the boundary maps of $(M^{ab}, \partial M^{ab})$	69
$(\cdot)^{\mathrm{tr}}$	the transpose of a matrix	70
σ	the factor $H \to \{-1, 1\}$ of ω	70
$\mathrm{supp}(P)$	the support of $P \in \mathbb{Z}[H]$	73
$N(P)$	the Newton polytope of $P \in \mathbb{Z}[H]$	73
$N^c(P)$	the centralised Newton polytope of $P \in \mathbb{Z}[H]$	74
$N^*(P)$	the polar dual set of $N^c(P)$	74
$\gamma_1, \ldots, \gamma_b$	Dehn filling slopes on $T_1, \ldots, T_b$	75
$N = M(\gamma_1, \ldots, \gamma_b)$	the Dehn filling of M along $\gamma_1, \ldots, \gamma_b$	75
H_N	$H_1(N; \mathbb{Z}) \,/_{\mathrm{torsion}}$	75
$b_1(M)$, $b_1(N)$	the ranks of H_M, H_N	75
$i_* : H_M \to H_N$	the epimorphism induced by the inclusion $M \hookrightarrow N$	75
$\varrho_C : H_M \to H^C_M$	the epimorphism determined by C	76
M^N	the free abelian cover of M determined by the Dehn filling N of M	79

$\mathcal{V}^N$	the triangulation of M^N induced by $\mathcal{V}$	79
σ_N	the factor $H_N \to \{-1, 1\}$ of ω	79
$\langle \cdot, \cdot \rangle$	the algebraic intersection of homology classes	81
$\|\cdot\|_{\mathrm{Th}}$	the Thurston norm on $H^1(N;\mathbb{R}) \cong H_2(N, \partial N;\mathbb{R})$	83
$B_{\mathrm{Th}}(\cdot)$	the Thurston norm unit ball	83
$\mathtt{F}$	a face of the Thurston norm ball (not necessarily fibred, not necessarily top-dimensional)	83
$\mathbb{R}_+ \cdot \mathtt{F}$	the cone on $\mathtt{F}$	83
$\mathtt{carried}(\mathcal{V})$	the cone in $\mathbb{R}^F$ of surfaces carried by $\mathcal{V}$	84
$\mathtt{hom}(\mathcal{V})$	the cone in $H_2(M, \partial M;\mathbb{R})$ of homology classes of surfaces carried by $\mathcal{V}$	84
$\mathtt{F}_{\mathcal{V}}$	the face of the Thurston norm ball determined by $\mathcal{V}$	84
φ	the projection $\mathbb{Z}^F \to H_M$	85
φ^*	the projection $\mathbb{Z}^F \to H_2(M, \partial M;\mathbb{Z})$	85
$e_{\mathcal{V}}$	the relative Euler class of $\mathcal{V}$, $e_{\mathcal{V}} \in H^2(M, \partial M;\mathbb{R})$	87
$[\Gamma]$	the class of Γ in $H_1(M;\mathbb{R})$	87
$\mathscr{L}$	the (stable) lamination associated to a fibred face $\mathtt{F}$	90
$\mathrm{sing}(\mathtt{F})$	the singular orbits of the suspension flow associated to a fibred face $\mathtt{F}$	90
$\Theta_{\mathtt{F}}$	the Teichmüller polynomial of a fibred face $\mathtt{F}$	90
Γ^β	the dual boundary graph of $(\mathcal{T}, \alpha)$	91
$\mathring{S}$	the surface obtained from S by puncturing it at the singularities of the invariant foliations of ψ	95
$\mathring{\psi}$	the restriction of ψ to $\mathring{S}$	95
$H_1(S;\mathbb{Z})^\psi$	the quotient of $H_1(S;\mathbb{Z})$ by the action of ψ_*	96
H_S^ψ	the torsion-free part of $H_1(S;\mathbb{Z})^\psi$	96
$\mathscr{L}^N$	the lamination induced by $\mathscr{L}$ in N^{ab} (or M^N)	97
$\mathscr{L}^{ab}$	the lamination induced by $\mathscr{L}$ in M^{ab}, where $M = N - \mathrm{sing}(\mathtt{F})$	97
$\mathrm{int}(\mathbb{R}_+ \cdot \mathtt{F})$	the interior of $\mathbb{R}_+ \cdot \mathtt{F}$	98

P^η	the specialisation of $P \in \mathbb{Z}[H_N]$ at $\eta \in H^1(N;\mathbb{Z})$	99
$\mathring{\mathcal{V}}$	a layered surgery parent of $\mathcal{V}$	116
$\mathscr{T}_M$	the torsion of the chain complex of homology modules of M^{ab}	118
$\mathscr{T}_\mathcal{V}$	the torsion of the veering chain complex of $\mathcal{V}$	119

Chapter 1

Introduction

A fibration of a hyperbolic 3-manifold N over the circle determines a *suspension flow* on N with nonzero, but finitely many, singular orbits. Ian Agol showed that the complement of the singular orbits admits a *veering triangulation* which combinatorially encodes the dynamics of the flow [2, Section 4].

Generically N fibres in infinitely many ways. The information about distinct fibrations is organised by the *Thurston norm* on the first cohomology group $H^1(N;\mathbb{R})$ [55, Theorem 3]. If two fibrations lie over the same *fibred face* of the Thurston norm ball, the suspension flows determined by them are isotopic [22, Theorem 14.11], and the obtained veering triangulations are the same [45, Proposition 2.7]. Hence every fibred face $\mathtt{F}$ of the Thurston norm ball gives a canonical veering triangulation, which in turn allows hands-on analysis of distinct fibrations lying over $\mathtt{F}$.

Veering triangulations exist also on non-fibred manifolds [31, Section 4]. In unpublished work Agol and Guéritaud showed that a veering triangulation can be derived from any *pseudo-Anosov flow* without *perfect fits*. Suspension flows of pseudo-Anosov homeomorphisms are special, but not the only, examples of such flows [19, p. 199]. Hence veering triangulations can be used to study not only fibred 3-manifolds but also the larger class of 3-manifolds supporting pseudo-Anosov flows without perfect fits. In particular, all results of this thesis until Chapter 12 hold also for veering triangulations which do not come from suspension flows.

Encoding analytical objects by combinatorial ones is not a novel idea. For instance, a very fruitful approach to study the geometry of hyperbolic 3-manifolds is to analyse their triangulations and ideal triangulations [33, 50, 54]. Similarly, train tracks were successfully used to study laminations in surfaces [28, 49]. Perhaps veering triangulations will play a similar role in the study of pseudo-Anosov flows without perfect fits.

Currently the idea to use veering triangulations to study pseudo-Anosov flows is still in its infancy. Even the conjecture that every veering triangulation comes from a pseudo-Anosov flow [51, p. 2] remains unresolved. Nevertheless, this direction of research seems very promising because it would allow us to tackle various problems regarding flows algorithmically. Veering triangulations also possess the advantage of being possible to rigorously classify and catalogue. This was used to build the Veering Census [26] which contains data on all veering triangulations consisting of up to 16 tetrahedra.

The key theme of this thesis is the relationship between the *taut polynomial* of a veering triangulation [38, Section 3] and the "classical" polynomial invariants of 3-manifolds. Most importantly, we study the relationship between the *specialisation of the taut polynomial* under a Dehn filling and the *Alexander polynomial* of the Dehn-filled manifold. Theorem 10.3.1, which is the main theoretical result of this thesis, gives a precise formula relating these two invariants.

Furthermore, we use the fact that the specialisation of the taut polynomial is a generalisation of the *Teichmüller polynomial* of a fibred face of the Thurston norm ball [38, Proposition 7.2] to obtain a formula relating the Alexander polynomial and the Teichmüller polynomial (Corollary 12.5.3). The connection between these two invariants was previously studied by McMullen [41, Theorem 7.1], but the precise formula that appears in Corollary 12.5.3 was not known. In Section 12.6 we explain that the close relationship between the Teichmüller polynomial and the Alexander polynomial is controlled by the existence of orientable fibred classes in the corresponding fibred cone.

Along the way, we give algorithms to compute the taut polynomial, the upper veering polynomial, and their specialisations. Using this and [38, Proposition 7.2] we give an algorithm to compute the Teichmüller polynomial of any fibred face of the Thurston norm ball. We also present an algorithm to find the face of the Thurston norm ball determined by a veering triangulation. All these algorithms are implemented which allowed us to include numerous computed examples.

1.1 Statement of results

Now we turn to give a more detailed exposition of the results contained in this thesis. Let M be a connected 3-manifold equipped with a finite veering triangulation $\mathcal{V}$. We study the *taut polynomial* $\Theta^{\uparrow}_{\mathcal{V}}$, the *veering polynomial* $V^{\uparrow}_{\mathcal{V}}$ and the *flow graph* $\Phi^{\uparrow}_{\mathcal{V}}$ of $\mathcal{V}$, as defined by Landry, Minsky and Taylor in [38].

1.1.1 Invariance under reversing the veering structure

A veering triangulation $\mathcal{V}$ is determined by a triple: an ideal triangulation $\mathcal{T}$, a coorientation α on its 2-dimensional faces and a 2-colouring ν on its edges. By reversing the coorientation on every face we obtain a new veering triangulation $-\mathcal{V} = (\mathcal{T}, -\alpha, \nu)$. If $\mathcal{V}$ comes from a pseudo-Anosov Ψ then $-\mathcal{V}$ comes from the pseudo-Anosov flow Ψ^{-1}.

The first question that we ask is whether the taut polynomial, the veering polynomial and the flow graph are invariant under the operation $(\mathcal{T}, \alpha, \nu) \mapsto (\mathcal{T}, -\alpha, \nu)$. This question can be restated in terms of a pair of canonical train tracks embedded in the 2-skeleton of $\mathcal{V}$. Namely, the authors of [38] define $\Theta^{\uparrow}_{\mathcal{V}}$, $V^{\uparrow}_{\mathcal{V}}$ and $\Phi^{\uparrow}_{\mathcal{V}}$ using the *upper track* of $\mathcal{V}$. Considering the upper track of $-\mathcal{V}$ is equivalent to considering the *lower track* of $\mathcal{V}$; see Remark 2.4.8. Therefore we compare the lower and upper taut polynomials $\Theta^{\downarrow}_{\mathcal{V}}$, $\Theta^{\uparrow}_{\mathcal{V}}$, the lower and upper veering polynomials $V^{\downarrow}_{\mathcal{V}}$, $V^{\uparrow}_{\mathcal{V}}$, and the lower and upper flow graphs $\Phi^{\downarrow}_{\mathcal{V}}$, $\Phi^{\uparrow}_{\mathcal{V}}$.

Let

$$H = H_M = H_1(M;\mathbb{Z}) \,/_{\text{torsion}}.$$

All polynomial invariants listed above are elements of the group ring $\mathbb{Z}[H]$. They are, however, well-defined only up to multiplication by $\pm h$, for $h \in H$. Therefore we compare them in the quotient semigroup $\mathbb{Z}[H] \,/_{\pm H}$.

In Proposition 5.1.1 we show that the upper taut polynomial $\Theta^{\uparrow}_{\mathcal{V}}$ of $\mathcal{V}$ is, up to a unit, equal to the lower taut polynomial $\Theta^{\downarrow}_{\mathcal{V}}$ of $\mathcal{V}$. Hence there is only one taut polynomial associated to a veering triangulation. We denote it by $\Theta_{\mathcal{V}}$. An analogous statement does not hold for the flow graphs and the veering polynomials. We give examples of veering triangulations whose lower and upper veering polynomials give different elements of $\mathbb{Z}[H] \,/_{\pm H}$ (Proposition 6.3.2) and whose lower and upper flow graphs are not isomorphic (Proposition 6.1.1).

1.1.2 Algorithms to compute the taut polynomial and the upper veering polynomial

Originally the taut polynomial $\Theta_{\mathcal{V}}$ is defined as the greatest common divisor of the maximal minors of a certain presentation matrix of the *taut module* of $\mathcal{V}$. This is an $n \times 2n$ matrix, where n denotes the number of tetrahedra in $\mathcal{V}$. We simplify the presentation for the taut module, so that the computation of the taut polynomial requires computing only linearly many minors instead of exponentially many (Proposition 5.2.3). Using this we give the algorithm `TautPolynomial` (Alg. 2). In Proposition 5.3.1 we prove that the output of `TautPolynomial` applied to $\mathcal{V}$ is equal to the taut polynomial $\Theta_{\mathcal{V}}$ of $\mathcal{V}$. We also give the algorithm `UpperVeeringPolynomial`

(Alg. 3). In Proposition 6.3.1 we show that it correctly computes the upper veering polynomial.

Both these algorithms rely on the algorithm `FacePairings` (Alg. 1). It performs basic homological computations which are necessary to encode the lifted triangulation of a free abelian cover of M.

1.1.3 A formula relating the taut polynomial and the Alexander polynomial

The Alexander polynomial Δ_M is an invariant of the homology module of the maximal free abelian cover M^{ab} of M. The taut polynomial $\Theta_{\mathcal{V}}$ is computed using the induced veering triangulation $\mathcal{V}^{ab}$ of M^{ab}. We define a combinatorial property of a veering triangulation, called *edge-orientability*, which is crucial for comparing these two invariants.

In Construction 8.2.4 we explain how to construct the *edge-orientation double cover* $\mathcal{V}^{or}$ of $\mathcal{V}$. It determines the *edge-orientation homomorphism* $\omega : \pi_1(M) \to \{-1, 1\}$. In Lemma 8.3.1 we show that ω factors through H if and only if $\mathcal{V}^{ab}$ is edge-orientable. We use the obtained factor $\sigma : H \to \{-1, 1\}$ to give a formula relating $\Theta_{\mathcal{V}}$ with Δ_M.

Proposition 9.3.1. *Let $\mathcal{V}$ be a veering triangulation of a 3-manifold M. Let $(h_1, \dots, h_r)$ be a basis of H. If $\mathcal{V}^{ab}$ is edge-orientable then*

$$\Theta_{\mathcal{V}}(h_1, \dots, h_r) = \Delta_M(\sigma(h_1) \cdot h_1, \dots, \sigma(h_r) \cdot h_r)$$

where $\sigma : H \to \{-1, 1\}$ is the factor of the edge-orientation homomorphism of $\mathcal{V}$.

In Corollary 9.3.2 we observe that $\mathcal{V}^{ab}$ can fail to be edge-orientable only if the torsion subgroup of $H_1(M; \mathbb{Z})$ is of even order. That is, in the absence of even torsion the supports of the taut polynomial and of the Alexander polynomial are always equal. In Subsection 9.3.1 we observe that the polynomials ($\Theta_{\mathcal{V}}$ mod 2) and (Δ_M mod 2) have a common factor, the zeroth Fitting invariant of the $\mathbb{Z}/2\mathbb{Z}[H]$-module $H_1(M^{ab}, \partial M^{ab}; \mathbb{Z}/2\mathbb{Z})$, even when $\mathcal{V}^{ab}$ is not edge-orientable.

We then consider a (not necessarily closed) Dehn filling N of M. We set

$$H_N = H_1(N; \mathbb{Z}) \,/_{\text{torsion}}.$$

The inclusion of M into N determines an epimorphism $i_* : H \to H_N$. Let $b_1(M)$, $b_1(N)$ denote the ranks of H, H_N, respectively. We compare the *specialisation* $i_*(\Theta_{\mathcal{V}})$ of the taut polynomial of $\mathcal{V}$ *under the Dehn filling* and the Alexander polynomial of the Dehn-filled manifold N. In order to do that we need to consider the intermediate free abelian cover M^N of M with the deck group isomorphic to H_N. It admits a

veering triangulation $\mathcal{V}^N$. By Lemma 8.3.1, if this triangulation is edge-orientable, then the edge-orientation homomorphism factors through $\sigma_N : H_N \to \{-1, 1\}$. Using Proposition 9.3.1, we prove the main theorem of this thesis.

Theorem 10.3.1. *Let $\mathcal{V}$ be a veering triangulation of a 3-manifold M. Let N be a Dehn filling of M such that $s = b_1(N)$ is positive. Denote by $\ell_1, \dots, \ell_k$ the core curves of the filling solid tori in N and by $i_* : H \to H_N$ the epimorphism induced by the inclusion of M into N. Assume that the veering triangulation $\mathcal{V}^N$ is edge-orientable and that for every $j \in \{1, \dots, k\}$ the class $[\ell_j] \in H_N$ is nontrivial. Let $\sigma_N : H_N \to \{-1, 1\}$ be the homomorphism through which the edge-orientation homomorphism of $\mathcal{V}$ factors.*

I. $b_1(M) \geq 2$ and

(a) $s \geq 2$. Then

$$i_*(\Theta_{\mathcal{V}})(h_1, \dots, h_s) = \Delta_N(\sigma_N(h_1) \cdot h_1, \dots, \sigma_N(h_s) \cdot h_s) \cdot \prod_{j=1}^{k} ([\ell_j] - \sigma_N([\ell_j])).$$

(b) $s = 1$. Let h denote the generator of H_N.

- *If $\partial N \neq \emptyset$ then*

$$i_*(\Theta_{\mathcal{V}})(h) = (h - \sigma_N(h))^{-1} \cdot \Delta_N(\sigma_N(h) \cdot h) \prod_{j=1}^{k} ([\ell_j] - \sigma_N([\ell_j])).$$

- *If N is closed then*

$$i_*(\Theta_{\mathcal{V}})(h) = (h - \sigma_N(h))^{-2} \cdot \Delta_N(\sigma_N(h) \cdot h) \cdot \prod_{j=1}^{k} ([\ell_j] - \sigma_N([\ell_j])).$$

II. $b_1(M) = 1$. Let h denote the generator of $H_N \cong H_M$.

(a) If $\partial N \neq \emptyset$ then

$$i_*(\Theta_{\mathcal{V}})(h) = \Delta_N(\sigma_N(h) \cdot h).$$

(b) If N is closed set $\ell = \ell_1$, and then

$$i_*(\Theta_{\mathcal{V}})(h) = (h - \sigma_N(h))^{-1}([\ell] - \sigma_N([\ell])) \cdot \Delta_N(\sigma_N(h) \cdot h).$$

We discuss edge-orientability of $\mathcal{V}^N$ in Subsection 10.3.1.

1.1.4 A formula relating the Teichmüller polynomial and the Alexander polynomial

The motivation for studying the specialisation of the taut polynomial under a Dehn filling comes from its connection with the *Teichmüller polynomial*. This invariant was introduced by McMullen in [41, Section 3] and is associated to a fibred face of the Thurston norm ball. By the results of Landry, Minsky and Taylor [38, Proposition 7.2], every Teichmüller polynomial can be expressed as the specialisation of the taut polynomial of a *layered* veering triangulation under Dehn filling it along the slopes parallel to the boundary components of a carried fibre. Theorem 10.3.1 can therefore be interpreted as a theorem which relates the Teichmüller polynomial $\Theta_{\mathtt{F}}$ of a fibred face $\mathtt{F}$ in $H^1(N;\mathbb{R})$ with the Alexander polynomial Δ_N of N. In [41, Theorem 7.1] McMullen proved

Theorem (McMullen). *Let N be a connected, oriented, hyperbolic 3-manifold which is fibred over the circle. Assume $b_1(N) \geq 2$. Let $\mathtt{F}$ be a fibred face of the Thurston norm ball in $H^1(N;\mathbb{R})$. Then $\mathtt{F} \subset \mathtt{A}$ for a unique face $\mathtt{A}$ of the Alexander norm ball in $H^1(N;\mathbb{R})$. If moreover the lamination $\mathscr{L}$ associated to $\mathtt{F}$ is transversely orientable, then $\mathtt{F} = \mathtt{A}$ and Δ_N divides $\Theta_{\mathtt{F}}$.*

The lamination $\mathscr{L}$ mentioned in the above theorem is just the stable lamination of the suspension flow associated to the fibred face $\mathtt{F}$. Theorem 10.3.1 extends McMullen's result in two ways.

(1) When the veering triangulation is layered and Dehn filling slopes are parallel to the boundary components of a carried fibre, it gives a stronger relation between the Teichmüller polynomial and the Alexander polynomial; see Corollary 12.5.3.

For a fibred face $\mathtt{F}$ whose associated lamination $\mathscr{L}$ is transversely orientable we give sufficient conditions for the equality between $\Theta_{\mathtt{F}}$ and Δ_N. When Δ_N only divides $\Theta_{\mathtt{F}}$ we give the formula for the remaining factors of $\Theta_{\mathtt{F}}$. We also give precise formulas relating $\Theta_{\mathtt{F}}$ and Δ_N in the case when $\mathscr{L}$ is not transversely orientable; we only need to assume that the lamination induced by $\mathscr{L}$ in the maximal free abelian cover N^{ab} of N is transversely orientable. Note that transverse orientability of the induced lamination in N^{ab} is a weaker condition than transverse orientability of $\mathscr{L}$ itself.

(2) Theorem 10.3.1 does not require a veering triangulation to be layered. When $\mathcal{V}$ is not layered, but does carry a surface, it determines a nonfibred face of the Thurston norm ball [38, Theorem 5.12]. In this case we obtain a relation between the Alexander polynomial of a 3-manifold and a polynomial invariant of a nonfibred face of its Thurston norm ball.

In Section 12.6 we consider *orientable fibred classes* in $H^1(N;\mathbb{R})$. They determine fibrations for which the stretch factor and the homological stretch factor of the monodromy are equal; see Theorem 3.2.2. Therefore they are responsible for the close relationship between the Teichmüller polynomial and the Alexander polynomial that we obtained in Corollary 12.5.3.

If the lamination $\mathscr{L}$ associated to $\mathtt{F}$ is transversely orientable, then every fibred class from the cone $\mathbb{R}_+\cdot\mathtt{F}$ is orientable. Indeed, by Corollary 12.5.3 in this case for every fibred class η in $\mathbb{R}_+\cdot\mathtt{F}$ the specialisation $\Delta_N^\eta(z)$ of the Alexander polynomial at η divides the specialisation $\Theta_{\mathtt{F}}^\eta(z)$ of the Teichmüller polynomial at η, and the remaining factors of $\Theta_{\mathtt{F}}^\eta(z)$ are cyclotomic.

The case when the lamination $\mathscr{L}$ associated to $\mathtt{F}$ is not transversely orientable, but its preimage in the maximal free abelian cover N^{ab} is transversely orientable, is slightly more involved. In Proposition 12.6.3 we give a simple characterisation of orientable fibred classes in $\mathbb{R}_+\cdot\mathtt{F}$. Restating it in a basis-dependent way gives an easy recipe to find orientable fibred classes, and proves that they always exist.

Corollary 12.6.4. *Let $\mathtt{F}$ be a fibred face of the Thurston norm ball in $H^1(N;\mathbb{R})$. Let $(h_1,\dots,h_s)$ be a basis of H_N and let $(h_1^*,\dots,h_s^*)$ be the dual basis of $H^1(N;\mathbb{Z})$. Denote by $\mathscr{L}$ the stable lamination associated to $\mathtt{F}$.*

If $\mathscr{L}$ is not transversely orientable, but the induced lamination $\mathscr{L}^N\subset N^{ab}$ is transversely orientable then a primitive class

$$\eta = a_1h_1^* + \ldots + a_rh_r^* \in \operatorname{int}(\mathbb{R}_+\cdot\mathtt{F})\cap H^1(N;\mathbb{Z})$$

is orientable if and only if for every $j=1,\dots,s$

$$a_j = \begin{cases} \text{odd} & \text{if } \sigma_N(h_j) = -1 \\ \text{even} & \text{if } \sigma_N(h_j) = 1. \end{cases} \tag{1.1}$$

In particular, with the above assumptions on $\mathscr{L}$ there are orientable fibred classes in $\mathbb{R}_+\cdot\mathtt{F}$. □

Using Corollary 12.5.3 one can check that if a fibred class η in $\mathbb{R}_+\cdot\mathtt{F}$ satisfies the condition (1.1), then $\Delta_N^\eta(-z)$ divides $\Theta_{\mathtt{F}}^\eta(z)$, and the remaining factors of $\Theta_{\mathtt{F}}^\eta(z)$ are cyclotomic.

We have not found a formula relating the Teichmüller polynomial $\Theta_{\mathtt{F}}$ with the Alexander polynomial Δ_N in the case when the lamination $\mathscr{L}^N$ in the maximal free abelian cover N^{ab} is not transversely orientable. We did, however, analyse the existence of orientable fibred classes in $\mathbb{R}_+\cdot\mathtt{F}$.

Proposition 12.6.5. *Let* $\mathtt{F}$ *be a fibred face of the Thurston norm ball in* $H^1(N;\mathbb{R})$. *Let* $\mathscr{L}$ *be the stable lamination associated to* $\mathtt{F}$. *If the induced lamination* $\mathscr{L}^N$ *in* N^{ab} *is not transversely orientable, then there is no orientable fibred class in the interior of* $\mathbb{R}_+ \cdot \mathtt{F}$.

Proposition 12.6.5 implies that when $\mathscr{L}^N$ is not transversely orientable then for every fibred class η in $\mathbb{R}_+ \cdot \mathtt{F}$ the largest in the absolute value real root of $\Delta_N^\eta(z)$ is strictly smaller than the largest real root of $\Theta_{\mathtt{F}}^\eta(z)$ [4, p. 1360].

1.1.5 Algorithm to compute the Teichmüller polynomial

Let $\mathtt{F}$ be a fibred face of the Thurston norm ball in $H^1(N;\mathbb{R})$. Let $\mathrm{sing}(\mathtt{F})$ be the set of singular orbits of the suspension flow determined by $\mathtt{F}$. By the results of Agol [2, Section 4], $M = N - \mathrm{sing}(\mathtt{F})$ admits a veering triangulation $\mathcal{V}$ which encodes the stable and unstable laminations of the flow. By [38, Proposition 7.2] the Teichmüller polynomial $\Theta_{\mathtt{F}}$ is equal to $i_*(\Theta_{\mathcal{V}})$, where $i_* : H \to H_N$ is induced by the inclusion of M into N. Recall that we have an algorithm to compute $\Theta_{\mathcal{V}}$ (`TautPolynomial`, Alg. 2). If $\mathtt{F}$ is not *fully-punctured*, there are two additional steps to compute $\Theta_{\mathtt{F}}$.

1. Finding Dehn filling slopes on the boundary tori of M which recover N.
2. Computing the specialisation of the taut polynomial of $\mathcal{V}$ under $i_* : H \to H_N$.

We give two algorithms, `BoundaryCycles` (Alg. 6) and `Specialisation` (Alg. 4), which realise the first and the second step, respectively. Then we give the algorithm `TeichmüllerPolynomial` (Alg. 7), which relies on algorithms `BoundaryCycles`, `TautPolynomial` and `Specialisation`. We prove that it correctly computes the Teichmüller polynomial in Proposition 12.3.1.

Different algorithms to compute the Teichmüller polynomial were previously known. First of all, there is McMullen's original algorithm [41, Section 3]. It relies on fixing a particular fibration lying in the fibred cone $\mathbb{R}_+ \cdot \mathtt{F}$ and analysing the lift of the stable train track of the monodromy to the maximal free abelian cover. This algorithm is general, but hard to implement. There are simpler algorithms which work in some special cases. In [39] Lanneau and Valdez give an algorithm to compute the Teichmüller polynomial of punctured disk bundles. The authors of [3] compute the Teichmüller polynomial of *odd-block surface* bundles. In [6] Billet and Lechti cover the case of alternating-sign Coxeter links.

The algorithm `TeichmüllerPolynomial` presented in this thesis is general and in principle can be applied to any hyperbolic, orientable 3-manifold fibred over the circle. Moreover, it has already been implemented, making abundant data on the Teichmüller polynomials available at the tip of our fingers.

1.1.6 Algorithm to find the face of the Thurston norm ball determined by a veering triangulation

Suppose that a veering triangulation $\mathcal{V}$ of M is *layered* or *measurable*. The set of homology classes of surfaces carried by $\mathcal{V}$ of M forms a cone in $H_2(M, \partial M; \mathbb{R}) \cong H^1(M; \mathbb{R})$. By the results of Landry, Minsky and Taylor this cone is equal to the cone on some (not necessarily fibred, not necessarily top-dimensional) face of the Thurston norm ball in $H^1(M; \mathbb{R})$ [38, Theorem 5.12]. We give the algorithm `VeeringFace` (Alg. 5) which takes as an input a veering triangulation $\mathcal{V}$ and outputs the vertices of the face of the Thurston norm unit ball determined by $\mathcal{V}$. An important feature of this algorithm is that the vertices are expressed in terms of the basis of $H^1(M; \mathbb{R})$ which is dual to the integral basis of $H_1(M; \mathbb{R})$ used to compute the taut polynomial of $\mathcal{V}$.

1.1.7 Examples

Numerous examples are scattered throughout this thesis. Their aim is either to falsify various hypotheses about the taut and veering polynomials, or to demonstrate the steps of presented algorithms on some particular veering triangulation, or to illustrate theoretical results of the thesis. We list the most important examples below.

By Proposition 6.3.2, the upper and lower veering polynomials of a given veering triangulation might not be equal in $\mathbb{Z}[H]/_{\pm H}$. In Example 6.3.5 we show that it is even possible that one veering polynomial vanishes and the other does not. We explain this phenomenon in Remark 6.3.6.

In [41, Section 7] McMullen studied the relationship between the *Alexander* and the *Teichmüller norms* on $H^1(N; \mathbb{R})$. By Proposition 9.3.1, if a fibred face is fully-punctured then transverse orientability of the associated lamination in the maximal free abelian cover implies equality of these norms. In Example 9.4.1 we show that the Alexander and the Teichmüller norms can agree even when the lamination in the maximal free abelian cover is not transversely orientable.

By [41, Theorem 6.1] and [38, Theorem 7.1], the cone in $H_2(M, \partial M; \mathbb{R})$ of homology classes of surfaces carried by a layered veering triangulation $\mathcal{V}$ is equal to the cone on some face of the dual polytope of the taut polynomial of $\mathcal{V}$. In Example 12.4.1 we show that this property does not extend to measurable veering triangulations.

In Chapter 13 we find the (fibred) face $\mathtt{F}$ of the Thurston norm ball determined by a veering triangulation of the 6_2^2 link complement. We use Corollary 12.6.4 to predict whether a given fibred class from the cone $\mathbb{R}_+ \cdot \mathtt{F}$ is orientable, and then verify

it experimentally.

All examples of multivariable Teichmüller polynomials previously known in the literature concern only fully-punctured fibred faces. In Chapter 14 we compute the Teichmüller polynomials of not fully-punctured fibred faces of 3-manifolds obtained by Dehn filling the 8_2^4 link complement. We also compute the corresponding specialisations of the Alexander polynomial. The aim is to show that the polynomials behave under the specialisation as predicted by Theorem 10.3.1.

1.2 Structure of the thesis

In Chapter 2 we recall the definition of veering triangulations and describe combinatorial structures which are naturally associated to them. We prove lemmas about the combinatorics of veering triangulations which are used later in the thesis. We also briefly overview past research on veering triangulations.

Chapter 3 is expository. We discuss pseudo-Anosov homeomorphisms, pseudo-Anosov flows and their connection to veering triangulations.

All polynomial invariants considered in this thesis are computed using the maximal free abelian cover of a 3-manifold. For this reason in Chapter 4 we recall the construction of this cover and other free abelian covers. Given a transverse taut triangulation $(\mathcal{T}, \alpha)$ of M we fix a convention for labelling ideal simplices of the triangulation induced by $(\mathcal{T}, \alpha)$ in a free abelian cover of M. We explain how to finitely encode this infinite triangulaton. This procedure is summarised in the algorithm `FacePairings` (Alg. 1). We also review the notions of Fitting ideals and Fitting invariants of modules.

In Chapter 5 we recall the definition of the taut polynomial introduced in [38, Section 3]. We prove that regardless of whether we use the lower or the upper track we obtain the same polynomial (Proposition 5.1.1). Then we give a recipe to systematically reduce the number of relations in the taut module (Proposition 5.2.3). We use it to accelerate the computation of the taut polynomial (Algorithm 2).

In Chapter 6 we recall the definitions of the (upper) flow graph and the (upper) veering polynomial introduced in [38, Sections 3 – 4]. We show that the lower and upper flow graphs are not always isomorphic (Proposition 6.1.1). We give an algorithm for the computation of the upper veering polynomial (Algorithm 3). Using this we present examples of veering triangulations whose lower and upper veering polynomials are not equal up to a unit (Proposition 6.3.2).

In Chapter 7 we follow the algorithms `TautPolynomial` and `UpperVeering Polynomial` to compute the taut and the upper veering polynomials of the veering triangulation `cPcbbbiht_12` of the figure-eight knot complement.

In Chapter 8 we introduce the notion of edge-orientability of a veering triangulation. We describe how to construct the edge-orientation double cover of a veering triangulation (Construction 8.2.4). We discuss the edge-orientation homomorphism and derive a combinatorial condition which ensures that it factors through a given quotient of the fundamental group (Lemma 8.3.1).

The aim of Chapter 9 is to prove a formula relating the taut polynomial of a veering triangulation $\mathcal{V}$ and the Alexander polynomial of the underlying manifold M. First we relate the Alexander polynomial of M with the zeroth Fitting invariant of the relative homology module $H_1(M^{ab}, \partial M^{ab}; \mathbb{Z})$ (Proposition 9.2.1). Using this we show that if the veering triangulation $\mathcal{V}^{ab}$ of the maximal free abelian cover is edge-orientable, then the supports of the taut polynomial of $\mathcal{V}$ and that of the Alexander polynomial of M are equal (Proposition 9.3.1).

In Chapter 10 we aim to generalise the results from Chapter 9 to Dehn fillings of veering triangulations. In this case we compare the specialisation of the taut polynomial under a Dehn filling and the Alexander polynomial of the Dehn filled manifold (Theorem 10.3.1). The computational part of this chapter includes an algorithm to compute the specialisation of $P \in \mathbb{Z}[H]$ under the epimorphism $\varrho_C : H \to H^C$ determined by a collection C of dual cycles (`Specialisation`, Algorithm 4).

In Chapter 11 we outline the connection between veering triangulations and the Thurston norm. We give the algorithm `VeeringFace` (Algorithm 5) to find the vertices spanning the face of the Thurston norm ball determined by a veering triangulation.

In Chapter 12 we use the results of Landry, Minsky and Taylor from [38, Proposition 7.2] to give the algorithm `TeichmüllerPolynomial` which computes the Teichmüller polynomial of any fibred face of any hyperbolic 3-manifold (Algorithm 7). We restate Theorem 10.3.1 in the fibred setting (Corollary 12.5.3). We interpret the obtained relation between the Teichmüller polynomial and the Alexander polynomial in terms of orientability of the laminations in the fibre which are invariant under the monodromy of a fibration (Section 12.6).

In Chapter 13 we follow the algorithm `VeeringFace` to find the face of the Thurston norm ball determined by the veering triangulation `eLMkbcdddedde_2100` of the 6_2^2 link complement. This triangulation is layered and hence the corresponding face is fibred. We analyse two fibrations lying over the interior of that face to show that their properties coincide with those anticipated by Corollary 12.6.4.

In Chapter 14 we compute the Teichmüller polynomials of not fully-punctured fibred faces of 3-manifolds obtained by Dehn filling the 8_2^4 link complement.

In Chapter 15 we outline two research projects which are closely related to the content of this thesis.

1.3 Conventions and assumed background

Throughout the thesis we assume familiarity with the basics of the following topics.

- Train tracks in surfaces. In particular, the notion of curves or laminations (fully) carried by a train track. Necessary definitions can be found in [49, Chapter 1].
- Branched surfaces in 3-manifolds. In particular, the notion of surfaces or laminations (fully) carried by a branched surface. Necessary definitions can be found in [25, Section 1].

1.3.1 Cusped and truncated models

In large parts of this thesis we consider 3-manifolds with torus cusps. If M is such a manifold it is often useful to truncate its torus cusps. By doing this we obtain a 3-manifold with toroidal boundary components whose interior is homeomorphic to M. For notational simplicity we still denote it by M. This is a slight abuse of notation, but it should not cause much confusion.

Throughout the thesis we freely alternate between the *cusped* and *truncated* models of M. The main advantage of the latter is that we can consider curves and train tracks in the boundary ∂M. For instance, the truncated model is used in Section 2.3 to define the boundary track associated to a transverse taut triangulation, in Section 9.2, where we compute the relative homology module $H_1(M^{ab}, \partial M^{ab}; \mathbb{Z})$, in Chapter 10, where we discuss Dehn fillings of M, and in Chapter 11, where we consider the Thurston norm on $H_2(M, \partial M; \mathbb{R})$.

Chapter 2

Veering triangulations

The aim of this chapter is to familiarise the reader with the basics of veering triangulations. We give necessary definitions and describe structures which are naturally associated with a veering triangulation. We also prove lemmas about the combinatorics of veering triangulations which are used later in the thesis. We end the chapter with a brief overview of the research on veering triangulations.

2.1 Ideal triangulations of 3-manifolds

An *ideal triangulation* of a 3-manifold M with torus cusps is a decomposition of M into ideal tetrahedra. We denote an ideal triangulation by $\mathcal{T} = (T, F, E)$, where T, F, E denote the set of tetrahedra, triangles (2-dimensional faces) and edges, respectively. Throughout the thesis we assume that ideal simplices of $\mathcal{T}$ are ordered and equipped with an orientation.

Every triangle of a triangulation has two *embeddings* into two, not necessarily distinct, tetrahedra. The number of (embeddings of) triangles attached to an edge is called the *degree* of this edge. An edge of degree d has d embeddings into triangles and d embeddings into tetrahedra.

By *edges of a triangle/tetrahedron* or *triangles of a tetrahedron* we mean embeddings of these ideal simplices into the boundary of a higher dimensional ideal simplex. Similarly, by *triangles/tetrahedra attached to an edge* we mean triangles/tetrahedra in which the edge is embedded, together with this embedding. When we claim that two lower dimensional simplices of a higher dimensional simplex are different we mean that at least their embeddings are different.

In this thesis we are mostly concerned with ideal triangulations that satisfy two additional combinatorial conditions. Namely, they are *transverse taut* and *veering*.

2.1.1 Transverse taut triangulations

Let t be an ideal tetrahedron. Assume that a coorientation is assigned to each of its faces. We say that t is *transverse taut* if on two of its faces the coorientation points into t and on the other two it points out of t [31, Definition 1.2]. We call the pair of faces whose coorientations point out of t the *top faces* of t and the pair of faces whose coorientations point into t the *bottom faces* of t. We also say that t is *immediately below* its top faces and *immediately above* its bottom faces.

We encode a transverse taut structure on a tetrahedron by drawing it as a quadrilateral with two diagonals — one on top of the other; see Figure 2.1. Then the convention is that the coorientations on all faces point towards the reader.

The *top diagonal* is the common edge of the two top faces of t and the *bottom diagonal* is the common edge of the two bottom faces of t. The remaining four edges of t are called its *equatorial edges*. Presenting a transverse tetrahedron as in Figure 2.1 naturally endows it with an abstract assignment of angles from $\{0, \pi\}$ to its edges. The angle π is assigned to the diagonal edges of the tetrahedron and the angle 0 is assigned to its equatorial edges. Such an assignment of angles is called a *taut structure* on t [31, Definition 1.1].

Definition 2.1.1. A triangulation $\mathcal{T} = (T, F, E)$ is *transverse taut* if

- every ideal triangle $f \in F$ is assigned a coorientation so that every ideal tetrahedron is transverse taut, and
- for every edge $e \in E$ the sum of angles of the underlying taut structure of $\mathcal{T}$, over all embeddings of e into tetrahedra, equals 2π [31, Definition 1.2].

We denote a triangulation with a transverse taut structure by $(\mathcal{T}, \alpha)$. Note that if M has a transverse taut triangulation $(\mathcal{T}, \alpha)$ then it also has a transverse taut triangulation obtained from $(\mathcal{T}, \alpha)$ by reversing coorientations on all faces of $\mathcal{T}$. We denote this triangulation by $(\mathcal{T}, -\alpha)$. These two triangulations have the same underlying taut structure, with tops and bottoms of tetrahedra swapped.

Remark. Triangulations as described above were introduced by Lackenby in [32]. Some authors, including Lackenby, call them *taut triangulations*. Then triangulations endowed only with a $\{0, \pi\}$ angle structure are called *angle taut triangulations*.

2.1.2 Veering triangulations

A (transverse taut) *veering tetrahedron* is an oriented transverse taut tetrahedron whose edges are coloured either red or blue, and the pattern of colouring on the

equatorial edges is precisely as in Figure 2.1. There is no restriction on how the diagonal edges are coloured; this is indicated by colouring them black.

A transverse taut triangulation is *veering* if a colour (red/blue) is assigned to each edge of the triangulation so that every tetrahedron is veering.

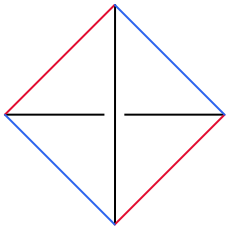

Figure 2.1: A veering tetrahedron as viewed from above. The taut angle structure assigns 0 to the equatorial edges and π to the diagonal edges of the tetrahedron.

We denote a veering triangulation by $\mathcal{V} = (\mathcal{T}, \alpha, \nu)$, where ν corresponds to the colouring on edges. If M has a veering triangulation $(\mathcal{T}, \alpha, \nu)$, then it also has a veering triangulation $(\mathcal{T}, -\alpha, \nu)$, where the coorientations on faces are reversed, $(\mathcal{T}, \alpha, -\nu)$, where the colours on edges are interchanged and $(\mathcal{T}, -\alpha, -\nu)$, where both coorientations of faces and colours on edges are interchanged.

The original veering condition due to Agol refers to the relative position of tetrahedra in the triangulation; see [2, Definition 4.1]. He introduced the notion of *right-* and *left-veering* edges, and defined a veering triangulation as a transverse taut triangulation whose every edge is either left- or right-veering. The Agol's veering property is never used in this thesis, hence we do not recall it here. It is, however, encoded by the colours of edges of a veering triangulation. Namely, by convention right-veering edges are coloured red and left-veering edges are coloured blue. The veering triangulations $(\mathcal{T}, -\alpha, -\nu)$ and $(\mathcal{T}, \alpha, -\nu)$ respect this convention if we reverse the orientation of M.

Assumption. Ideal triangulations $\mathcal{T}$, $\mathcal{V}$ are finite.

The veering census

The data on transverse taut veering structures on ideal triangulations of orientable 3-manifolds consisting of up to 16 tetrahedra is available in the Veering Census [26]. A veering triangulation in the census is described by a string of the form

```
[isoSig]_[taut angle structure].
```
(2.1)

The first part of this string is the isomorphism signature of the triangulation. It identifies a triangulation uniquely up to combinatorial isomorphism [8, Section 3].

The second part of the string records the transverse taut structure, up to a sign.

The above description suggests that an entry from the Veering Census determines $([\mathcal{T}], \pm\alpha, \pm\nu)$, where $[\mathcal{T}]$ denotes the isomorphism class of $\mathcal{T}$. However, in the Veering Census certain (non-canonical) choices have been made. In fact, each entry corresponds to an ideal triangulation with numbered simplices, a fixed coorientation on its triangles, and a fixed orientation on its ideal simplices.

We use a string of the form (2.1) whenever we refer to a concrete example of a veering triangulation. Implementations of all algorithms given in this thesis take (2.1) as an input.

2.2 The horizontal branched surface

Let $(\mathcal{T}, \alpha)$ be a transverse taut triangulation with the set T of tetrahedra, the set F of triangular faces, and the set E of edges. By Definition 2.1.1 the triangles attached to an edge $e \in E$ are grouped into two *sides*, separated by a pair of π angles at e; see Figure 2.2. Therefore a transverse taut structure on an ideal triangulation $\mathcal{T}$ makes it possible to view the 2-skeleton $\mathcal{T}^{(2)}$ as a 2-dimensional complex with a well-defined tangent space everywhere, including along its 1-skeleton. Following [51, Subsection 2.12] we call $\mathcal{T}^{(2)}$ the *horizontal branched surface* of $(\mathcal{T}, \alpha)$ and denote it by $\mathscr{B}$. The branch locus of $\mathscr{B}$ is equal to the 1-skeleton $\mathcal{T}^{(1)}$. In particular, $\mathscr{B}$ is *ideally triangulated* by the triangular faces of $\mathcal{T}$. We denote this triangulation of $\mathscr{B}$ by (F, E). For a more general definition of a branched surface see [47, p. 532].

2.2.1 Branch equations

Let $e \in E$ be an edge of degree d of a transverse taut triangulation $\mathcal{T}$. Let $f_1, f_2, \ldots, f_k$ be triangles attached to e on the right side, ordered from the bottom to the top. Let $f'_1, f'_2, \ldots, f'_{d-k}$ be triangles attached to e on the left side, also ordered from the bottom to the top. Then e determines the following relation between the triangles of $\mathcal{T}$

$$f_1 + f_2 + \ldots + f_k = f'_1 + f'_2 + \ldots + f'_{d-k}. \tag{2.2}$$

We call this equation the *branch equation* of e. An example is given in Figure 2.2. A transverse taut triangulation with n tetrahedra determines a system of n branch equations. They can be organised into a matrix

$$B : \mathbb{Z}^E \to \mathbb{Z}^F, \tag{2.3}$$

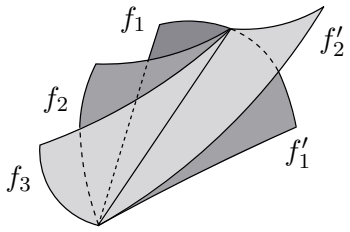

Figure 2.2: Edge with the branch equation $f_1 + f_2 + f_3 = f_1' + f_2'$.

which we call the *branch equations matrix* for $(\mathcal{T}, \alpha)$. For $e \in E$ as in (2.2) we have

$$B(e) = f_1 + f_2 + \ldots + f_k - \left(f_1' + f_2' + \ldots + f_{d-k}'\right).$$

Branch equations of transverse taut triangulations are important in these thesis for two reasons. First, they allow us to easily check whether the horizontal branch surface carries any surfaces; see Subsection 2.2.2. Second, the branch equations matrix B can be interpreted as a boundary map from the 2-chains to the 1-chains of the 2-complex dual to the triangulation. We use this fact in Section 4.2 where we build free abelian covers of transverse taut triangulations.

2.2.2 Surfaces carried by a transverse taut triangulation

Let $(\mathcal{T}, \alpha)$ be a transverse taut ideal triangulation of a 3-manifold M. Suppose that it consists of n ideal tetrahedra. For brevity, if a properly embedded surface S is carried by the horizontal branched surface $\mathscr{B}$ of $(\mathcal{T}, \alpha)$ we say that it is *carried by the triangulation* $(\mathcal{T}, \alpha)$. In this case there exists a nonzero, nonnegative, integral solution $w = (w_1, \ldots, w_{2n})$ to the system of branch equations of $(\mathcal{T}, \alpha)$ such that S can be realised as the relative 2-cycle [21, p. 117]

$$S^w = \sum_{i=1}^{2n} w_i f_i. \tag{2.4}$$

We call w a *weight vector* which puts S in a *fixed carried position*.

If there exists a strictly positive integral solution w to the system of branch equations of $(\mathcal{T}, \alpha)$ we say that $(\mathcal{T}, \alpha)$ is *layered*. In this case S^w is (a multiple of) the fibre of a fibration of M over the circle [38, Theorem 5.15]. If there exists a nonnegative, nonzero integral solution, but no strictly positive integral solution, then we say that $(\mathcal{T}, \alpha)$ is *measurable*. If zero is the only nonnegative solution to the system of branch equations of $(\mathcal{T}, \alpha)$ then we say that $(\mathcal{T}, \alpha)$ is *nonmeasurable*.

2.3 The boundary track

An object which is strictly related to the horizontal branched surface is the *boundary track*. To define it, it is necessary to view the manifold M with a transverse taut triangulation $(\mathcal{T}, \alpha)$ in the truncated model.

Definition 2.3.1. Let $(\mathcal{T}, \alpha)$ be a (truncated) transverse taut triangulation of a 3-manifold M. Let $\mathscr{B}$ be the horizontal branched surface of $(\mathcal{T}, \alpha)$. The *boundary track* β of $(\mathcal{T}, \alpha)$ is the intersection $\mathscr{B} \cap \partial M$.

In Figure 2.3 we present a local picture of a boundary track around one of its switches. A global picture of the boundary track for the veering triangulation `cPcbbbiht_12` of the figure-eight knot complement is presented in Figure 12.1. The boundary track carries boundary components of surfaces carried by the horizontal branched surface. We discuss this in details in Section 12.2.

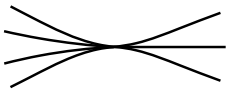

Figure 2.3: The boundary track around one of its switches. This switch corresponds to an endpoint of an edge of degree 7.

Each edge of $\mathcal{T}$ has two endpoints. Therefore for every $e \in E$ the boundary track β has two switches of the same degree that can be labelled with e. Each triangle $f \in F$ has three arcs around its corners; see Figure 2.4. These corner arcs are in a bijective correspondence with branches of β. Therefore for every $f \in F$ the track β has three branches that we label with f. If M has $b \geq 1$ boundary components $T_1, \ldots, T_b$, then β is a disjoint union of train tracks $\beta_1, \ldots, \beta_b$ in boundary tori $T_1, \ldots, T_b$, respectively.

We orient branches of the boundary track β using the transverse taut structure α and the right hand rule; see Figure 2.4. Therefore every switch has a collection of *incoming* branches and a collection of *outgoing branches*. Moreover, branches within these collections can be ordered from the bottom to the top. In particular, for every branch ϵ of β we can consider

- branches outgoing from the initial switch of ϵ above ϵ,
- branches incoming to the terminal switch of ϵ above ϵ.

We use this property of the boundary track in the algorithm `BoundaryCycles` (Alg. 6).

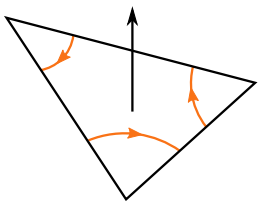

Figure 2.4: Coorientation on a triangle of $\mathcal{T}$ determines orientation on the branches of β embedded in that triangle by the right hand rule.

If a transverse taut triangulation $(\mathcal{T}, \alpha)$ is additionally veering we can colour the switches and branches of the boundary track β by the following rules

- if a switch v of β is an endpoint of an edge e of $\mathcal{T}$ then we colour v with the colour of e,
- if a branch ϵ of β corresponds to a corner arc of a face f of $\mathcal{T}$ then we colour ϵ with the colour of the *opposite* edge of f (the edge of f disjoint from ϵ).

Then, following Section 1.2 of [27], we define *ladderpole branches* as branches of β which connect two switches of the same colour. Ladderpole branches of a boundary track β_j arrange into parallel simple closed curves, called *ladderpoles*, in T_j. The colours of these curves alternate red and blue. A *ladder* is the region between two consecutive ladderpoles. For instance, the boundary torus of the figure-eight knot complement, presented in Figure 12.1, admits a decomposition into four ladders.

In this thesis ladderpoles and ladders do not play any significant role. We mention them because of their relation to the invariant foliations of pseudo-Anosov flows; see Proposition 3.4.2.

More information on the boundary track can be found in [23, Section 2].

2.4 Train tracks in the horizontal branched surface

Let $(\mathcal{T}, \alpha)$ be a transverse taut triangulation. In this section we discuss train tracks embedded in the horizontal branched surface $\mathscr{B}$ of $(\mathcal{T}, \alpha)$ which are dual to its triangulation (F, E). We need to modify the standard definition of a train track so that it is applicable to our setting.

We construct train tracks in $\mathscr{B}$ dual to the triangulation (F, E) by gluing together "ordinary" train tracks in individual triangles of that triangulation. We restrict the class of train tracks that we allow in those triangles. We call the allowed train tracks *triangular*.

Definition 2.4.1. Let f be an ideal triangle. By a *triangular train track* in f we mean a graph $\tau_f \subset f$ with four vertices and three edges, such that

- one vertex v is in the interior of f and the remaining three vertices are at the midpoints of the three edges in the boundary of f, one for each edge,
- for each vertex v' different than v there is an edge joining v and v',
- all edges are C^1-embedded,
- there is a well-defined tangent line to τ_f at v.

See Figure 2.5. We call the vertex v in the interior of f a *switch* of τ_f. The edges of τ_f are called *half-branches*. Each half-branch has one *switch endpoint* and one *edge endpoint*. We say that a half-branch b *meets* $e \in E$, or vice versa, if the edge endpoint of b is the midpoint of e.

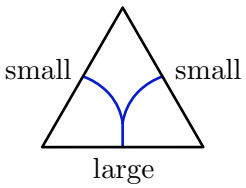

Figure 2.5: A triangular train track.

A tangent line to τ_f at a switch v distinguishes two *sides* of v. Two half-branches are on different sides of v if an only if the path contained in τ_f which joins their edge endpoints is smooth. A switch v has one half-branch on one side and two on the other. We call the half-branch which is the unique half-branch on one side of v the *large half-branch* of τ_f. The remaining two half-branches are called *small half-branches* of τ_f.

Definition 2.4.2. A *dual train track* in $(\mathscr{B}, F)$ is a finite graph $\tau \subset \mathscr{B}$ whose restriction to any ideal triangle f of the ideal triangulation (F, E) of $\mathscr{B}$ is a triangular train track, which we denote by τ_f. Every *switch*/*half-branch* of τ is a *switch*/*half-branch* of τ_f for some $f \in F$, respectively.

2.4.1 The upper and lower tracks of a transverse taut triangulation

A transverse taut structure on a triangulation endows its horizontal branched surface $\mathscr{B}$ with a pair of canonical dual train tracks which we call, following [51, Definition 4.7], the *upper* and *lower* tracks of $\mathscr{B}$.

Definition 2.4.3. Let $(\mathcal{T}, \alpha)$ be a transverse taut triangulation and let $\mathscr{B}$ be the corresponding horizontal branched surface equipped with the ideal triangulation

(F, E). The *upper track* $\tau^{\uparrow}$ of $\mathcal{T}$ is the dual train track in $\mathscr{B}$ such that for every $f \in F$ the large-half branch of $\tau_f^{\uparrow}$ meets the bottom diagonal of the tetrahedron immediately above f. The *lower track* $\tau^{\downarrow}$ of $\mathcal{T}$ is the dual train track in $\mathscr{B}$ such that for every $f \in F$ the large-half branch of $\tau_f^{\downarrow}$ meets the top diagonal of the tetrahedron immediately below f.

We introduce the following names for the edges of $f \in F$ which are dual to large half-branches of $\tau_f^{\uparrow}$ or $\tau_f^{\downarrow}$.

Definition 2.4.4. Let $(\mathcal{T}, \alpha)$ be a transverse taut triangulation. We say that an edge in the boundary of $f \in F$ is the *upper large* (respectively *lower large*) edge of f if it meets the large half-branch of $\tau_f^{\uparrow}$ (respectively $\tau_f^{\downarrow}$).

To define the upper and lower tracks we do not need a veering structure on the triangulation. However, in the case of veering triangulations we can figure out the lower and upper tracks restricted to the faces of a given tetrahedron t without looking at the tetrahedra adjacent to t. Instead, the tracks are encoded by the colours of the edges of t. This follows from the following lemma, which is a reformulation of [38, Lemma 3.2].

Lemma 2.4.5. *Let $\mathcal{V}$ be a veering triangulation. Let t be one of its tetrahedra. Through its top faces t is adjacent to two (not necessarily distinct) tetrahedra t_1, t_2 of $\mathcal{V}$. The embeddings of the bottom diagonals of t_1, t_2 into t are the equatorial edges of t which are of the same colour as the top diagonal of t.*

Proof. First note that the top diagonal of t cannot be the bottom diagonal of t_i, $i = 1, 2$, as this would immediately violate the colouring pattern from Figure 2.1. Now suppose that two consecutive equatorial edges of t are the bottom diagonals of the two tetrahedra t_1, t_2 immediately above t. Such a situation is shown in Figure 2.6.

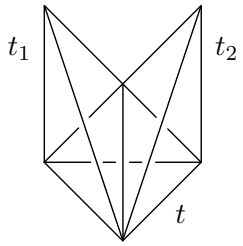

Figure 2.6: The bottom diagonals of t_1, t_2 are not opposite equatorial edges of t.

There is no consistent choice for the colour of the top diagonal of t. Tetrahedron t_1 requires it to be red, while tetrahedron t_2 requires it to be blue; see Figure 2.1.

Hence $(\mathcal{T}, \alpha)$ does not admit a veering structure.

It follows that in a veering triangulation the bottom diagonals of t_1, t_2 are opposite equatorial edges of t. The fact that they have the same colour as the top diagonal of t follows again from analysing Figure 2.1. □

Analogously we have

Lemma 2.4.6. *Let $\mathcal{V}$ be a veering triangulation. Let t be one of its tetrahedra. Through its bottom faces t is adjacent to two (not necessarily distinct) tetrahedra t_1, t_2 of $\mathcal{V}$. The embeddings of the top diagonals of t_1, t_2 into t are the equatorial edges of t which are of the same colour as the bottom diagonal of t.* □

Corollary 2.4.7. *Let $\mathcal{V}$ be a veering triangulation. Let t be one of its tetrahedra. The upper large edges of the top faces of t are the equatorial edges of t which are of the same colour as the top diagonal of t. The lower large edges of the bottom faces of t are the equatorial edges of t which are of the same colour as the bottom diagonal of t.* □

It follows that if a transverse taut triangulation is veering then its upper track $\tau^{\uparrow}$ restricted to the pair of bottom faces of any tetrahedron t differs from $\tau^{\uparrow}$ restricted to the pair of top faces of t by a splitting. The direction of this splitting depends on the colour of the top diagonal of t, with a red top diagonal indicating a left splitting and a blue top diagonal — a right splitting; see Figure 2.7(a). Analogously, the lower track $\tau^{\downarrow}$ restricted to the pair of top faces of t differs from $\tau^{\downarrow}$ restricted to the pair of bottom faces of t by a right (respectively left) splitting if the bottom diagonal of t is red (respectively blue); see Figure 2.7(b).

For both the lower and upper track every tetrahedron of a veering triangulation corresponds to a splitting. The upper track splits upwards, while the lower track splits downwards through tetrahedra. This property is responsible for good dynamical properties of veering triangulations. We discuss this further in Section 3.4.

Remark 2.4.8. The operation $\nu \mapsto -\nu$ does not affect the lower and upper tracks as their definitions do not depend on the 2-colouring on the edges of a veering triangulation. The operation $\alpha \mapsto -\alpha$ interchanges the lower and upper tracks.

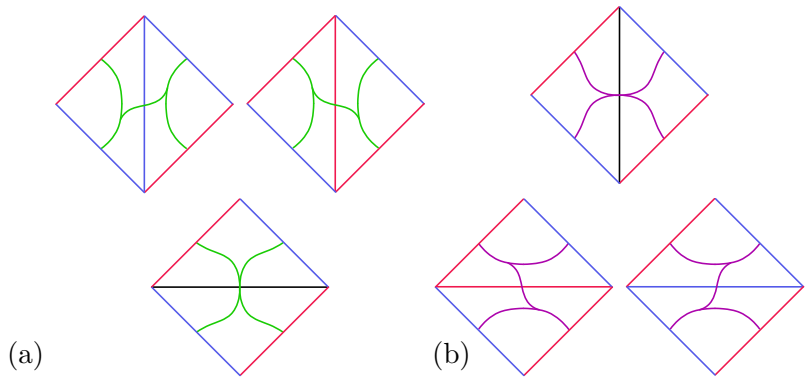

Figure 2.7: Squares in the top row represent the top faces of a tetrahedron and squares in the bottom row represent the bottom faces of a tetrahedron. (a) The upper track in a veering tetrahedron. In the top faces there are two options, depending on the colour of the top diagonal. (b) The lower track in a veering tetrahedron. In the bottom faces there are two options, depending on the colour of the bottom diagonal.

2.5 Colours of triangles of a veering triangulation

Note that any triangle of a veering triangulation has two edges of the same colour and one edge of the other colour; see Figure 2.1. This motivates the following definition.

Definition 2.5.1. We say that a triangle of a veering triangulation is *red* (respectively *blue*) if two of its edges are red (respectively blue).

Recall that triangles attached to an edge e are grouped into two sides. In particular, we distinguish a pair of the *lowermost* and a pair of the *uppermost* (relative to the coorientation) triangles attached to e. For instance, in Figure 2.2 triangles f_1, f_1' are the lowermost and triangles f_3, f_2' are the uppermost.

In the following lemma and the subsequent corollary we show how colours of triangles attached to an edge e depend on the colour of e. We later use this in the proof of Proposition 6.3.1, where we prove that the algorithm `UpperVeeringPolynomial` correctly computes the upper veering polynomial.

Lemma 2.5.2. *Let $\mathcal{V}$ be a veering triangulation with the set T of tetrahedra, the set F of triangular faces, and the set E of edges. Then for any $f \in F$ the bottom diagonal of a tetrahedron immediately above f and the top diagonal of the tetrahedron immediately below f are of the same colour.*

Proof. Denote by b the bottom diagonal of the tetrahedron immediately above f and by t the top diagonal of the tetrahedron immediately below f. Then clearly b, t are distinct edges in the boundary of f, otherwise $\mathcal{V}$ would not be veering. Since

b, t are diagonal edges, there is another edge of f which has the same colour as b and an edge of f which has the same colour as t. Thus b, t cannot be of a different colour. □

Corollary 2.5.3. *Let $\mathcal{V}$ be a veering triangulation with the set T of tetrahedra, the set F of triangular faces, and the set E of edges. Among all triangles attached to an edge $e \in E$ there are exactly four which have the same colour as e. They are the two uppermost and the two lowermost triangles attached to e.*

Proof. By Lemma 2.5.2 the lowermost and uppermost triangles attached to e are of the same colour as e. Conversely, suppose $f \in F$ is neither a lowermost nor an uppermost triangle around e. Then e is an equatorial edge of both the tetrahedron immediately above f and the tetrahedron immediately below f. Again by Lemma 2.5.2 the bottom diagonal of the first and the top diagonal of the latter are of the same colour. Since they are different edges of f (otherwise $\mathcal{V}$ would not be veering), it follows that f is of a different colour than e. □

We distinguish two types of veering tetrahedra: *hinges* and *non-hinges*. We say that a tetrahedron is *hinge* if it has two faces of one colour and two faces of the other colour. We say that a tetrahedron is *non-hinge* if it has all four faces of the same colour. This distinction is not particularly relevant in this thesis, but it is important in many results regarding veering triangulations and we refer to it in Section 2.6.

Remark. Hinge tetrahedra are called *toggles* and non-hinge tetrahedra are called *fans* in [51, Definition 5.8].

2.6 State of knowledge on veering triangulations

Veering triangulations were introduced by Ian Agol in [2, Section 4]. He constructed only layered triangulations of pseudo-Anosov mapping tori, but noticed that veering triangulations can potentially exist on non-fibred 3-manifolds. That is indeed the case. In [31, Section 4] Hodgson, Rubinstein, Segerman and Tillmann presented the first known example of a nonlayered veering triangulation. They also showed that veering triangulations admit strict angle structures [31, Theorem 1.5]. An alternative constructive proof was given by Futer and Guéritaud in [23, Theorem 1.4]. It follows that veering triangulations exist only on hyperbolic manifolds [33, Corollary 4.6].

However, veering triangulations are not always *geometric*, that is realised in a complete hyperbolic metric with all tetrahedra positively oriented [30, Section 7]. Futer, Taylor and Worden proved that layered veering triangulations are in fact

generically non-geometric [24, Theorems 1.1 and 1.2]. This result was preceded by an experimental analysis undertaken by Worden in [60]. Worden also observed a relation between the number of *hinge* tetrahedra in a veering triangulation and the hyperbolic volume of the underlying manifold [60, Section 6], as well as a relation between the length of the maximal chain of *non-hinge* tetrahedra in the triangulation and the systole length [60, Corollary 7.4].

A different connection between veering triangulations and the hyperbolic geometry was obtained by Guéritaud in [27]. He showed that the combinatorics of a layered veering triangulation informs about the order in which the image of the associated *Cannon-Thurston map* fills out the sphere at infinity of the hyperbolic 3-space. Additionally, Guéritaud gave an alternative construction of layered veering triangulations [27, Theorem 1.1]. Agol's construction relied on properties of the train tracks carrying the stable lamination of a pseudo-Anosov homeomorphism, while Guéritaud used a singular Euclidean metric on the fibre determined by the pseudo-Anosov monodromy. In unpublished work Agol and Guéritaud together generalised the construction from [27] and showed that a veering triangulation can be derived from any *pseudo-Anosov flow without perfect fits*.

Guéritaud's result on the connection between veering triangulations and Cannon-Thurston maps was recently generalised by Schleimer in Segerman in [51, Theorem 9.15]. They proved that even a nonlayered veering triangulation determines a *veering sphere* admitting a continuous, faithful and orientation-preserving action of the fundamental group of the underlying manifold. They conjecture that the veering sphere is equivariantly homeomorphic to the sphere at infinity $\partial\mathbb{H}^3$. This would imply that veering triangulations determine sphere-filling curves, similar to the ones obtained by Cannon and Thurston in [11], but not arising from surface subgroups.

The work of Schleimer and Segerman [51] is the first step in proving the converse to the result of Agol and Guéritaud, that *every* veering triangulation is constructed from a pseudo-Anosov flow without perfect fits. Given a veering triangulation $\mathcal{V}$ they construct the *link space* which is homeomorphic to $\mathbb{R}^2$ and is supposed to model the orbit space of a pseudo-Anosov flow without perfect fits on the universal cover of the manifold.

Another interesting aspect of veering triangulations is their connection to the Thurston norm. This was mainly studied by Landry in [34, 35, 36]. For instance, using veering triangulations he gave a sufficient condition for when given a fibred face $\mathtt{F}$ of the Thurston norm ball in $H_2(N, \partial N; \mathbb{R})$ there exists a *unique* taut oriented branched surface in N which carries representatives of all integral homology classes in the cone $\mathbb{R}_+ \cdot \mathtt{F} \subset H_2(N, \partial N; \mathbb{R})$ [36, Theorem 3.9]. He analysed nonfibred faces of

the Thurston norm ball in [35]. On a different note, Minsky and Taylor proved that a layered veering triangulation informs about *subsurface projections* associated to each fibre in the corresponding fibred face of the Thurston norm ball [45].

Finally, Landry, Minsky and Taylor defined two polynomial invariants of veering triangulations: the taut polynomial and the veering polynomial [38]. These polynomial invariants are the main research focus of this thesis.

Chapter 3

Pseudo-Anosov flows

The combinatorial definition of a veering triangulation given in Section 2.1 is easy to state and has computational advantages. However, it comes with a price — it hides the dynamical meaning of veering triangulations. In Section 2.6 we alluded to the fact that veering triangulations are tightly related to *pseudo-Anosov flows without perfect fits*. In this chapter we discuss this relation further.

3.1 Foliations of codimension one

Both pseudo-Anosov homeomorphisms and pseudo-Anosov flows are defined in terms of the existence of a pair of codimension one foliations with certain properties.

Definition 3.1.1. [10, p. 22] A *codimension one foliation* of an n-dimensional manifold M is an atlas of charts $\mathscr{F}$ on M into $\mathbb{R}^n$ with the following properties

- $\varphi(U) = U_1 \times U_2 \subset \mathbb{R}^{n-1} \times \mathbb{R}$ for any $(U, \varphi) \in \mathscr{F}$, where U_1, U_2 are open disks in $\mathbb{R}^{n-1}, \mathbb{R}$, respectively,
- the transition functions are of the fom

$$\varphi_j \varphi_i^{-1}(x, y) = (f_{ij}(x, y), g_{ij}(y))$$

for $x \in \mathbb{R}^{n-1}, y \in \mathbb{R}$ and some smooth functions $f_{ij}, g_{ij} : \mathbb{R}^n \to \mathbb{R}^n$.

A codimension one foliation of M determines its decomposition into a disjoint union of $(n-1)$-dimensional subsets, which are called the *leaves* of the foliation.

The foliations determined by pseudo-Anosov homeomorphisms and pseudo-Anosov flows do *not* satisfy Definition 3.1.1, because they admit (finitely many) *singularities*. In the case of surfaces singularities that occur are *k-prongs*, $k \geq 3$. Around these points the leaves of the foliation arrange into level sets of the k-prong

saddle; see Figure 3.1 for $k = 6$. We note that 1-prongs are allowed in surfaces with boundary or punctures.

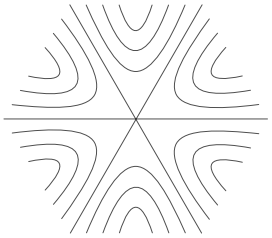

Figure 3.1: A 6-prong singularity of a 1-dimensional foliation.

Let ℓ be a closed curve contained in a leaf of a 2-dimensional foliation $\mathscr{F}$. We say that ℓ is a *suspended k-prong* if it admits a small regular neighbourhood $U(\ell)$ such that for every meridonal disk D of $U(\ell)$ the foliation $\mathscr{F} \cap D$ of D admits only one singularity, of the k-prong type, which appears at $\ell \cap D$. We also say that ℓ has k-prongs. The curve ℓ forms a singularity of $\mathscr{F}$. Generally, singular codimension one foliations of 3-manifolds can have different types of singularities, but in this thesis we only encounter singularities as above.

A leaf of a singular foliation is *singular* if it contains a singularity of the foliation. For a 1-dimensional foliation $\mathscr{F}$ we define a *generalised leaf* of $\mathscr{F}$ to be either a nonsingular leaf of $\mathscr{F}$ or the union of two singular leaves of $\mathscr{F}$ which share a common singularity. Two singular foliations are *transverse* if they have the same set of singular points/curves and their leaves are transverse away from the singularities. A singular foliation $\mathscr{F}$ is *orientable* if its leaves can be oriented in continuously varying way. It is *transversely orientable* if there is a continuous choice of a nonvanishing transverse vector field on $\mathscr{F}$. Throughout the thesis we assume that all surfaces and 3-manifolds are orientable, therefore orientability of a foliation is equivalent to its transverse orientability [10, p. 39].

3.2 Pseudo-Anosov homeomorphisms of surfaces

Pseudo-Anosov homeomorphisms of surfaces leave invariant a pair of transverse singular foliations in the surface, contracting the leaves of one foliation and stretching the leaves of the other foliation. In order to formalise this concept we need to introduce a notion of a *transverse measure* on a singular foliation.

Let S be an orientable surface of finite type. A singular codimension one foliation $\mathscr{F}$ on S is *measured* if there exists a nonnegative function μ on arcs transverse to $\mathscr{F}$ which is countably additive under a disjoint union of arcs and invariant under a homotopy from a transverse arc β to a transverse arc β' during which every point

of β stays in a fixed leaf of $\mathscr{F}$ [9, p. 39]. A measured foliation is typically denoted by $(\mathscr{F}, \mu)$. A homeomorphism ψ of S transforms $(\mathscr{F}, \mu)$ into another measured foliation $(\psi(\mathscr{F}), \psi_*\mu)$ where for an arc β transverse to $\psi(\mathscr{F})$ we have $(\psi_*\mu)(\beta) = \mu(\psi^{-1}(\beta))$ [15, p. 319].

If ψ is pseudo-Anosov then there is a pair of singular measured foliations $(\mathscr{F}^s, \mu^s)$, $(\mathscr{F}^u, \mu^u)$ in S such that $\mathscr{F}^s$ and $\mathscr{F}^u$ coincide at the singularities, are transverse to each other away from the singularities, both are invariant under ψ, and moreover there is a number $\lambda > 1$ such that $\psi_*\mu^s = \lambda^{-1}\mu^s$ and $\psi_*\mu^u = \lambda\mu^u$ [15, Subsection 13.2.3]. Example 3.2.1 illustrates the behaviour of a pseudo-Anosov homeomorphism.

The numerical invariant λ is called the *stretch factor* of ψ. Foliations $\mathscr{F}^s$, $\mathscr{F}^u$ are called the *stable* and *unstable* foliation of ψ, respectively, or just *invariant foliations* of ψ. Informally, ψ contracts the leaves of the stable foliation by λ and stretches the leaves of the unstable foliation by λ. We also consider invariant laminations $\mathscr{L}^s, \mathscr{L}^u$ of ψ obtained from $\mathscr{F}^s$ and $\mathscr{F}^u$ by splitting them open along their singular leaves.

Example 3.2.1. Consider the octagon $Q \subset \mathbb{R}^2$ presented in Figure 3.2(a) on the left. Identifying its opposite sides of equal lengths by translations yields a closed genus 2 surface S. All eight vertices of Q are identified to one point in S. This representation of S endows it with a singular Euclidean metric. The singularity of the metric occurs precisely at the image of the vertices of Q in S. The angle around this point equals 6π.

Let $\kappa = \frac{1+\sqrt{13}+\sqrt{2\sqrt{13}-2}}{4} \approx 1.72208$. Consider the linear homomorphism

$$A = \begin{bmatrix} \kappa & 0 \\ 0 & \kappa^{-1} \end{bmatrix}.$$

The image $A(Q)$ is presented in Figure 3.2(a) on the right. Figure 3.2(b) illustrates that $A(Q)$ can be cut along a straight line into two pieces, which can then be glued along a pair of sides identified in S to give Q back. This implies that A descends to a homeomorphism ψ of S. It is pseudo-Anosov; the horizontal and vertical foliations in Q give the unstable and stable foliations of ψ. These foliations have one 6-prong singularity in the singular point of the metric.

Apart from the stretch factor of ψ, in Chapter 12 we also consider the *homological stretch factor* of ψ. This is the absolute value of the largest real eigenvalue of the homomorphism $\psi_* : H_1(S; \mathbb{Z}) \to H_1(S; \mathbb{Z})$ induced by ψ. There is an easy criterion which tells when these two numerical invariants of ψ are equal.

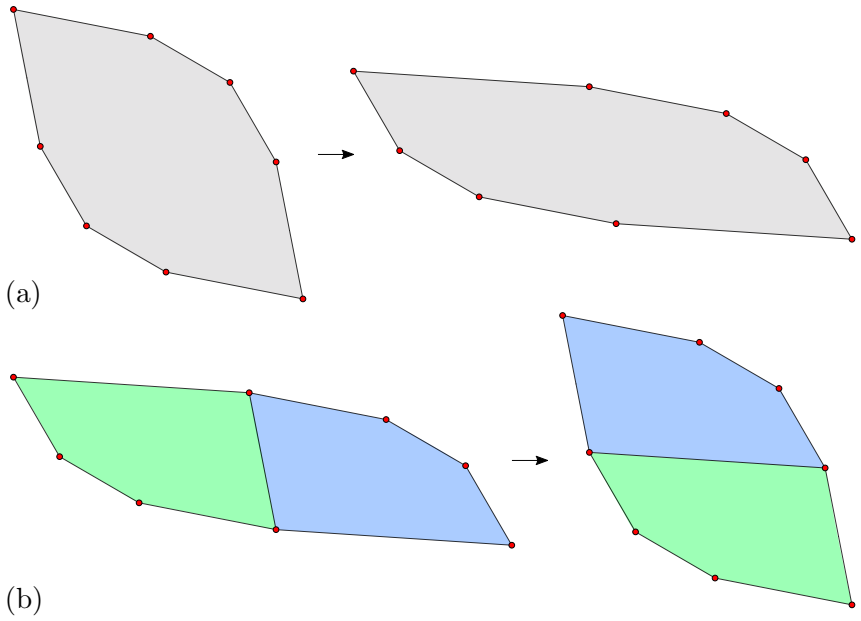

Figure 3.2: (a) Transforming Q by the affine transformation A. (b) Cutting $A(Q)$ along a straight line and gluing the obtained pieces along a pair of sides which are identified in S gives Q back.

Theorem 3.2.2 (Lemma 4.3 of [4]). *Let $\psi : S \to S$ be a pseudo-Anosov homeomorphism. The stretch factor and the homological stretch factor of ψ are equal if and only if the invariant foliations of ψ are orientable.* □

3.3 Pseudo-Anosov flows

Let N be a closed 3-manifold. Following [17, Definition 7.1] we say that a flow $\Psi : N \times \mathbb{R} \to N$ is a *(topological) pseudo-Anosov flow* if it has no point orbits and there is a pair of singular codimension one foliations $\mathscr{F}^s$, $\mathscr{F}^u$ in N such that

- $\mathscr{F}^s$, $\mathscr{F}^u$ intersect at flowlines and away from the singularities they are transverse to each other,
- all singularities of $\mathscr{F}^s$, $\mathscr{F}^u$ are k-prong suspensions, $k \geq 3$,
- two orbits in a leaf of $\mathscr{F}^s$ are forward asymptotic and two orbits in a leaf of $\mathscr{F}^u$ are backward asymptotic.

We call the singularities of $\mathscr{F}^s$, $\mathscr{F}^u$ the *singular orbits* of Ψ and denote their set by $\mathrm{sing}(\Psi)$. The foliations $\mathscr{F}^s$, $\mathscr{F}^u$ are called the *stable* and *unstable foliations* of the flow. We also consider the stable and unstable laminations $\mathscr{L}^s, \mathscr{L}^u$ of Ψ obtained from $\mathscr{F}^s$ and $\mathscr{F}^u$ by splitting them open along their singular leaves.

An important class of pseudo-Anosov flows can be constructed using pseudo-Anosov homeomorphisms. Namely, let $\psi : S \to S$ be a pseudo-Anosov homeomorphism of a closed surface. We construct the *mapping torus* of ψ

$$N = N_\psi = (S \times [0,1]) \Big/ \{(x,1) \sim (\psi(x),0)\}.$$

It is equipped with the *suspension flow* Ψ of ψ defined as the unit speed flow along the curves $\{x\} \times [0,1]$. This flow is pseudo-Anosov. The mapping tori of the invariant foliations of ψ give the stable and unstable foliations of the flow Ψ.

There are pseudo-Anosov flows which are not suspension flows of pseudo-Anosov homeomorphisms [18, Theorem H]. Such flows do not admit an embedded surface which transversely intersects every flowline. However, by a theorem of Brunella [7, Theorem 1] every pseudo-Anosov flow Ψ admits a *surface of section*. This is an embedded surface S with (possibly empty) boundary such that the interior of S is transverse to Ψ and ∂S is a finite collection of closed orbits of Ψ. In other words, every pseudo-Anosov flow restricts to a suspension flow in the complement of finitely many of its closed orbits.

3.4 Connection with veering triangulations

In this section we recall the construction of layered veering triangulations of pseudo-Anosov mapping tori due to Guéritaud [27, Section 2]. Then we outline how his arguments can be generalised to the case of general *pseudo-Anosov flows without perfect fits*.

Let $\psi : S \to S$ be a pseudo-Anosov homeomorphism with the stretch factor κ. There is a singular Euclidean metric d_ψ on S, with only conical singularities, such that ψ can be realised by the affine transformation

$$A_\psi = \begin{bmatrix} \kappa & 0 \\ 0 & \kappa^{-1} \end{bmatrix}$$

of (S, d_ψ). The stable and unstable foliations of ψ correspond to the vertical and horizontal foliations of (S, d_ψ). Compare this with Example 3.2.1. See also [27, Fact A].

Now let $\mathring{S}$ be obtained from S by puncturing it at the singularities of d_ψ. It admits a pseudo-Anosov homeomorphism $\mathring{\psi}$ obtained by restricting ψ to $\mathring{S}$. Guéritaud's construction [27, Section 2], described below, yields a veering triangulation of the mapping torus of $\mathring{\psi}$.

Let $\mathring{d_\psi}$ be the incomplete Euclidean metric on $\mathring{S}$ induced by d_ψ. Let $(\hat{S}, \hat{d_\psi})$

be the metric completion of the universal cover of $(\mathring{S}, \mathring{d}_\psi)$. Denote by $\hat{\mathscr{F}}^s$, $\hat{\mathscr{F}}^u$ the lifts of the stable and unstable foliations of ψ to $\hat{S}$. A *singularity-free rectangle* in $\hat{S}$ is an embedded rectangle in $\hat{S}$ cobounded by two generalised leaf segments of $\hat{\mathscr{F}}^s$ and two generalised leaf segments of $\hat{\mathscr{F}}^u$. Such a rectangle has a well-defined width and height, in particular we can tell when it is a square. Among singularity-free squares in $\hat{S}$ we are interested in the *maximal* ones, which are not properly contained in any other singularity-free square. They determine a cellulation of $\hat{S}$, where every cell is the convex hull of the singularities in the boundary of a maximal singularity-free square. Generically they are triangles. Quadrilaterals occur when there is a maximal singularity-free square which has precisely four singularities in its boundary [27, Proposition 2.1].

We continuously transform the metric on $\hat{S}$ by applying the flow

$$\mathfrak{F}_t = \begin{bmatrix} e^t & 0 \\ 0 & e^{-t} \end{bmatrix}$$

and observe how the cellulation changes with $t \in \mathbb{R}$. One possibility is depicted in Figure 3.3.

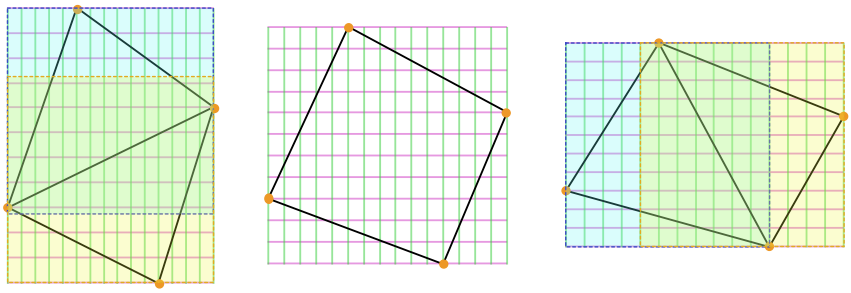

Figure 3.3: Change of the cellulation of $\hat{S}$ under $\mathfrak{F}_t$. The stable foliation is green and the unstable foliation is purple. Orange dots indicate singularities of foliations. On the far left and far right there is one maximal singularity-free rectangle but two maximal singularity-free squares (shaded). In the middle picture there is only one singularity-free rectangle which happens to be a square.

Clearly, the cellulation of $\hat{S}$ undergoes *diagonal exchanges* in the maximal singularity-free *rectangles*. Therefore to every maximal singularity-free rectangle R we associate a transverse taut tetrahedron t as in Figure 3.4. Since $\mathfrak{F}_t$ stretches in the horizontal direction and contracts in the vertical direction, the edge e joining the singularities in the two vertical sides of R appears *before* the edge e' joining the singularities in the two horizontal sides of R. Hence e' is above e in t.

We colour an edge of t red if its slope is positive and blue if the slope is

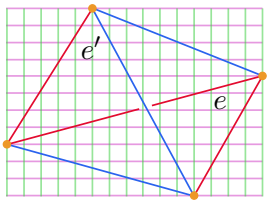

Figure 3.4: A veering tetrahedron associated to a maximal singularity-free rectangle. The stable foliation is green and the unstable foliation is purple. Orange dots indicate singularities of foliations.

negative. Note that every edge has either positive or negative slope. Slopes 0 or ∞ never occur, because invariant foliations of pseudo-Anosov homeomorphisms do not admit leaf segments with two singular endpoints [15, Lemma 14.11]. Therefore a transverse taut triangulation obtained from this construction is necessarily veering. It descends to a veering triangulation of the mapping torus of $\mathring{\psi}$ [27, Theorem 1.1].

This line of reasoning generalises to pseudo-Anosov flows which are not suspension flows of pseudo-Anosov homeomorphisms, as long as they do not admit *perfect fits*. This work is due to Guéritaud and Agol, but unfortunately there is no written reference for these results.

Let Ψ be a pseudo-Anosov flow on a 3-manifold N. We consider the flow $\widetilde{\Psi}$ induced on the universal cover $\widetilde{N}$. Denote by $\widetilde{\mathscr{F}^s}$, $\widetilde{\mathscr{F}^u}$ the stable and unstable foliations of $\widetilde{\Psi}$, respectively. All flowlines of $\widetilde{\Psi}$ are homeomorphic to $\mathbb{R}$. By collapsing each of them to a point we obtain the *orbit space* $\mathcal{O}$ of $\widetilde{\Psi}$, which is homeomorphic to $\mathbb{R}^2$ [20, Proposition 4.2]. The foliations $\widetilde{\mathscr{F}^s}$, $\widetilde{\mathscr{F}^u}$ project to give 1-dimensional transverse singular foliations $\mathcal{O}^s$, $\mathcal{O}^u$ in $\mathcal{O}$, respectively.

If s_1, u_1 are leaves of $\mathcal{O}^s$ and $\mathcal{O}^u$, respectively, then they intersect at most once [16, p. 637]. If they intersect once and furthemore s_1 intersects another leaf u_2 of $\mathcal{O}^u$, and u_1 intersects another leaf s_2 of $\mathcal{O}^s$, then we say that s_1, u_1, s_2, u_2 form a *rectangle* R in $\mathcal{O}$. In this case there is no singularity of $\mathcal{O}^s$ or $\mathcal{O}^u$ in the interior of R [16, p. 638].

Now suppose that s_1, u_1 are disjoint. We say that s_1, u_1 form a *perfect fit* if there are closed leaf segments ϵ_1, ϵ_2 of $\mathcal{O}^s$ and $\mathcal{O}^u$, respectively, and closed rays s_1', u_1' in s_1, u_1, respectively, such that $s_1' \cup u_1' \cup \epsilon_1 \cup \epsilon_2$ separates $\mathcal{O}$ and forms a rectangle R° with one vertex removed [19, Definition 2.3]. This is illustrated in Figure 3.5. We say that Ψ does not admit perfect fits if no pair of leaves of $\mathcal{O}^s$ and $\mathcal{O}^u$ form a perfect fit.

Assume that Ψ does not admit perfect fits. Let $M = N - \mathrm{sing}(\Psi)$. The restriction of Ψ to M gives a flow Ψ_M. Let $\mathring{\mathcal{O}}$ denote the surface obtained from $\mathcal{O}$

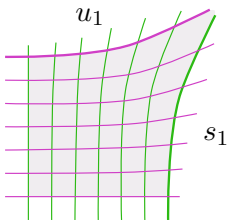

Figure 3.5: Leaves u_1, s_1 form a perfect fit.

by puncturing it at the singularities of $\mathcal{O}^s$ and $\mathcal{O}^u$. The universal cover $\widetilde{\mathcal{O}}_M$ of $\mathring{\mathcal{O}}$ is the orbit space of the flow $\widetilde{\Psi}_M$ induced on the universal cover $\widetilde{M}$. Its completion gives the branched cover $\hat{\mathcal{O}}_M \to \mathcal{O}$, infinitely branched over the singularities of $\mathcal{O}$. The space $\hat{\mathcal{O}}_M$ is equipped with a pair of transverse singular foliations $\hat{\mathcal{O}}^s_M$, $\hat{\mathcal{O}}^u_M$. Since Ψ does not admit perfect fits, $\hat{\mathcal{O}}^s_M$, $\hat{\mathcal{O}}^u_M$ determine singularity-free rectangles (with all vertices) in $\hat{\mathcal{O}}_M$. To each maximal singularity-free rectangle we associate a veering tetrahedron as in Figure 3.4. As in the fibred case, the obtained veering triangulation of $\widetilde{\mathcal{O}}_M \times \mathbb{R} \approx \widetilde{M}$ descends to a veering triangulation of M.

Now that we have a veering triangulation $\mathcal{V}$ constructed from a pseudo-Anosov flow Ψ we are interested in how much information about the flow Ψ is encoded in $\mathcal{V}$. Recall from Subsection 2.4.1 that the 2-skeleton of a veering triangulation $\mathcal{V}$ is equipped with the upper and lower tracks. Following [51, Section 6.1] inside every tetrahedron t we embed a contractible branched surface $\mathscr{B}^{\uparrow}_t$ which intersects the faces in the boundary of t along the upper track; see Figure 3.6. Analogously, inside every t there is a branched surface $\mathscr{B}^{\downarrow}_t$ in t which intersects the faces of t along the lower track.

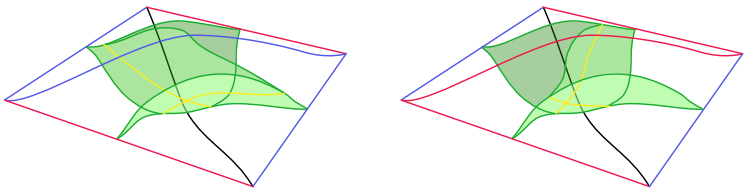

Figure 3.6: Two options for the upper branched surface in a veering tetrahedron. Yellow curves indicate the branch locus. This is a modified version of Figure 6.2.(B) of [51].

The union

$$\mathscr{B}^{\uparrow} = \bigcup_{t \in T} \mathscr{B}^{\uparrow}_t \tag{3.1}$$

is called the *upper branched surface* of $\mathcal{V}$ and the union

$$\mathscr{B}^{\downarrow} = \bigcup_{t \in T} \mathscr{B}_t^{\downarrow}$$

is called the *lower branched surface* of $\mathcal{V}$ [51, Subsection 6.1]. Note that combinatorially both $\mathscr{B}^{\uparrow}$ and $\mathscr{B}^{\downarrow}$ are dual to $\mathcal{V}$.

Theorem 3.4.1 (Agol, Guéritaud)**.** *Suppose that a veering triangulation $\mathcal{V}$ is constructed from a pseudo-Anosov flow Ψ. Then*

- *the stable lamination $\mathscr{L}^s$ of Ψ is fully carried by $\mathscr{B}^{\uparrow}$,*
- *the unstable lamination $\mathscr{L}^u$ of Ψ is fully carried by $\mathscr{B}^{\downarrow}$.* □

Different pseudo-Anosov flows can give rise to the same veering triangulation. This notoriously happens even in the case of suspension flows of pseudo-Anosov homeomorphisms, as different fibres carried by a veering triangulation of M may determine different Dehn filling slopes on the boundary tori of M.

The number of prongs of the singular orbits of the flow can be computed from the combinatorics of the veering triangulation and Dehn filling data.

Proposition 3.4.2 (Section 4 of [35])**.** *Let Ψ be a pseudo-Anosov flow without perfect fits and let $\mathcal{V}$ be the derived veering triangulation of $M = N - \mathrm{sing}(\Psi)$. Suppose that M in the truncated model has b boundary tori $T_1, \dots, T_b$. Let δ_j denote the union of all ladderpoles in T_j. Let γ_j be a Dehn filling slope on T_j such that N is obtained from M by Dehn filling T_j along γ_j for $j = 1, \dots, b$. Let ℓ_j be the core curve of the filling solid torus in N whose boundary is identified with T_j. Then ℓ_j is a singular orbit of Ψ and the number of prongs of ℓ_j is equal to*

$$\frac{\iota(\delta_j, \gamma_j)}{2},$$

where $\iota(\cdot, \cdot)$ denotes the geometric intersection number in T_j. □

Conjecturally, every veering triangulation satisfies the assumption of Theorem 3.4.1 [52]. If this conjecture is true then a pseudo-Anosov flow is uniquely determined by a veering triangulation and Dehn filling slopes on the boundary tori of the underlying manifold.

Chapter 4

Free abelian covers of transverse taut triangulations

This thesis concerns various polynomial invariants of 3-manifolds. All of them are derived from certain modules associated to the *maximal free abelian cover* M^{ab} of a 3-manifold M. This covering space corresponds to the kernel of the homomorphism

$$\pi_1(M) \to H_1(M;\mathbb{Z}) /_{\text{torsion}}.$$

The deck group of the covering $M^{ab} \to M$ is isomorphic to

$$H = H_1(M;\mathbb{Z}) /_{\text{torsion}}. \tag{4.1}$$

We will be more general and consider a free abelian quotient H' of $H_1(M;\mathbb{Z})$. This generalisation is important in Chapter 10, where the group H' will arise as the maximal free abelian quotient of the homology group $H_1(N;\mathbb{Z})$ of a Dehn filling N of M. Associated to H' there is an *intermediate* free abelian cover of M

$$M^{ab} \to M' \to M$$

with the deck group isomorphic to H'.

Let r denote the rank of H'. The integral group ring $\mathbb{Z}[H']$ on H' is isomorphic to the ring $\mathbb{Z}[u_1^{\pm 1}, \ldots, u_r^{\pm 1}]$ of Laurent polynomials. If a basis $(b_1, \ldots, b_r)$ of H' is fixed then we choose the isomorphism to be $b_i \mapsto u_i$. Then an element $v = \sum_{i=1}^{r} v_i b_i \in H'$, $v_i \in \mathbb{Z}$, can be encoded by the Laurent monomial $u^v = u_1^{v_1} \cdots u_r^{v_r}$.

Suppose M is equipped with a transverse taut triangulation $(\mathcal{T}, \alpha)$. A free abelian cover M' admits a triangulation $\mathcal{T}'$ induced by $\mathcal{T}$ via the covering map

$M' \to M$. It is also transverse taut, as coorientations on triangular faces can be lifted from $\mathcal{T}$. If $\mathcal{T}$ is additionally veering, then so is $\mathcal{T}'$.

Ideal tetrahedra, triangles and edges of $\mathcal{T}'$ are lifts of elements of T, F, E, respectively. They can be indexed by elements of H', hence we denote their sets by $H' \cdot T, H' \cdot F, H' \cdot E$. We endow the free abelian groups generated by $H' \cdot T$, $H' \cdot F$ and $H' \cdot E$ with a $\mathbb{Z}[H']$-module structure. That is, we identify them with $\mathbb{Z}[H']^T, \mathbb{Z}[H']^F, \mathbb{Z}[H']^E$, respectively.

4.1 Labelling ideal simplices of the cover

Let $(\mathcal{T}, \alpha)$ be a transverse taut triangulation of M. Let $\mathcal{F}$ be a connected fundamental domain for the action of H' on M' whose closure $\overline{\mathcal{F}}$ is triangulated by lifts of tetrahedra $t \in T$. We label the tetrahedra in $\overline{\mathcal{F}}$ with $1 \in H$. Every other tetrahedron in the triangulation $\mathcal{T}'$ is a translate of some $1 \cdot t$ by an element $h \in H'$, hence we denote it by $h \cdot t$. We also say that $h \cdot t$ has *H'-coefficient* h.

For the remaining of the thesis the labelling for the lower dimensional ideal simplices is as follows:

- triangle $h \cdot f$, for $f \in F$, $h \in H'$, is a bottom triangle of a tetrahedron with H'-coefficient h,
- edge $h \cdot e$, for $e \in E$, $h \in H'$, is the bottom diagonal of a tetrahedron with H'-coefficient h.

In other words, triangles and edges inherit their H'-coefficient from the unique tetrahedron immediately above them. Once a basis for H is fixed, we replace the H'-coefficients of simplices with their *Laurent coefficients*. They are the images of H'-coefficients under the inclusion $H' \to \mathbb{Z}[H']$.

Remark. Throughout the thesis we use the multiplicative convention for H'.

Every triangle of $\mathcal{T}'$ is a top triangle of $h_1 \cdot t_1$ and a bottom triangle of $h_2 \cdot t_2$ for some $h_1, h_2 \in H'$, $t_1, t_2 \in T$. Moreover, for all lifts of a triangle $f \in F$ the corresponding product $h_2 h_1^{-1}$ is the same. This motivates the following definition.

Definition 4.1.1. The *H'-pairings* for $(\mathcal{T}, \mathcal{F})$ are elements $h_i \in H'$ associated to triangles $f_i \in F$ such that the tetrahedron immediately below $h \cdot f_i$ is in $h_i^{-1} h \cdot \mathcal{F}$. We also say that h_i is the *H'-pairing* of f_i relative to $\mathcal{F}$.

Remark. The meaning of H'-pairings is explained in Remark 4.2.2.

A transverse taut triangulation $\mathcal{T}'$ together with a fixed fundamental domain $\mathcal{F}$ determine the H'-pairings and, once a basis of H' is fixed, the *face Laurents*,

their images under the inclusion $H' \to \mathbb{Z}[H']$. We, however, need to reverse this process. Namely, given a triangulation $\mathcal{T}$ of M consisting of n tetrahedra, we compute a list $\mathcal{H}$ of $2n$ H'-pairings, which determines a consistent labelling of ideal simplices of $\mathcal{T}'$ by elements of H'. In this way we encode the whole infinite triangulation $\mathcal{T}'$ with a pair of finite objects $(\mathcal{T}, \mathcal{H})$. This procedure is a subject of the next subsection.

4.2 Encoding the triangulation of the cover

We want to encode the triangulation $\mathcal{T}'$ by $\mathcal{T}$ and a finite list of H'-pairings associated to the triangles of $\mathcal{T}$. The latter depends on the chosen fundamental domain $\mathcal{F}$ for the action of H' on $\mathcal{T}'$. We fix it using the *dual graph* of $\mathcal{T}$.

4.2.1 The dual 2-complex and the dual graph

Let $\mathcal{T} = (T, F, E)$ be an ideal triangulation. By $\mathcal{D}$ we denote its dual complex. It is a 2-dimensional CW-complex: it has n vertices, each corresponding to some $t \in T$, $2n$ edges, each corresponding to a triangular face $f \in F$, and n two-cells, each corresponding to an edge $e \in E$. We abuse the notation slightly and denote the vertex of $\mathcal{D}$ dual to tetrahedron t by t, the edge of $\mathcal{D}$ dual to face f by f and the 2-cell of $\mathcal{D}$ dual to edge e by e.

By Γ we denote the 1-skeleton of $\mathcal{D}$. We call Γ the *dual graph* of $\mathcal{T}$. Whenever $\mathcal{T}$ is transverse taut we endow Γ with the "upward" orientation on edges coming from the coorientation on their dual faces.

4.2.2 Fixing a fundamental domain

Let $(\mathcal{T}, \alpha)$ is a transverse taut triangulation. Let Γ be the dual graph of $\mathcal{T}$ with edges oriented by α. Let Υ be a spanning tree of Γ. If $\mathcal{T}$ has n tetrahedra, then Υ has n vertices $t \in T$ and $n - 1$ edges.

The dual 2-complex $\mathcal{D}'$ of $\mathcal{T}'$ is a free abelian cover of $\mathcal{D}$. Fix a lift $\widetilde{\Upsilon}$ of Υ to $\mathcal{D}'$. The lift $\widetilde{\Upsilon}$ determines a fundamental domain $\mathcal{F}$ for the action of H' on $\mathcal{T}'$ built from:

- the interiors of all tetrahedra of $\mathcal{T}'$ dual to vertices of $\widetilde{\Upsilon}$,
- bottom diagonal edges of tetrahedra of $\mathcal{T}'$ dual to vertices of $\widetilde{\Upsilon}$,
- the interiors of triangles of $\mathcal{T}'$ dual to the edges of Γ' which join two vertices of $\widetilde{\Upsilon}$,
- the interiors of triangles of $\mathcal{T}'$ dual to the edges of Γ' which run from a vertex not in $\widetilde{\Upsilon}$ to a vertex of $\widetilde{\Upsilon}$.

Definition 4.2.1. We say that $\mathcal{F}$ constructed as above is the (downwardly closed) fundamental domain for the action of H' on $\mathcal{T}'$ *determined by the spanning tree* Υ of Γ.

4.2.3 Finding H'-pairings

A choice of a spanning tree Υ of the dual graph Γ not only determines the fundamental domain $\mathcal{F}$ for the action of H' on $\mathcal{T}'$, but also gives an easy way to find a presentation for $\pi_1(\mathcal{D})$, and hence for H', in terms of elements of F.

First note that $\mathcal{D}$ is a deformation retract of M and therefore

$$H_1(M;\mathbb{Z}) \cong H_1(\mathcal{D};\mathbb{Z}).$$

It follows that $H_1(M;\mathbb{Z})$ is generated by simplicial 1-cycles in $\mathcal{D}$. For brevity we call any simplicial 1-cycle in $\mathcal{D}$ a *dual cycle*. This is different from [38, Section 5], where by dual cycles the authors mean only directed cycles, with the orientation on the dual graph coming from the transverse taut structure α on $\mathcal{T}$.

Given a collection C of dual cycles we consider the subgroup $\langle C\rangle$ generated by $\{[c] \in H_1(M;\mathbb{Z}) \mid c \in C\}$. Let

$$H_1(M;\mathbb{Z})^C = H_1(M;\mathbb{Z}) \Big/ \langle C\rangle$$

and set

$$H^C = H_1(M;\mathbb{Z})^C \,/_{\text{torsion}}. \tag{4.2}$$

Every free abelian quotient H' of $H_1(M;\mathbb{Z})$ is equal to H^C for some finite collection C of dual cycles. Below we supress C from notation, but we regularly use the notation H^C and $\mathcal{T}^C$ later in the text.

Let Υ be a spanning tree of Γ. Denote by F_Υ the subset of F consisting of triangles dual to the edges *not* in Υ. We call the elements of F_Υ the *non-tree edges*, and elements of $F - F_\Upsilon$ — the *tree edges*. Recall the branch equations matrix (2.3)

$$B : \mathbb{Z}^E \to \mathbb{Z}^F$$

associated to $(\mathcal{T}, \alpha)$. Let

$$B_\Upsilon : \mathbb{Z}^E \to \mathbb{Z}^{F_\Upsilon}$$

be the matrix obtained from B by deleting the rows corresponding to the tree edges.

Denote by $\mathcal{D}_\Upsilon$ the 2-complex obtained from $\mathcal{D}$ by contracting Υ to a point. Then B_Υ is the boundary map from the 2-chains to the 1-chains of $\mathcal{D}_\Upsilon$. Thus $H_1(\mathcal{D}_\Upsilon;\mathbb{Z})$, and hence $H_1(M;\mathbb{Z})$, is isomorphic to the cokernel of B_Υ. It follows that

$H_1(M;\mathbb{Z})$ is generated by $n+1$ non-tree edges $f_1,\dots,f_{n+1}$ which satisfy n relations $r_1,\dots,r_n$. The group H, that is the maximal free abelian quotient of $H_1(M;\mathbb{Z})$, is isomorphic to

$$\langle f_1,\dots,f_{n+1} \mid r_1,\dots,r_n\rangle \,/_{\text{torsion}}.$$

More generally, let C be a finite collection of dual cycles. Under the contraction $\mathcal{D}\to\mathcal{D}_\Upsilon$ they become simplicial 1-cycles in $\mathcal{D}_\Upsilon$. If we denote them by $c_1,\dots,c_k$ then $H'=H^C$ is isomorphic to

$$\langle f_1,\dots,f_{n+1} \mid r_1,\dots,r_n,c_1,\dots,c_k\rangle \,/_{\text{torsion}}.$$

Suppose that H' is of rank r. Let $(B|C)_\Upsilon$ denote the matrix obtained from B_Υ by augmenting it with the columns $c_1,\dots,c_k$. Let

$$S = U(B|C)_\Upsilon V \tag{4.3}$$

be the Smith normal form of $(B|C)_\Upsilon$. Let $f_1,\dots,f_{n+1}$ denote the elements of F_Υ. The matrix U transforms the basis $(f_1,\dots,f_{n+1})$ of $\mathbb{Z}^{F_\Upsilon}$ to another basis $(\mu_1,\dots,\mu_{n+1})$. The last r rows of both S and $U(B|C)_\Upsilon$ are zero, therefore $\{\mu_{n-r+2},\dots,\mu_{n+1}\}$ are simplicial 1-cycles in $\mathcal{D}_\Upsilon$ whose images under the projection $\mathbb{Z}^{F_\Upsilon}\to H'$ form a basis of H'. For brevity, we say that $(\mu_{n-r+2},\dots,\mu_{n+1})$ is a basis of H'.

The consecutive entries of the i-th column of U give the coefficients of f_i expressed as a linear combination of $(\mu_1,\dots,\mu_{n+1})$. Since $\mu_1,\dots,\mu_{n-r+1}$ are 0 in H', it follows that the last r entries of the i-th column of U correspond to the H'-pairing of f_i written in terms of the basis $(\mu_{n-r+2},\dots,\mu_{n+1})$ of H'.

On the other hand, the coefficients of μ_i expressed as a linear combination of $(f_1,\dots,f_{n+1})$ are equal to the consecutive entries of the i-th column of U^{-1}. Therefore the last r columns of the matrix U^{-1} give a representation of the basis elements of H' as simplicial 1-cycles in $\mathcal{D}_\Upsilon$.

Remark 4.2.2. Adding a non-tree edge $f\in F_\Upsilon$ to the tree Υ creates a unique cycle $\zeta(f)$ in the subgraph $f\cup\Upsilon$ of Γ. The H'-pairing of f is equal to the image of the homology class of $\zeta(f)$ under the epimorphism $H_1(M;\mathbb{Z})\to H'$.

Definition 4.2.3. The dual cycles $\{\zeta(f)\mid f\in F_\Upsilon\}$ are called the *non-tree cycles*.

Remark 4.2.4. The H'-pairings for $f\in F-F_\Upsilon$ are all trivial because tree edges correspond to contractible cycles contained in the tree Υ.

Remark. All computations presented in this section can be easily generalised to ideal triangulations which are not transverse taut. The only benefit of having a

transverse taut structure is that we get a canonical choice of orientation on the edges of the dual graph.

4.2.4 Algorithm `FacePairings`

We give the algorithm `FacePairings` which lays a foundation for all other algorithms given in this thesis. It performs computations discussed in Subsection 4.2.3 to find the projection $\mathbb{Z}^F \to H'$ which sends a dual cycle to the image of its homology class under $H_1(M;\mathbb{Z}) \to H'$. A free abelian quotient H' is specified by a finite collection C of dual cycles as in (4.2).

In this algorithm by `SpanningTree` we denote an algorithm which takes as an input an ideal triangulation $\mathcal{T} = (T, F, E)$, fixes a spanning tree Υ of its dual graph, and returns the subset of F consisting of triangles dual to the edges Υ. There are standard algorithms to find spanning trees of finite graphs, so we do not include pseudocode here.

Algorithm 1. `FacePairings`
Encoding the triangulation of a free abelian cover

Input:

- A transverse taut triangulation $(\mathcal{T}, \alpha)$ of a cusped 3-manifold M with n ideal tetrahedra, $\mathcal{T} = (T, F, E)$
- A list C of dual cycles of $(\mathcal{T}, \alpha)$
- Optional: return type = "matrix"

Output:

- Default: a tuple of $2n$ face Laurents encoding the triangulation $\mathcal{T}^C$ of a free abelian cover of M with the deck group isomorphic to H^C
- If return type = "matrix": a pair (U, r) where r is the rank of H^C and U is as in (4.3)

1: $B :=$ the branch equations matrix of $(\mathcal{T}, \alpha)$ # $2n \times n$ integer matrix
2: $B := B$.AddColumns(C)
3: $Y :=$ `SpanningTree`($\mathcal{T}$)
4: NonTree $:= F - Y$
5: $B := B$.DeleteRows(Y) # $(n+1) \times n$ integer matrix
6: $S, U, V :=$ SmithNormalForm(B) # $S = UBV$
7: $r :=$ the number of zero rows of S

continued on the next page

Algorithm `FacePairings` continued

if return type = "matrix" **then**
    return U, r
else
    $\mathcal{H}$:= the zero matrix with r rows and columns indexed by elements of F
    for f in NonTree **do**
        column $\mathcal{H}(f)$:= the last r entries of the column $U(f)$
    end for
    FaceLaurents:= the tuple of zero Laurent polynomials, indexed by F
    for f in F **do**
        FaceLaurents$(f) := u^{\mathcal{H}(f)}$ # $u = (u_1, \ldots, u_r)$ and $u^v = u_1^{v_1} \cdots u_r^{v_r}$
    end for
    return FaceLaurents
end if

Remark 4.2.5. We can ensure that the algorithm `FacePairings` is deterministic. That is, if we do not permute ideal simplices of $\mathcal{T}$, nor change the order of dual cycles in C, the output of `FacePairings`$((\mathcal{T}, \alpha), C)$ is always the same.

4.3 Polynomial invariants of 3-manifolds

As we shall see in Chapters 5, 6, 9 and 12, the definitions of the taut, the veering, the Alexander and the Teichmüller polynomials all follow the same pattern. Namely, they are derived from Fitting ideals of certain modules associated to the maximal free abelian cover of a 3-manifold. For this reason in this section we recall definitions of Fitting ideals and their invariants.

Let H be a finitely generated free abelian group. Let $\mathcal{M}$ be a finitely presented module over $\mathbb{Z}[H]$. Then there exist integers $k, l \in \mathbb{N}$ and an exact sequence

$$\mathbb{Z}[H]^k \xrightarrow{A} \mathbb{Z}[H]^l \longrightarrow \mathcal{M} \longrightarrow 0$$

of $\mathbb{Z}[H]$-homomorphisms called a *free presentation* of $\mathcal{M}$. The matrix of A, written in terms of any bases of $\mathbb{Z}[H]^k$ and $\mathbb{Z}[H]^l$, is called a *presentation matrix* for $\mathcal{M}$.

Definition 4.3.1. [46, Section 3.1] Let $\mathcal{M}$ be a finitely presented $\mathbb{Z}[H]$-module with a presentation matrix A of dimension $l \times k$. We define the i-th *Fitting ideal* $\mathrm{Fit}_i(\mathcal{M})$ of $\mathcal{M}$ to be the ideal in $\mathbb{Z}[H]$ generated by $(l-i) \times (l-i)$ minors of A.

In particular $\mathrm{Fit}_i(\mathcal{M}) = \mathbb{Z}[H]$ for $i \geq l$, as the determinant of the empty matrix equals 1, and $\mathrm{Fit}_i(\mathcal{M}) = 0$ for $i < 0$ or $i < l - k$. The Fitting ideals are

independent of the choice of a free presentation for $\mathcal{M}$ [46, p. 58].

Remark. Fitting ideals are called *determinantal ideals* in [57] and *elementary ideals* in [12, Chapter VIII].

The ring $\mathbb{Z}[H]$ is not a principal ideal domain, but it is a GCD domain [12, p. 117]. Therefore for any finitely generated ideal $I \subset \mathbb{Z}[H]$ there exists a unique minimal principal ideal $\overline{I} \subset \mathbb{Z}[H]$ which contains it. The ideal $\overline{I}$ is generated by the greatest common divisor of the generators of I [12, p. 118]. This motivates the following definition.

Definition 4.3.2. Let $\mathcal{M}$ be a finitely presented $\mathbb{Z}[H]$-module. We define the i-th *Fitting invariant* of $\mathcal{M}$ to be the greatest common divisor of elements of $\mathrm{Fit}_i(\mathcal{M})$. When $\mathrm{Fit}_i(\mathcal{M}) = (0)$ we set the i-th Fitting invariant of $\mathcal{M}$ to be equal to 0.

Note that Fitting invariants are well-defined only up to a unit in $\mathbb{Z}[H]$. Therefore all equalities proved in this thesis hold only up to a unit in the appropriate integral group ring.

Chapter 5

The taut polynomial

Let $\mathcal{V} = (\mathcal{T}, \alpha, \nu)$ be a veering triangulation of a 3-manifold M, with the set T of tetrahedra, the set F of 2-dimensional faces and the set E of edges. Recall that

$$H = H_1(M;\mathbb{Z})\,/_{\text{torsion}}.$$

Following [38, Section 3] we define the *upper taut module* $\mathcal{E}^{\uparrow}_{\alpha}(\mathcal{V})$ of $\mathcal{V}$ by the presentation

$$\mathbb{Z}[H]^F \xrightarrow{D^{\uparrow}} \mathbb{Z}[H]^E \longrightarrow \mathcal{E}^{\uparrow}_{\alpha}(\mathcal{V}) \longrightarrow 0. \tag{5.1}$$

The definition of $D^{\uparrow}$ depends on the upper track of $\mathcal{V}$, as explained below.

Let $\tau^{\uparrow ab}$ be the upper track of the veering triangulation $\mathcal{V}^{ab}$ of M^{ab}. Consider the restriction of $\tau^{\uparrow ab}$ to $1 \cdot f \in H \cdot F$; see Figure 5.1. This train track determines a *switch relation* between its three half-branches: the large half-branch is equal to the sum of the two small half-branches. By identifying the half-branches with the edges in the boundary of $1 \cdot f$ which they meet, we obtain a switch relation between the edges in the boundary of $1 \cdot f$.

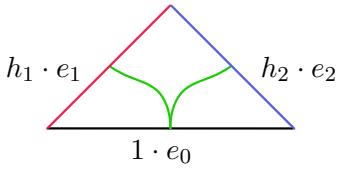

Figure 5.1: The upper track in a triangle determines the switch relation $1 \cdot e_0 = h_1 \cdot e_1 + h_2 \cdot e_2$ between the edges in its boundary.

We rearrange the switch relation of $1 \cdot f$ into a linear combination of edges from $H \cdot E$. This linear combination is the value of $D^{\uparrow}$ at $1 \cdot f$. For example, the

image of the triangle presented in Figure 5.1 under $D^{\uparrow}$ is equal to

$$1 \cdot e_0 - h_1 \cdot e_1 - h_2 \cdot e_2 \in \mathbb{Z}[H]^E.$$

The *upper taut polynomial* $\Theta^{\uparrow}_{\mathcal{V}}$ is defined as the zeroth Fitting polynomial of $\mathcal{E}^{\uparrow}_{\alpha}(\mathcal{V})$. In other words

$$\Theta^{\uparrow}_{\mathcal{V}} = \gcd\left\{\text{maximal minors of } D^{\uparrow}\right\}.$$

We can analogously define the *lower taut module* $\mathcal{E}^{\downarrow}_{\alpha}(\mathcal{V})$ with the presentation matrix $D^{\downarrow}$ which assigns to $1 \cdot f \in H \cdot F$ the switch equation of $\tau^{\downarrow ab}$ in $1 \cdot f$. Then the *lower taut polynomial* $\Theta^{\downarrow}_{\mathcal{V}}$ is the greatest common divisor of the maximal minors of $D^{\downarrow}$.

Remark. The subscript α in $\mathcal{E}^{\uparrow}_{\alpha}$, $\mathcal{E}^{\downarrow}_{\alpha}$ reflects the fact that to define these modules we just need a transverse taut structure α on the triangulation. This is because the upper and lower tracks exist in transverse taut triangulations even when they are not veering; see Definition 2.4.3.

We, however, consider only the taut polynomials of veering triangulations. In our proofs we rely on the veering structure. For example, in Proposition 5.1.1 we use Lemma 2.5.2 and in Lemma 5.2.1 we use Lemma 2.4.6.

5.1 Only one taut polynomial

At the beginning of this chapter we defined two taut polynomials. In this section we prove that they are in fact equal up to a unit in $\mathbb{Z}[H]$.

Proposition 5.1.1. *Let $\mathcal{V}$ be a veering triangulation. The lower taut module of $\mathcal{V}$ is isomorphic to the upper taut module of $\mathcal{V}$. Hence*

$$\Theta^{\downarrow}_{\mathcal{V}} = \Theta^{\uparrow}_{\mathcal{V}}$$

up to a unit in $\mathbb{Z}[H]$.

Proof. Let $1 \cdot f \in H \cdot F$ be a red triangle of $\mathcal{V}^{ab}$. By Lemma 2.5.2 the tetrahedron immediately below $1 \cdot f$ has a red top diagonal t and the tetrahedron immediately above $1 \cdot f$ has a red bottom diagonal r, for some $t, r \in H \cdot E$. We have

$$D^{\downarrow}(1 \cdot f) = t - r - l$$
$$D^{\uparrow}(1 \cdot f) = r - t - l$$

for some $l \in H \cdot E$, so the signs of the two red edges of f are interchanged. A similar statement is true for blue triangles: the images of $D^{\downarrow}$ and $D^{\uparrow}$ on them differ by swapping the signs of the two blue edges.

If we multiply all columns of $D^{\downarrow}$ corresponding to red triangles of $\mathcal{V}$ by -1, and all rows corresponding to blue edges by -1, we obtain the matrix $D^{\uparrow}$. Hence the maximal minors of $D^{\downarrow}$ and $D^{\uparrow}$ differ at most by a sign. □

Thus from now on we only write about the *taut polynomial* $\Theta_{\mathcal{V}}$ and the taut module $\mathcal{E}_{\alpha}(\mathcal{V})$.

Corollary 5.1.2. *The taut polynomials of* $(\mathcal{T}, \alpha, \nu)$, $(\mathcal{T}, -\alpha, \nu)$, $(\mathcal{T}, \alpha, -\nu)$ *and* $(\mathcal{T}, -\alpha, -\nu)$ *are equal.*

Proof. This follows from Proposition 5.1.1 and Remark 2.4.8. □

5.2 Reducing the number of relations

Suppose that $\mathcal{V}$ consists of n tetrahedra. The original definition of the taut polynomial requires computing $\binom{2n}{n} > 2^n$ minors of $D^{\uparrow}$, which is an obstacle for efficient computation. However, the relations satisfied by the generators of the taut module are not linearly independent. In this subsection we give a recipe to systematically eliminate $n-1$ relations.

The following lemma follows from [38, Lemma 3.2]. We include its proof, because it is important in Proposition 5.2.3.

Lemma 5.2.1. *Let* $\mathcal{V}$ *be a veering triangulation. Each tetrahedron* $t \in T$ *induces a linear dependence between the columns of* $D^{\uparrow}$ *corresponding to the triangles in the boundary of* t.

Proof. Suppose that $1 \cdot t$ has red equatorial edges r_1, r_2, blue equatorial edges l_1, l_2, bottom diagonal d_b and top diagonal d_t, where $r_1, r_2, l_1, l_2,\ d_b, d_t \in H \cdot E$. Such a tetrahedron is illustrated in Figure 5.2.

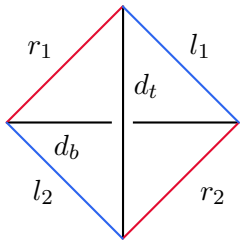

Figure 5.2: Edges of the tetrahedron $1 \cdot t$ of $\mathcal{V}^{ab}$.

Let $f_1,\ f_2 \in H \cdot F$ be two bottom triangles of $1 \cdot t$ such that

$$D^{\uparrow}(f_1) = d_b - r_1 - l_1$$
$$D^{\uparrow}(f_2) = d_b - r_2 - l_2.$$

For $i = 1, 2$ denote by f_i' the top triangle of $1 \cdot t$ such that f_i' and f_i are adjacent in $1 \cdot t$ along the upper large edge of f_i'.

By Lemma 2.4.6 the upper large edges of f_i''s are the equatorial edges of $1 \cdot t$ which are of the same colour as the top diagonal of $1 \cdot t$; see also Figure 2.7. Therefore

$$D^{\uparrow}(f_1 + f_1') = D^{\uparrow}(f_2 + f_2') = d_b - d_t - s_1 - s_2$$

where $(s_1, s_2) = \begin{cases} (r_1, r_2) & \text{if } d_t \text{ is blue} \\ (l_1, l_2) & \text{if } d_t \text{ is red.} \end{cases}$ □

Remark 5.2.2. Lemma 5.2.1 does not hold for transverse taut triangulations which do not admit a veering structure. One can check that if the upper large edges of the top faces of a tetrahedron t are not the opposite equatorial edges of t, then no nontrivial linear combination of the images of faces of t under $D^{\uparrow}$ gives zero.

Let Υ be a spanning tree of the dual graph of $\mathcal{V}$. Recall that by F_Υ we denote the subset of triangles which are dual to the edges of Γ which are not in Υ (non-tree edges). We define a $\mathbb{Z}[H]$-module homomorphism

$$D^{\uparrow}_{\Upsilon} : \mathbb{Z}[H]^{F_\Upsilon} \to \mathbb{Z}[H]^{E}$$

obtained from $D^{\uparrow}$ by deleting the columns corresponding to the edges of Υ.

Proposition 5.2.3. *Let $\mathcal{V}$ be a veering triangulation and let Υ be a spanning tree of its dual graph Γ. The image of $D^{\uparrow}$ and that of $D^{\uparrow}_{\Upsilon}$ are equal.*

Proof. We say that a dual edge $h \cdot f \in H \cdot F$ is a *linear combination of dual edges* $h_{i_1} \cdot f_{i_1}, h_{i_2} \cdot f_{i_2}, \ldots, h_{i_k} \cdot f_{i_k} \in H \cdot F$, or *in the span of* these edges, if $D^{\uparrow}(h \cdot f)$ is a linear combination with $\mathbb{Z}[H]$ coefficients of $D^{\uparrow}(h_{i_1} \cdot f_{i_1})$, $D^{\uparrow}(h_{i_2} \cdot f_{i_2}), \ldots, D^{\uparrow}(h_{i_k} \cdot f_{i_k})$. It is enough to prove that every tree edge is in the span of non-tree edges.

By Lemma 5.2.1 each tree edge $h \cdot f \in H \cdot F$ is a linear combination of three dual edges that share a vertex with $h \cdot f$. In particular, the terminal edges of Υ — there are at least two of them — are in the span of non-tree edges. Now consider a subtree Υ' obtained from Υ by deleting its terminal edges. The terminal edges of Υ' can be expressed as linear combinations of non-tree edges and terminal edges of Υ,

hence as linear combinations of non-tree edges only. Since Υ is finite, we eventually exhaust all its edges. □

Corollary 5.2.4. *Let Υ be a spanning tree of the dual graph Γ of a veering triangulation $\mathcal{V}$. The taut polynomial $\Theta_{\mathcal{V}}$ is equal to the greatest common divisor of the maximal minors of the matrix $D^{\uparrow}_{\Upsilon}$.*

Proof. By Proposition 5.2.3 we obtain another presentation for the taut module

$$\mathbb{Z}[H]^{F_\Upsilon} \xrightarrow{D^{\uparrow}_{\Upsilon}} \mathbb{Z}[H]^{E} \longrightarrow \mathcal{E}_{\alpha}(\mathcal{V}) \longrightarrow 0.$$

Since Fitting invariants of a finitely presented module do not depend on a chosen presentation [46, p. 58], the greatest common divisor of the maximal minors of $D^{\uparrow}_{\Upsilon}$ is equal to the taut polynomial of $\mathcal{V}$. □

5.3 Algorithm `TautPolynomial`

In this subsection we present pseudocode for an algorithm which takes as an input a veering triangulation $\mathcal{V}$ and outputs the taut polynomial $\Theta_{\mathcal{V}}$ of $\mathcal{V}$.

In Chapter 7 we follow the algorithm `TautPolynomial` applied to the veering triangulation `cPcbbbiht_12` of the figure-eight knot complement.

Algorithm 2. `TautPolynomial`
Computation of the taut polynomial of a veering triangulation

Input: A veering triangulation $\mathcal{V}$ with the set T of tetrahedra, the set F of triangular faces and the set E of edges

Output: The taut polynomial $\Theta_{\mathcal{V}}$

```
1:  Pairing := FacePairings(V, [ ])                    # Face Laurents encoding V^ab
2:  D := the zero matrix with rows indexed by E and columns by F
3:  for e in E do
4:      L := list of triangles on the left of e, ordered from the top to the bottom
5:      R := list of triangles on the right of e, ordered from the top to the bottom
6:      for A in {L, R} do
7:          CurrentCoefficient := 1                    # Counting from 1, not 0
8:          add CurrentCoefficient to the entry (e, A[1]) of D
9:          for i from 2 to length(A) do               # Inclusive
10:             CurrentCoefficient := CurrentCoefficient·Pairing(A[i − 1])
11:             subtract CurrentCoefficient from the entry (e, A[i]) of D
12:         end for
```

continued on the next page

Algorithm `TautPolynomial` continued

13: **end for**
14: **end for**
15: $Y :=$ `SpanningTree`(Y)
16: $D_Y := D$.DeleteColumns(Y) # Accelerate the computation
17: minors $:= D_Y$.minors$(|E|)$
18: **return** gcd(minors)

Proposition 5.3.1. *The output of* `TautPolynomial` *applied to a veering triangulation* $\mathcal{V}$ *is equal to the taut polynomial* $\Theta_{\mathcal{V}}$ *of* $\mathcal{V}$*.*

Proof. The output `FacePairings`$(\mathcal{V}, [\,])$ is a list of face Laurents encoding the triangulation $\mathcal{V}^{ab}$. First note that $1 \cdot f \in H \cdot F$ has $h \cdot e$ in its boundary, for some $e \in E$, $h \in H$, if and only if $h^{-1} \cdot f$ is attached to $1 \cdot e$. Using this "dual" approach we fill in the rows of the presentation matrix $D^{\uparrow}$ for the taut module. Each for loop, starting at line 3 of the algorithm, is responsible for filling one row.

By our conventions for labelling the triangles of $\mathcal{V}^{ab}$ established in Section 4.1 the uppermost triangles attached to $1 \cdot e$ have the H-coefficient equal to 1. Then the H-coefficients of the consecutive (from the top) triangles attached to $1 \cdot e$ are obtained by multiplying the H-coefficient of the previous triangle by the *inverse* of its H-pairing. This explains line 10 of the algorithm. We do not invert H-pairings because of the duality mentioned at the beginning of this proof.

Since $1 \cdot e$ is the upper large edge only in the two uppermost triangles attached to $1 \cdot e$, we add the coefficients in line 8 and subtract in line 11.

Thus the matrix D on line 15 of the algorithm is equal to the presentation matrix $D^{\uparrow}$ of the taut module $\mathcal{E}_{\alpha}(\mathcal{V})$ as in (5.1). Deleting the tree columns of D, for some spanning tree Υ of the dual graph Γ of $\mathcal{V}$, gives another presentation matrix for the taut module $\mathcal{E}_{\alpha}(\mathcal{V})$ by Corollary 5.2.4. The greatest common divisor of its maximal minors is equal to the zeroth Fitting invariant of $\mathcal{E}_{\alpha}(\mathcal{V})$, that is the taut polynomial $\Theta_{\mathcal{V}}$ of $\mathcal{V}$. □

Chapter 6

The veering polynomials

Let $\mathcal{V} = (\mathcal{T}, \alpha, \nu)$ be a veering triangulation of a 3-manifold M, with the set T of tetrahedra, the set F of triangular faces and the set E of edges. We still use the notation

$$H = H_1(M; \mathbb{Z}) \,/_{\text{torsion}}.$$

In Section 4 of [38] Landry, Minsky and Taylor defined the *flow graph* $\Phi_\mathcal{V}$ of $\mathcal{V}$. In Section 3 of the same paper they defined the *veering polynomial* $V_\mathcal{V}$ of $\mathcal{V}$. These two invariants are closely related: the veering polynomial is the image of the *Perron polynomial* of $\Phi_\mathcal{V}$ under the epimorphism induced by the inclusion of $\Phi_\mathcal{V}$ into M [38, Theorem 4.8]. Similarly as with the taut polynomial, here we explicitly connect $\Phi_\mathcal{V}$ and $V_\mathcal{V}$ with the upper track of $\mathcal{V}$. Thus we call them the *upper flow graph* and the *upper veering polynomial*, and denote them by $\Phi^U_\mathcal{V}$ and $V^U_\mathcal{V}$, respectively. Furthermore, using the lower track of $\mathcal{V}$ we define the lower flow graph $\Phi^L_\mathcal{V}$, and the lower veering polynomial $V^L_\mathcal{V}$.

The aim of this chapter is twofold. First, we show examples of veering triangulations whose upper and lower flow graphs are not isomorphic (Proposition 6.1.1) and whose upper and lower veering polynomials are not equal in $\mathbb{Z}[H] \,/_{\pm H}$ (Proposition 6.3.2). The second aim of this chapter is to present pseudocode for the computation of the upper veering polynomial; see Section 6.3.

6.1 Flow graphs

Landry, Minsky and Taylor defined the *flow graph* $\Phi^\uparrow_\mathcal{V}$ of a veering triangulation $\mathcal{V}$ [38, Subsection 4.3]. The vertices of $\Phi^\uparrow_\mathcal{V}$ are in bijective correspondence with edges $e \in E$. Every tetrahedron $t \in T$ determines three directed edges of $\Phi^\uparrow_\mathcal{V}$:

- from the bottom diagonal of t to the top diagonal of t,

- from the bottom diagonal of t to the equatorial edges of t which have a different colour than the top diagonal of t.

In this thesis we call the obtained graph the *upper flow graph* of $\mathcal{V}$, hence the superscript $\uparrow$. We analogously define the *lower flow graph* $\Phi^{\downarrow}_{\mathcal{V}}$. Its vertices also correspond to the edges of the veering triangulation. Every $t \in T$ determines the following three directed edges of $\Phi^{\downarrow}_{\mathcal{V}}$:

- from the top diagonal of t to the bottom diagonal of t,
- from the top diagonal of t to the equatorial edges of t which have a different colour than the bottom diagonal of t.

Remark. The name flow graph is motivated by the fact that if $\mathcal{V}$ is constructed from a pseudo-Anosov flow Ψ on N then for almost every closed orbit ℓ of Ψ there is a directed cycle in $\Phi^{\uparrow}_{\mathcal{V}}$ which, after embedding $\Phi^{\uparrow}_{\mathcal{V}}$ in N, is homotopic to ℓ. Only finitely many orbits and their multiples are exceptions to this statement. If ℓ is such an exceptional orbit we can find a directed cycle in $\Phi^{\uparrow}_{\mathcal{V}}$ which is homotopic to ℓ^2 [37].

By computer search we have found that the lower and upper flow graphs are not always isomorphic.

Proposition 6.1.1. *There are veering triangulations whose lower and upper flow graphs are not isomorphic.*

Proof. The first entry of the Veering Census for which the upper and lower flow graphs are not isomorphic is given by the string `hLMzMkbcdefggghhhqxqkc_1221002` which encodes a veering triangulation of the manifold v2898.

The graphs are presented in Figure 6.1. In 6.1(a) there are two vertices of valency 6 (labelled 4 and 6) which are joined to a vertex of valency 10 (labelled 0), while in 6.1(b) there is only one vertex of valency 6 (labelled 6) which is joined to a vertex of valency 10 (labelled 0). Hence the graphs are not isomorphic. □

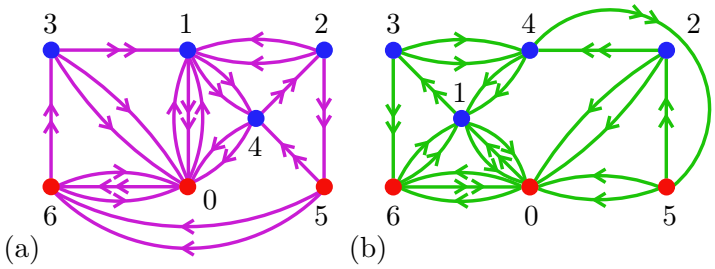

Figure 6.1: Flow graphs of `hLMzMkbcdefggghhhqxqkc_1221002`. Edges with double arrows join top diagonals to bottom diagonals of tetrahedra, or vice versa.

6.2 Veering polynomials

Let $\mathcal{V}$ be a veering triangulation. The matrix $D^{\uparrow}$ assigns to the faces of a tetrahedron the set of four relations between its edges. By Lemma 5.2.1, we can group these triangles into pairs such that $D^{\uparrow}$ evaluated on each pair equals

$$d_b - d_t - s_1 - s_2, \tag{6.1}$$

where d_t, d_b denote the top end the bottom diagonals of the tetrahedron, respectively, and s_1, s_2 — its two equatorial edges of a different colour than d_t.

Following [38] we use this fact to define a $\mathbb{Z}[H]$-module homomorphism

$$K^{\uparrow} : \mathbb{Z}[H]^T \to \mathbb{Z}[H]^E \tag{6.2}$$

assigning to each tetrahedron of the veering triangulation $\mathcal{V}^{ab}$ a linear combination (6.1) of its edges. We call the cokernel of $K^{\uparrow}$ the *upper veering module* and denote it by $\mathcal{E}^{\uparrow}_{\alpha,\nu}(\mathcal{V})$. The subscripts α, ν reflect the fact that to define this module one needs both the transverse taut structure α and the colouring ν on $\mathcal{V}$.

Definition 6.2.1. The *upper veering polynomial* $V^{\uparrow}_{\mathcal{V}}$ is the determinant of $K^{\uparrow}$.

That is, the upper veering polynomial is the zeroth Fitting invariant of the upper veering module. Analogously, the *lower veering polynomial* $V^{\downarrow}_{\mathcal{V}}$ is the determinant of the map $K^{\downarrow}$ which assigns to a tetrahedron with the top diagonal d_t, the bottom diagonal d_b and equatorial edges w_1, w_2 of a different colour than d_b the linear combination

$$d_t - d_b - w_1 - w_2.$$

Remark 6.2.2. In [38, Section 3] the (upper) veering polynomial is well-defined as an element of $\mathbb{Z}[H]$, and not just up to a unit. This is accomplished by identifying a tetrahedron of $\mathcal{V}^{ab}$ with its bottom diagonal. Then the map $K^{\uparrow}$ has $\mathbb{Z}[H]^E$ as both the domain and codomain. The upper veering polynomial $V_{\mathcal{V}}^{\uparrow}$ is then equal to the determinant of $K^{\uparrow}$, where the basis for the domain and codomain is chosen to be the same. By our conventions for labelling ideal simplices of $\mathcal{V}^{ab}$ established in Section 4.1 the bases for $\mathbb{Z}[H]^T \cong \mathbb{Z}[H]^E$ differ at most by a permutation (and not by multiplying by elements of H).

For the lower veering polynomial we identify a tetrahedron of $\mathcal{V}^{ab}$ with its top diagonal.

6.3 Algorithm `UpperVeeringPolynomial`

In this section we present pseudocode for an algorithm which takes as an input a veering triangulation and returns its upper veering polynomial. In Chapter 7 we follow this algorithm applied to the veering triangulation `cPcbbbiht_12` of the figure-eight knot complement.

Algorithm 3. `UpperVeeringPolynomial`
Computation of the upper veering polynomial

Input: A veering triangulation $\mathcal{V}$, with the set T of tetrahedra, the set F of triangular faces and the set E of edges

Output: The upper veering polynomial $V_{\mathcal{V}}^{\uparrow}$ of $\mathcal{V}$

permute the elements of T so that $E[i]$ is the bottom diagonal of $T[i]$
Pairing := `FacePairings`$(\mathcal{V}, [\,])$ # Face Laurents encoding $\mathcal{V}^{ab}$
K := the zero matrix with rows indexed by E and columns by T
for e in E **do**
    L := triangles on the left of e, ordered from the top to the bottom
    R := triangles on the right of e, ordered from the top to the bottom
    TT := tetrahedron immediately above $L[1]$ # Counting from 1, not 0
    add 1 to the entry (e, TT) of K
    BT := tetrahedron immediately below $L[\text{length}(L)]$
    BottomCoefficient:= $\prod_{i=1}^{\text{length}(L)} \text{Pairing}(L[i])$
    subtract BottomCoefficient from the entry (e, BT) of K
    for A in $\{L, R\}$ **do**
        CurrentCoefficient := 1

continued on the next page

Algorithm `UpperVeeringPolynomial` continued

```
14:         for i from 1 to length(A)−1 do          # Inclusive, counting from 1, not 0
15:             T := tetrahedron immediately below A[i]
16:             CurrentCoefficient := CurrentCoefficient·Pairing(A[i])
17:             if i > 1 then
18:                 subtract CurrentCoefficient from the entry (e, T) of K
19:             end if
20:         end for
21:     end for
22: end for
23: return determinant of K
```

Proposition 6.3.1. *The output of* `UpperVeeringPolynomial` *applied to a veering triangulation $\mathcal{V}$ is equal to the upper veering polynomial of $\mathcal{V}$.*

Proof. We claim that the matrix K on line 22 of the algorithm is equal to $K^{\uparrow}$ as in (6.2). Hence its determinant is equal to the upper veering polynomial of $\mathcal{V}$. The proof is similar to that of Proposition 5.3.1. The main difference here is that when we explore an edge $e \in E$ we do not take into account all tetrahedra attached to it, but only the one immediately below e, immediately above e and the ones on the sides of e which have the top diagonal of a different colour than e. However, by Corollary 2.5.3 we know that the only tetrahedra on the sides of e whose top diagonal has the same colour as e are the two uppermost side tetrahedra of e. This explains line 17 of `UpperVeeringPolynomial`.

Line 1 of `UpperVeeringPolynomial` ensures that the polynomial is correctly computed not only up to a sign; see Remark 6.2.2. □

An analogous algorithm can be written for the lower veering polynomial. Alternatively, by Remark 2.4.8 to compute the upper veering polynomial of $(\mathcal{T}, \alpha, \nu)$ we can apply `UpperVeeringPolynomial` to the triangulation $(\mathcal{T}, -\alpha, \nu)$.

Using an implementation of `UpperVeeringPolynomial` we have found that the upper veering polynomial is not invariant under reversing a transverse taut veering structure via $(\alpha, \nu) \mapsto (-\alpha, -\nu)$.

Proposition 6.3.2. *There are veering triangulations whose upper and lower veering polynomials are not equal up to a unit in $\mathbb{Z}[H]$.*

Proof. The first entry of the Veering Census for which we have $V_{\mathcal{V}}^{L} \neq V_{\mathcal{V}}^{U}$ in $\mathbb{Z}[H]/\pm H$ is given by the string `iLLLAQccdffgfhhhqgdatgqdm_21012210`. It encodes a veering

triangulation of the 3-manifold t10133. Its lower and upper veering polynomials are up to a unit equal to

$$(1-u)^{-1}(1-u^{25})(1-u^{13})$$
$$(1-u+u^2-u^3+u^4-u^5+u^6)(1-u^2-u^7-u^{12}+u^{14})$$

and

$$(1-u)^{-1}(1-u^{29})(1-u^{9})$$
$$(1-u+u^2-u^3+u^4-u^5+u^6)(1-u^2-u^7-u^{12}+u^{14}).$$

Their greatest common divisor

$$(1-u+u^2-u^3+u^4-u^5+u^6)(1-u^2-u^7-u^{12}+u^{14})$$

is equal to the taut polynomial $\Theta_{\mathcal{V}}$ of $\mathcal{V}$. □

Remark 6.3.3. The flow graphs of the triangulation from the proof of Proposition 6.3.2 are not isomorphic. In fact, one of them is planar, and the other is not.

Remark 6.3.4. In the proof of Proposition 6.1.1 we showed that the upper and lower flow graphs of the veering triangulation `hLMzMkbcdefggghhhqxqkc_1221002` of the manifold v2898 are not isomorphic. However, its lower and upper veering polynomial are both (up to a unit) equal to

$$(1+u)(1-20u+u^2).$$

There are even veering triangulations for which one veering polynomial vanishes and the other does not.

Example 6.3.5. The entry `lLLLAPAMcbcfeggihijkktshhxfpikaqj_20102220020` of the Veering Census encodes a veering triangulation whose upper veering polynomial vanishes, but

$$V_{\mathcal{V}}^{\downarrow} = (u-1)^2(u+1)^3(u^2-u+1)(u^4+1).$$

Remark 6.3.6. By the results of Landry, Minsky and Taylor the taut polynomial divides the upper veering polynomial [38, Theorem 6.1 and Remark 6.18] and hence also the lower veering polynomial. The remaining factor of the upper/lower veering polynomial is called the upper/lower *AB-polynomial*. It is related to a special family

of cycles in the dual graph of the veering triangulation, called the upper/lower *AB-cycles* [38, Section 4]. We refer the reader to [38, Subsection 6.1] to find out the formula for the upper AB-polynomial.

If $\Theta_{\mathcal{V}} \neq 0$ and $V_{\mathcal{V}}^{\uparrow} = 0$ ($V_{\mathcal{V}}^{\downarrow} = 0$), then $\mathcal{V}$ has an upper (lower) AB-cycle of even length whose homology class is either trivial or torsion.

In Corollary 7.3 of [38] Landry, Minsky and Taylor proved than when $\mathcal{V}$ is layered and the first Betti number of the underlying manifold is at least 2 we can compute the taut polynomial of $\mathcal{V}$ using the following formula

$$\Theta_{\mathcal{V}} = \frac{V_{\mathcal{V}}^{\uparrow}}{\text{upper AB-polynomial.}} \tag{6.3}$$

This works because the AB-polynomial of a layered triangulation never vanishes [38, Corollary 7.3].

The AB-polynomial can be computed using a square matrix. Hence, by using (6.3) we would avoid computing multiple minors and their greatest common divisor. However, as Example 6.3.5 illustrates, this method is not general and cannot be applied to nonlayered veering triangulations. In Section 15.2 we discuss how considering the *veering torsion* could give us another way of computing the taut polynomial which avoids dealing with multiple minors.

Chapter 7

Example: polynomial invariants of `cPcbbbiht_12`

In this chapter we follow algorithms `TautPolynomial` (Alg. 2) and `UpperVeering Polynomial` (Alg. 3) on the veering triangulation `cPcbbbiht_12` of the figure-eight knot complement.

7.1 Triangulation of the maximal free abelian cover

Let $\mathcal{V}$ denote the veering triangulation `cPcbbbiht_12` of the figure-eight knot complement. We do not include a picture of tetrahedra of this triangulation, because they can be reconstructed from Figure 7.1 and this figure is more useful for our purposes.

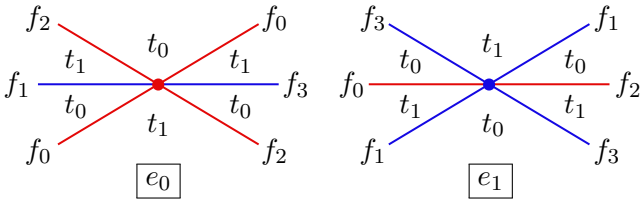

Figure 7.1: Cross-sections of the neighbourhoods of edges e_0, e_1 of $\mathcal{V}$. The colours of edges and triangles are indicated.

First we follow the algorithm `FacePairings` (Alg. 1) to encode the triangulation $\mathcal{V}^{ab}$ of the maximal free abelian cover of the figure-eight knot complement. Figure 7.1 shows triangles attached to the edges e_0, e_1 of $\mathcal{V}$. It allows us to find the

branch equations matrix B of $\mathcal{V}$:

$$B = \begin{array}{c} \\ f_0 \\ f_1 \\ f_2 \\ f_3 \end{array} \begin{array}{c} \begin{array}{cc} e_0 & e_1 \end{array} \\ \begin{bmatrix} 0 & 1 \\ 1 & 0 \\ 0 & -1 \\ -1 & 0 \end{bmatrix} \end{array}.$$

Again using Figure 7.1 we draw the dual graph Γ of $\mathcal{V}$. It is presented in Figure 7.2. As a spanning tree Υ of Γ we choose $\{f_0\}$. The matrix B_Υ is obtained

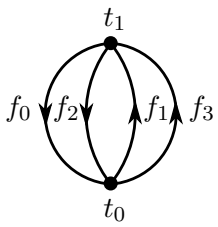

Figure 7.2: The dual graph of `cPcbbbiht_12`.

from B by deleting its first row, corresponding to f_0. Let S be the Smith normal form of B_Υ. It satisfies $S = UB_\Upsilon V$, where

$$U = \begin{array}{c} \begin{array}{ccc} f_1 & f_2 & f_3 \end{array} \\ \begin{bmatrix} -1 & 0 & 0 \\ 0 & 1 & 0 \\ 1 & 0 & 1 \end{bmatrix} \end{array}.$$

Since S is of rank 2, the face Laurents of the non-tree edges are determined by the last row of U. All face Laurents for $\mathcal{V}$ relative to the fundamental domain determined by $\Upsilon = \{f_0\}$ are listed in Table 7.1.

face	f_0	f_1	f_2	f_3
face Laurent	1	u	1	u

Table 7.1: The face Laurents encoding $\mathcal{V}^{ab}$.

Using Table 7.1 and Figure 7.1 we draw triangles and tetrahedra attached to the edges $1 \cdot e_0$ and $1 \cdot e_1$ of $\mathcal{V}^{ab}$ in Figure 7.3.

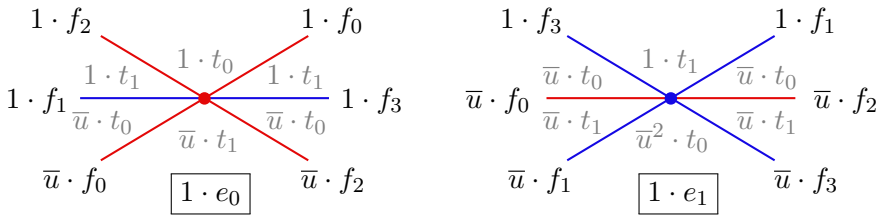

Figure 7.3: Cross-sections of the neighbourhoods of edges $1 \cdot e_0$, $1 \cdot e_1$ of $\mathcal{V}^{ab}$. The colours of edges and triangles are indicated. To not overcrowd the figure we use $\overline{u} = u^{-1}$.

7.2 The taut polynomial

To find the presentation matrix $D^{\uparrow}$ it is enough to know the (inverses of) Laurent coefficients of the triangles attached to $1 \cdot e_0$ and $1 \cdot e_1$. They can be read off from Figure 7.3. Note that $1 \cdot e_i$ is upper large only in its two uppermost triangles. Recall that by Corollary 5.2.4 the taut polynomial of $\mathcal{V}$ is equal to the greatest common divisor of the matrix $D^{\uparrow}_{\Upsilon}$, obtained from $D^{\uparrow}$ by deleting its first column, corresponding to the tree $\Upsilon = \{f_0\}$. We have

$$D^{\uparrow}_{\Upsilon}(u) = \begin{array}{c} \\ e_0 \\ e_1 \end{array} \begin{array}{c} \begin{array}{ccc} f_1 & f_2 & f_3 \end{array} \\ \begin{bmatrix} -1 & 1-u & -1 \\ 1-u & -u & 1-u \end{bmatrix} \end{array}$$

and hence

$$\Theta_{\mathcal{V}} = 1 - 3u + u^2$$

up to a unit in $\mathbb{Z}[u^{\pm 1}]$.

7.3 The upper veering polynomial

To find the presentation matrix $K^{\uparrow}$ it is enough to know the (inverses of) Laurent coefficients of the tetrahedra attached to $1 \cdot e_i$. They can be read off from Figure 7.3. Recall that among side tetrahedra we only take into account the ones which have the top diagonal of a different colour than $1 \cdot e_i$. By Corollary 2.5.3 this boils down to skipping the uppermost tetrahedra. We get

$$K^{\uparrow}(u) = \begin{array}{c} \\ e_0 \\ e_1 \end{array} \begin{array}{c} \begin{array}{cc} t_0 & t_1 \end{array} \\ \begin{bmatrix} 1-2u & -u \\ -u^2 & 1-2u \end{bmatrix} \end{array}.$$

Thus

$$V_{\mathcal{V}}^{\uparrow} = -(u^3 - 4u^2 + 4u - 1).$$

Up to a unit we have

$$V_{\mathcal{V}}^{\uparrow} = (u - 1) \cdot \Theta_{\mathcal{V}}.$$

Chapter 8

Edge-orientable veering triangulations

In this chapter we divide veering triangulations into two classes — *edge-orientable* ones and not *edge-orientable* ones. We describe how to construct the *edge-orientation double cover* of a veering triangulation. We also discuss the *edge-orientation homomorphism* and derive a combinatorial condition which ensures that it factors through a given quotient of $\pi_1(M)$. All these notions are used in Chapter 9, where we prove a relation between the taut polynomial of a veering triangulation and the Alexander polynomial of the underlying manifold.

8.1 Transversely orientable dual tracks

Let $\mathcal{V}$ be a veering triangulation, with the set T of tetrahedra, the set F of triangular faces and the set E of edges. Recall that by $\mathscr{B}$ we denote the horizontal branched surface of $\mathcal{V}$.

Definition 8.1.1. We say that a dual train track $\tau \subset \mathscr{B}$ is *transversely orientable* if there exists a nonvanishing continuous vector field on τ which is tangent to $\mathscr{B}$ and transverse to τ.

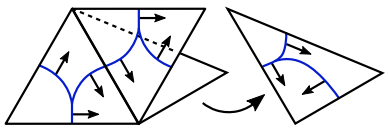

Figure 8.1: A local picture of a transversely oriented dual train track in the horizontal branched surface. For clarity the train track in the bottom triangle is presented separately on the right.

Figure 8.1 presents a local picture of a transversely oriented dual train track. The transverse orientation is indicated by arrows which point in one of the two possible directions.

Remark 8.1.2. Let τ be a dual train track in $\mathscr{B}$ and let $f \in F$. If we fix a transverse orientation on one half-branch of τ_f there is no obstruction to extend it over all half-branches of τ_f. Hence the train track τ_f is always transversely orientable.

Example 8.1.3. Figure 8.2 presents the upper track $\tau^\uparrow$ of the veering triangulation `cPcbbbdxm_10` of the manifold m003, also known as the figure-eight knot sister. The union of two half-branches of $\tau^\uparrow$ in the face f_0 form the core curve of the Möbius band (shaded in yellow). Hence $\tau^\uparrow$ cannot be transversely oriented.

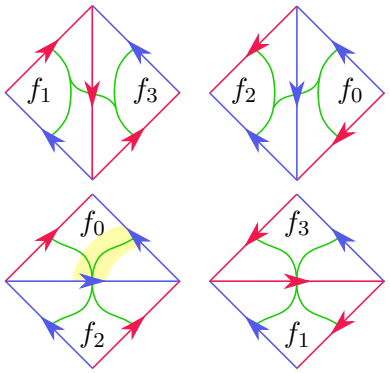

Figure 8.2: The upper track of the veering triangulation $\mathcal{V}$ =`cPcbbbdxm_10` of the figure-eight knot sister. The yellow shaded region is homeomorphic to the Möbius band.

If a dual track is transversely oriented it is often useful to pick the orientation on the edges of the triangulation which agrees with the transverse orientation on the track.

Definition 8.1.4. Suppose that a dual train track τ in the horizontal branched surface of $(\mathcal{T}, \alpha)$ is transversely oriented. The restriction of the transverse orientation to the edge midpoints endows the edges of $\mathcal{T}$ with an orientation. We say that these orientations on edges are *determined* by the transverse orientation on τ.

We divide all veering triangulations into two classes. The division depends on whether their lower/upper track is transversely orientable. First we prove that it does not matter which track we consider.

Lemma 8.1.5. *Let $\mathcal{V}$ be a veering triangulation. The lower track of $\mathcal{V}$ is transversely orientable if and only if the upper track of $\mathcal{V}$ is transversely orientable.*

Proof. Suppose $\tau^{\downarrow}$ is transversely oriented. Pick the orientation on the edges of $\mathcal{V}$ determined by the transverse orientation on $\tau^{\downarrow}$.

By Lemma 2.5.2 for any triangle $f \in F$ the lower large edge of f and the upper large edge of f are different edges of f, but both are of the same colour as f. Figure 8.3 presents the lower and upper tracks in a red and a blue triangle. If we reverse the orientation of all edges of one colour, say blue, then the new orientations determine a transverse orientation on $\tau^{\uparrow}$. □

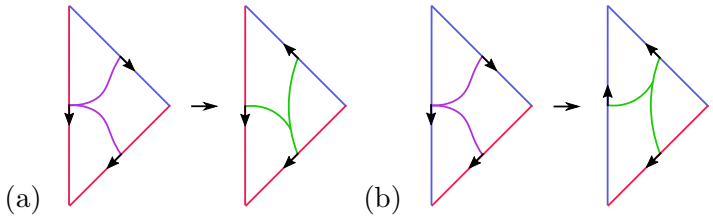

Figure 8.3: Using a transverse orientation on the lower track to find a transverse orientation on the upper track. (a) In red a triangle. (b) In a blue triangle.

Definition 8.1.6. We say that a veering triangulation $\mathcal{V}$ is *edge-orientable* if the upper track of $\mathcal{V}$ is transversely orientable.

By Lemma 8.1.5 a veering triangulation $\mathcal{V}$ is edge-orientable if and only if the lower track of $\mathcal{V}$ is transversely orientable.

Example 8.1.7. Figure 8.2 presents the upper track of the veering triangulation $\mathcal{V}$ = `cPcbbbdxm_10` of the figure-eight knot sister. Since the track is not transversely orientable, $\mathcal{V}$ is not edge-orientable.

Note that the upper track of $\mathcal{V}$ is edge-orientable if and only if the upper branched surface $\mathscr{B}^{\uparrow}$ of $\mathcal{V}$ is transversely orientable. It follows from Theorem 3.4.1 that edge-orientability of a veering triangulation is equivalent to transverse orientability of the stable and unstable laminations of the underlying flow.

Lemma 8.1.8. *Suppose that a veering triangulation $\mathcal{V}$ is constructed from a pseudo-Anosov flow Ψ. Let $\mathscr{L}^s$ denote the stable lamination of Ψ. Then $\mathcal{V}$ is edge-orientable if and only if $\mathscr{L}^s$ is transversely orientable.* □

8.2 The edge-orientation double cover

Let $\mathcal{V}$ be a veering triangulation of a 3-manifold M. Let $\tau = \tau^{\uparrow}$ be the upper track of $\mathcal{V}$. In this section we construct the *edge-orientation double cover* $\mathcal{V}^{or}$ of $\mathcal{V}$.

Definition 8.2.1. Let $f \in F$. Fix a transverse orientation on the upper track τ_f; this is possible by Remark 8.1.2. We say that f is *edge-oriented* if the orientation of the edges in the boundary of f agrees with the orientation determined by the transverse orientation on τ_f; see Figure 8.4.

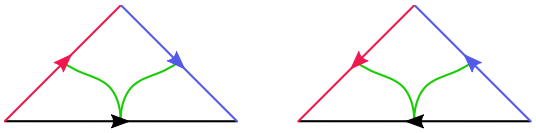

Figure 8.4: Edge-oriented triangles. There are two possibilities depending on the chosen transverse orientation on τ_f.

Naturally, if $\mathcal{V}$ is edge-orientable, then there is a choice of orientations on the edges of $\mathcal{V}$ such that every $f \in F$ is edge-oriented.

In Remark 8.1.2 we noted that every dual train track restricted to a single face of the triangulation is transversely orientable. We are interested in extending this transverse orientation further, not yet over the whole 2-skeleton of the triangulation, but over the four faces of a given tetrahedron. This is not possible for all dual train tracks. But it is possible in the case of the upper and lower tracks of a veering triangulation.

Corollary 8.2.2. *Let $\mathcal{V}$ be a veering triangulation. Fix a tetrahedron $t \in T$ and let $f_i \in F$, $i = 1, 2, 3, 4$ be the four faces of t. Denote by τ_i the restriction $\tau^{\uparrow}_{f_i}$ of the upper track $\tau^{\uparrow}$ of $\mathcal{V}$ to f_i. Then the train track*

$$\tau_t = \bigcup_{i=1}^{4} \tau_i \subset \bigcup_{i=1}^{4} f_i$$

is transversely orientable. □

Proof. We can transport a fixed transverse orientation of τ_1 to τ_i, $i = 2, 3, 4$, across the upper branched surface $\mathscr{B}^{\uparrow}_t$ in t without twisting; see Figure 3.6. □

Definition 8.2.3. Let $t \in T$. Fix a transverse orientation on the upper track τ_t restricted to the faces of t; this is possible by Corollary 8.2.2. We say that t is *edge-oriented* if the orientation on the edges of t agrees with the orientation determined by the transverse orientation on τ_t. In that case every face of t is edge-oriented.

We construct the edge-orientation double cover $\mathcal{V}^{or}$ of $\mathcal{V}$ using edge-oriented tetrahedra — twice as many as the number of tetrahedra of $\mathcal{V}$. Then we use the fact

that every face can be edge-oriented in precisely two ways (see Figure 8.4) to argue that faces of the edge-oriented tetrahedra can be identified in pairs to give a double cover of $\mathcal{V}$.

Construction 8.2.4. (Edge-orientation double cover) Let $\mathcal{V}$ be a veering triangulation with the set T of tetrahedra, the set F of triangular faces, and the set E of edges. For $t \in T$ we take two copies of t and denote them by $t, \bar{t}$. Both $t, \bar{t}$ are endowed with the upper track of $\mathcal{V}$ restricted to the faces of t. We denote the track in t by τ_t and the track in $\bar{t}$ by $\overline{\tau}_t$.

We fix the orientation on the bottom diagonal of t and choose the *opposite* orientation on the bottom diagonal of $\bar{t}$. This determines (opposite) transverse orientations on τ_t, $\overline{\tau}_t$ by Corollary 8.2.2. We orient the edges of $t, \bar{t}$ so that they are edge-oriented by τ_t, $\overline{\tau}_t$, respectively.

Let $\overline{T} = \{\bar{t} \mid t \in T\}$. Every face $f \in F$ appears four times as a face of an edge-oriented tetrahedron from $T \cup \overline{T}$: twice as a bottom face and twice as a top face. Moreover, its two bottom copies are edge-oriented in the opposite way; the same is true for its two top copies. Hence we can identify the faces of the tetrahedra $T \cup \overline{T}$ in pairs to obtain an edge-oriented veering triangulation which double covers $\mathcal{V}$.

Definition 8.2.5. Let $\mathcal{V}$ be a veering triangulation. The *edge-orientation double cover* $\mathcal{V}^{or}$ of $\mathcal{V}$ is the ideal triangulation obtained by Construction 8.2.4.

Example 8.2.6. Let $\mathcal{V}$ denote the veering triangulation `cPcbbbdxm_10` of the figure-eight knot sister (manifold m003). It is presented in Figure 8.2. We follow Construction 8.2.4 to build the edge-orientation double cover $\mathcal{V}^{or}$ of $\mathcal{V}$. The result is presented in Figure 8.5.

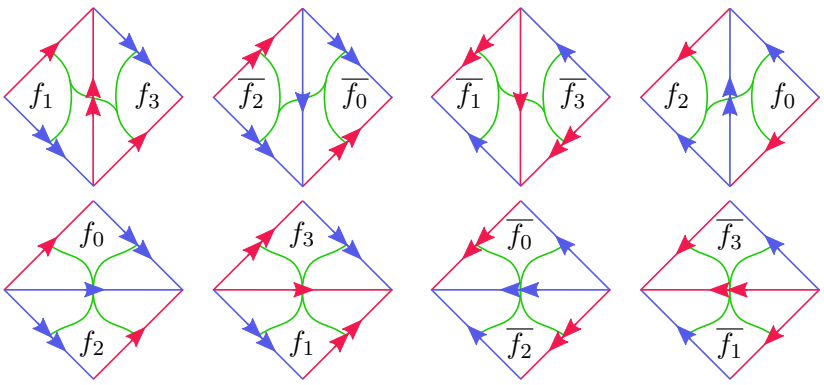

Figure 8.5: The edge-orientation double cover of the veering triangulation $\mathcal{V}$ = `cPcbbbdxm_10` of the figure-eight knot sister. We distinguish two lifts of the same edge of $\mathcal{V}$ to $\mathcal{V}^{or}$ by using a single or a double arrow to indicate their orientation.

Since we build the cover $\mathcal{V}^{or}$ using edge-oriented tetrahedra, we immediately get the following lemma.

Lemma 8.2.7. *Let $\mathcal{V}$ be a veering triangulation. The edge-orientation double cover $\mathcal{V}^{or}$ of $\mathcal{V}$ is edge-orientable.* □

Lemma 8.2.8. *Let $\mathcal{V}$ be a veering triangulation. The edge-orientation double cover $\mathcal{V}^{or}$ is connected if and only if $\mathcal{V}$ is not edge-orientable.*

Proof. Suppose that $\mathcal{V}$ is edge-orientable. Fix the orientations on the edges of $\mathcal{V}$ such that every face of $\mathcal{V}$ is edge-oriented. With this choice of orientations following Construction 8.2.4 gives a disjoint union of two copies of $\mathcal{V}$. Conversely, if $\mathcal{V}^{or}$ is disconnected, then it is a disjoint union of two copies of $\mathcal{V}$. By Lemma 8.2.7 the triangulation $\mathcal{V}^{or}$ is edge-orientable and hence so is $\mathcal{V}$. □

8.3 The edge-orientation homomorphism

The edge-orientation double cover $\mathcal{V}^{or} \to \mathcal{V}$ determines a homomorphism

$$\omega : \pi_1(M) \to \{-1, 1\}$$
$$\gamma \mapsto \begin{cases} 1 & \text{if } \gamma \text{ lifts to a loop in } \mathcal{V}^{or} \\ -1 & \text{otherwise.} \end{cases}$$

We call this homomorphism the *edge-orientation homomorphism* of $\mathcal{V}$. We say that $\gamma \in \pi_1(M)$ is *twisted* if $\omega(\gamma) = -1$ and *untwisted* otherwise.

Let G be a quotient of $\pi_1(M)$. We are interested in a combinatorial condition which ensures that the edge-orientation homomorphism $\omega : \pi_1(M) \to \{-1, 1\}$ factors through G. The obtained factors $G \to \{-1, 1\}$ are used in Proposition 9.3.1 and Theorem 10.3.1.

Note that there is a regular cover M^G of M with the deck group isomorphic to G and the fundamental group isomorphic to the kernel of the projection $\pi_1(M) \to G$. This cover admits a veering triangulation $\mathcal{V}^G$ induced by the veering triangulation $\mathcal{V}$ of M.

The reasoning in the following lemma is completely analogous to the case of factoring the orientation character; see for example [1, Lemma 1.1].

Lemma 8.3.1. *The veering triangulation $\mathcal{V}^G$ is edge-orientable if and only if the edge-orientation homomorphism $\omega : \pi_1(M) \to \{-1, 1\}$ factors through G.*

Proof. Let $q : \pi_1(M) \to G$ be the natural projection. Its kernel is isomorphic to $\pi_1\left(M^G\right)$. To show that ω factors through G it is enough to show that $\ker q \leq \ker \omega$.

This is clearly the case when $\mathcal{V}^G$ is edge-orientable, because then the edge-orientation homomorphism $\omega^G : \pi_1\left(M^G\right) \to \{-1, 1\}$ is trivial. Therefore for every $\gamma \in \ker q \cong \pi_1\left(M^G\right)$ we have $\omega(\gamma) = 1$.

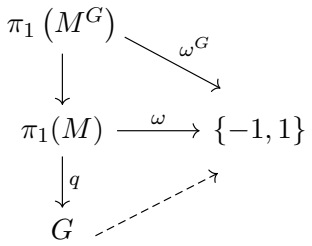

Conversely, suppose that $\mathcal{V}^G$ is not edge-orientable. Then the edge-orientation homomorphism $\omega^G : \pi_1\left(M^G\right) \to \{-1, 1\}$ is not trivial. Let $\gamma \in \ker q \cong \pi_1\left(M^G\right)$ be an element such that $\omega(\gamma) = -1$ and let $\beta \in \pi_1(M)$. Then $q(\beta) = q(\beta\gamma)$ and

$$\omega(\beta\gamma) = \omega(\beta)\omega(\gamma) = -\omega(\beta) \neq \omega(\beta).$$

This implies that ω does not factor through G. □

Chapter 9

The Alexander polynomial

The aim of this chapter is to prove a relation between the taut polynomial of a veering triangulation and the Alexander polynomial of the underlying manifold. On our way we prove that the Alexander polynomial can be computed using the relative homology module $H_1(M^{ab}, \partial M^{ab}; \mathbb{Z})$. This can be deduced from Milnor's result on the Reidemeister torsion [43, Theorem 1']. Our proof is direct and uses only an ideal triangulation of the manifold.

9.1 Computing the Alexander polynomial

Let M be a 3-manifold. Recall that by M^{ab} we denote the maximal free abelian cover of M and that H denotes the torsion-free part of $H_1(M; \mathbb{Z})$ (4.1). Since there is an action of H on M^{ab}, the first homology group $H_1(M^{ab}; \mathbb{Z})$ admits a $\mathbb{Z}[H]$-module structure. Its zeroth Fitting invariant is called the *Alexander polynomial* of M. We denote it by Δ_M.

An efficient algorithm to compute the Alexander polynomial of M directly from the presentation of $\pi_1(M)$ relies on the *Fox calculus* [40, pp. 116 – 118] and has been implemented in SnapPy [13]. We will be assuming that M admits an ideal triangulation and computing the Alexander polynomial using the triangulation will be more useful for our purposes. We explain the computation below; see also [42, Section 5]. We refer back to this computation in Proposition 9.2.1.

Let $\mathcal{T} = (T, F, E)$ be an ideal triangulation of M. Let $\mathcal{D}$, Υ, $\mathcal{D}_\Upsilon$, F_Υ be as in Section 4.2. The only difference here is that we do not assume that $\mathcal{T}$ is transverse taut. Let $\mathcal{D}_\Upsilon^{ab}$ be the maximal free abelian cover of $\mathcal{D}_\Upsilon$. Note that

$$H_1(\mathcal{D}_\Upsilon^{ab}; \mathbb{Z}) \cong H_1(M^{ab}; \mathbb{Z}). \tag{9.1}$$

It follows that the Alexander polynomial of M is equal to the zeroth Fitting invariant

of $H_1(\mathcal{D}^{ab}_\Upsilon;\mathbb{Z})$. The chain groups of $\mathcal{D}^{ab}_\Upsilon$ fit into

$$0 \longrightarrow \mathbb{Z}[H]^E \xrightarrow{d_2^\Upsilon} \mathbb{Z}[H]^{F_\Upsilon} \xrightarrow{d_1^\Upsilon} \mathbb{Z}[H] \longrightarrow 0. \tag{9.2}$$

If by v we denote the unique vertex of $\mathcal{D}_\Upsilon$, and by v^{ab} the full preimage of v under the covering map $\mathcal{D}^{ab}_\Upsilon \to \mathcal{D}_\Upsilon$, then

$$H_1(\mathcal{D}^{ab}_\Upsilon, v^{ab};\mathbb{Z}) \cong \mathbb{Z}[H]^{F_\Upsilon} \Big/ \operatorname{im} d_2^\Upsilon .$$

Lemma 9.1.1. *Let M be a 3-manifold with an ideal triangulation $\mathcal{T}$. Denote by $\mathcal{D}$ the 2-complex dual to $\mathcal{T}$. Let Υ be a spanning tree of the 1-skeleton of $\mathcal{D}$. Then the first Fitting invariant of $H_1(\mathcal{D}^{ab}_\Upsilon, v^{ab};\mathbb{Z})$ is equal to the Alexander polynomial of M.*

Proof. Denote by IH the kernel of the map $\epsilon : \mathbb{Z}[H] \to \mathbb{Z}$ defined by $h \mapsto 1$ for every $h \in H$. Since $H_1(v^{ab};\mathbb{Z}) \cong 0$, $H_0(v^{ab};\mathbb{Z}) \cong \mathbb{Z}[H]$ $H_0(\mathcal{D}^{ab}_\Upsilon;\mathbb{Z}) \cong \mathbb{Z} \cong \mathbb{Z}[H] \,/_{\mathrm{IH}}$, and the long exact sequence of the pair $(\mathcal{D}^{ab}_\Upsilon, v^{ab})$ is exact, we obtain the short exact sequence

$$0 \longrightarrow H_1(\mathcal{D}^{ab}_\Upsilon;\mathbb{Z}) \longrightarrow H_1(\mathcal{D}^{ab}_\Upsilon, v^{ab};\mathbb{Z}) \longrightarrow \mathrm{IH} \longrightarrow 0.$$

This is an augmentation sequence in the sense of [57]. In particular, it follows from [57, Corollary 1.2] that the first Fitting invariant of $H_1(\mathcal{D}^{ab}_\Upsilon, v^{ab};\mathbb{Z})$ and the zeroth Fitting invariant of of $H_1(\mathcal{D}^{ab}_\Upsilon;\mathbb{Z})$ are equal. The latter is equal to the Alexander polynomial of M by (9.1). □

Remark. If M admits a veering triangulation $\mathcal{V}$, it is useful to express the taut polynomial of $\mathcal{V}$ and the Alexander polynomial of M in terms of the same basis of H. For this reason we implemented the computation of the Alexander polynomial of M which relies on Lemma 9.1.1 and the algorithm `FacePairings` (Alg. 1). The source code is available at [48]. We use this in Example 9.4.1, Section 13.2 and Section 14.1.

9.2 The relative homology module

The first boundary relative homology group $H_1(M^{ab}, \partial M^{ab};\mathbb{Z})$ also admits a $\mathbb{Z}[H]$-module structure. We denote its zeroth Fitting invariant by $\Delta_{(M,\partial M)}$.

Recall that M is endowed with an ideal triangulation $\mathcal{T} = (T, F, E)$. Let Υ be a spanning tree of the dual graph Γ of $\mathcal{T}$. Let F_Υ be as in Section 4.2. By merging all tetrahedra into one 3-cell as dictated by Υ, we can compute the homology groups of the pair $(M^{ab}, \partial M^{ab})$ using the following chain complex.

$$0 \longrightarrow \mathbb{Z}[H] \xrightarrow{\partial_3^\Upsilon} \mathbb{Z}[H]^{F_\Upsilon} \xrightarrow{\partial_2^\Upsilon} \mathbb{Z}[H]^E \xrightarrow{0} 0 \longrightarrow 0. \tag{9.3}$$

Therefore $\mathrm{Fit}_0(H_1(M^{ab}, \partial M^{ab}))$ is generated by the $|T| \times |T|$ minors of ∂_2^Υ.

Proposition 9.2.1. *Let M be a 3-manifold endowed with an ideal triangulation $\mathcal{T} = (T, F, E)$. Then*

$$\Delta_{(M,\partial M)} = \Delta_M.$$

Proof. Let $\mathcal{D}$ be the dual 2-complex of $\mathcal{T}$. We fix the orientation on the edges of $\mathcal{T}$ and then choose the orientation on the dual 2-cells of $\mathcal{D}$ as determined by the right hand rule. We fix the orientation on the edges of $\mathcal{D}$ and then choose the orientation on the corresponding faces of $\mathcal{T}$ to be determined by the right hand rule.

Let Υ be a spanning tree of the dual graph Γ of $\mathcal{T}$. We consider the $\mathbb{Z}[H]$-module homomorphisms d_2^Υ and ∂_2^Υ as in (9.2) and (9.3), respectively. Let r be the rank of H and let $(h_1, \ldots, h_r)$ be a basis of H. With the above-mentioned choice of orientations we have the equality of matrices

$$d_2^\Upsilon(h_1, \ldots, h_r) = \left(\partial_2^\Upsilon(h_1^{-1}, \ldots, h_r^{-1})\right)^{\mathrm{tr}}.$$

Inverting the variables is necessary, because a triangle $1 \cdot f \in H \cdot F$ of $\mathcal{T}^{ab}$ has $h \cdot e$ in its boundary, for some $e \in E$, $h \in H$, if and only if the 2-cell $1 \cdot e$ of $\mathcal{D}_\Upsilon^{ab}$ has edge $h^{-1} \cdot f$ in its boundary.

Let $n = |T|$. By Lemma 9.1.1 have

$$\Delta_M = \gcd\left\{n \times n \text{ minors of } d_2^\Upsilon\right\}.$$

At the beginning of this section we explained that

$$\Delta_{(M,\partial M)} = \gcd\left\{n \times n \text{ minors of } \partial_2^\Upsilon\right\}.$$

Since the Alexander polynomial satisfies

$$\Delta_M(h_1, \ldots, h_r) = \Delta_M(h_1^{-1}, \ldots, h_r^{-1})$$

up to a unit in $\mathbb{Z}[H]$ [59, Corollary 4.5], we obtain the desired equality. □

9.3 The taut polynomial and the Alexander polynomial

In this section we give a sufficient condition on the veering triangulation for its taut polynomial to be very closely related to the Alexander polynomial of the underlying manifold.

Recall from Section 8.3 that a veering triangulation $\mathcal{V}$ of M determines the edge-orientation homomorphism $\omega : \pi_1(M) \to \{-1, 1\}$. By Lemma 8.3.1, if $\mathcal{V}^{ab}$ is

edge-orientable then ω factors through $\sigma : H \to \{-1, 1\}$.

Proposition 9.3.1. *Let $\mathcal{V}$ be a veering triangulation of a 3-manifold M. Let $(h_1, \ldots, h_r)$ be a basis of H. If $\mathcal{V}^{ab}$ is edge-orientable then*

$$\Theta_{\mathcal{V}}(h_1, \ldots, h_r) = \Delta_M(\sigma(h_1) \cdot h_1, \ldots, \sigma(h_r) \cdot h_r)$$

where $\sigma : H \to \{-1, 1\}$ is the factor of the edge-orientation homomorphism of $\mathcal{V}$.

Proof. The relative homology module $H_1(M^{ab}, \partial M^{ab}; \mathbb{Z})$ admits a free presentation

$$\mathbb{Z}[H]^F \xrightarrow{\partial_2} \mathbb{Z}[H]^E \longrightarrow H_1(M^{ab}, \partial M^{ab}; \mathbb{Z}) \longrightarrow 0.$$

Observe that it resembles the presentation (5.1) for the taut module. The difference is that the presentation matrix $D^{\uparrow}$ of the taut module does not depend on the orientations of the triangles and edges of $\mathcal{V}^{ab}$ — it only depends on the transverse taut structure α on the triangulation.

If $\mathcal{V}$ is edge-orientable choose an orientation on its edges so that it is edge-oriented. Otherwise, pick any orientation on the edges of $\mathcal{V}$. The edges of $\mathcal{V}^{ab}$ are oriented so that the covering map $M^{ab} \to M$ restricted to any edge is orientation-preserving. Therefore clearly when $\mathcal{V}$ is edge-orientable then for any $h \cdot f \in H \cdot F$ we have $D^{\uparrow}(h \cdot f) = \pm\partial_2(h \cdot f)$ and thus $\Theta_{\mathcal{V}} = \Delta_{(M,\partial M)}$.

More generally, the group homomorphism σ induces a ring homomorphism $\overline{\sigma} : \mathbb{Z}[H] \to \mathbb{Z}[H]$ defined by

$$\overline{\sigma}\left(\sum_{h \in H} a_h \cdot h\right) = \sum_{h \in H} \sigma(h) \cdot a_h \cdot h.$$

Consider the following diagram.

$$\begin{array}{ccccccc} \mathbb{Z}[H]^F & \xrightarrow{\partial_2} & \mathbb{Z}[H]^E & \longrightarrow & H_1(M^{ab}, \partial M^{ab}; \mathbb{Z}) & \longrightarrow & 0 \\ \downarrow{\scriptstyle id} & & \downarrow{\scriptstyle \overline{\sigma}^{\oplus E}} & & \downarrow & & \\ \mathbb{Z}[H]^F & \xrightarrow{D^{\uparrow}} & \mathbb{Z}[H]^E & \longrightarrow & \mathcal{E}_{\alpha}(\mathcal{V}) & \longrightarrow & 0 \end{array} \tag{9.4}$$

The diagram commutes (after reversing the orientation of some triangular faces of $\mathcal{V}$ if necessary) because reversing the orientation of the edge $h \cdot e$ of $\mathcal{V}^{ab}$ if and only if

$$\sigma(h) = -1$$

makes $\mathcal{V}^{ab}$ into an edge-oriented triangulation. It follows that the presentation

matrices for $H_1(M^{ab}, \partial M^{ab}; \mathbb{Z})$ and $\mathcal{E}_\alpha(\mathcal{V})$ differ by reversing the sign of variables corresponding to the basis elements of H with a nontrivial image under σ. And so do their Fitting invariants. Therefore

$$\Theta_{\mathcal{V}}(h_1, \dots, h_r) = \Delta_{(M,\partial M)}(\sigma(h_1) \cdot h_1, \dots, \sigma(h_r) \cdot h_r).$$

The claim now follows from Proposition 9.2.1. □

Remark. If $\mathcal{V}$ is not edge-orientable then $\mathcal{E}_\alpha(\mathcal{V})$ and $H_1(M^{ab}, \partial M^{ab}; \mathbb{Z})$ are not isomorphic as $\mathbb{Z}[H]$-modules (otherwise their Fitting invariants would be the same). When σ is nontrivial the induced ring homomorphism $\overline{\sigma} : \mathbb{Z}[H] \to \mathbb{Z}[H]$ is not a $\mathbb{Z}[H]$-module homomorphism. For $h \in H$ such that $\sigma(h) = -1$ we have

$$h \cdot \overline{\sigma}(h) = -h^2,$$

but

$$\overline{\sigma}(h \cdot h) = h^2.$$

Proposition 9.3.1 allows us to easily identify veering triangulations for which the equality $\Theta_{\mathcal{V}}(h_1, \dots, h_r) = \Delta_M(\pm h_1, \dots, \pm h_r)$ might fail.

Corollary 9.3.2. *Let $\mathcal{V}$ be a veering triangulation of a 3-manifold M. Let $(h_1, \dots, h_r)$ be a basis of H. If*

$$\Theta_{\mathcal{V}}(h_1, \dots, h_r) \neq \Delta_M(\pm h_1, \dots, \pm h_r) \tag{9.5}$$

up to a unit in $\mathbb{Z}[H]$ then the torsion subgroup of $H_1(M; \mathbb{Z})$ has even order.

Proof. By Proposition 9.3.1, the condition (9.5) implies that $\mathcal{V}^{ab}$ is not edge-orientable. If follows that the deck group of $\mathcal{V}^{or} \to \mathcal{V}$ is a quotient of the torsion subgroup of $H_1(M; \mathbb{Z})$. □

9.3.1 Reduction modulo 2

We consider the ring epimorphism

$$\begin{aligned} \bmod 2 : \mathbb{Z}[H] &\to \mathbb{Z}/2[H] \\ \sum_{h \in H} a_h \cdot h &\mapsto \sum_{h \in H} (a_h \bmod 2) \cdot h. \end{aligned}$$

Let ∂_2, $D^\uparrow$ be as in (9.4). Reducing them modulo 2 yields an isomorphism of $\mathbb{Z}/2[H]$-modules

$$\mathcal{E}_\alpha(\mathcal{V}) \otimes_{\mathbb{Z}[H]} \mathbb{Z}/2\mathbb{Z}[H] \cong H_1(M^{ab}, \partial M^{ab}; \mathbb{Z}/2\mathbb{Z}) \tag{9.6}$$

obtained from $\mathcal{E}_\alpha(\mathcal{V})$ and $H_1(M^{ab}, \partial M^{ab}; \mathbb{Z})$ by the extension of scalars through mod 2. Let $\Delta_M^{\text{mod } 2}$ denote the zeroth Fitting invariant of the module (9.6). Then $\Delta_M^{\text{mod } 2}$ is a common factor of ($\Theta_\mathcal{V}$ mod 2) and (Δ_M mod 2). In Section 15.2 we suggest a method to find the precise formula relating ($\Theta_\mathcal{V}$ mod 2) and (Δ_M mod 2).

9.4 Supports, Newton polytopes and dual polytopes

Given a Laurent polynomial

$$P = \sum_{h \in H} a_h \cdot h \in \mathbb{Z}[H]$$

we define the *support* of P

$$\text{supp}(P) = \{h \in H \mid a_h \neq 0\}$$

and the *Newton polytope* of P

$$N(P) = \text{the convex hull of supp}(P) \text{ in } H_1(M; \mathbb{R}).$$

Proposition 9.3.1 says that edge-orientability of $\mathcal{V}^{ab}$ is a sufficient condition for the equality

$$\text{supp}(\Theta_\mathcal{V}) = \text{supp}(\Delta_M).$$

In Example 9.4.1 we present a veering triangulation for which this equality does not hold, but the Newton polytopes of the taut and Alexander polynomial are nonetheless equal.

Example 9.4.1. Let

$$\mathcal{V} = \texttt{oLLLLLPwQQcccefgijlmkklnnnlnewbnetafobnkj\_12001112122200}.$$

This triangulation is layered. Since $\mathcal{V}^{ab}$ is not edge-orientable the formula given in Proposition 9.3.1 does not have to hold. The taut and Alexander polynomials expressed in terms of the same basis of H are as follows.

$$\begin{aligned}\Theta_\mathcal{V} = {} & a^7b - a^6b^2 - a^5b^3 + a^4b^4 - a^6b - 2a^5b^2 + 2a^4b^3 + 2a^3b^4 - ab^6 \\ & - a^6 + 2a^4b^2 + 2a^3b^3 - 2a^2b^4 - ab^5 + a^3b^2 - a^2b^3 - ab^4 + b^5 \\ \Delta_M = {} & a^7b + a^6b^2 + a^5b^3 + a^4b^4 + a^6b + 2a^4b^3 + 2a^3b^4 + 2a^2b^5 + ab^6 \\ & + a^6 + 2a^5b + 2a^4b^2 + 2a^3b^3 + ab^5 + a^3b^2 + a^2b^3 + ab^4 + b^5\end{aligned}$$

In Figure 9.1 we see that

$$\operatorname{supp}(\Theta_{\mathcal{V}}) \neq \operatorname{supp}(\Delta_M)$$

but

$$N(\Theta_{\mathcal{V}}) = N(\Delta_M).$$

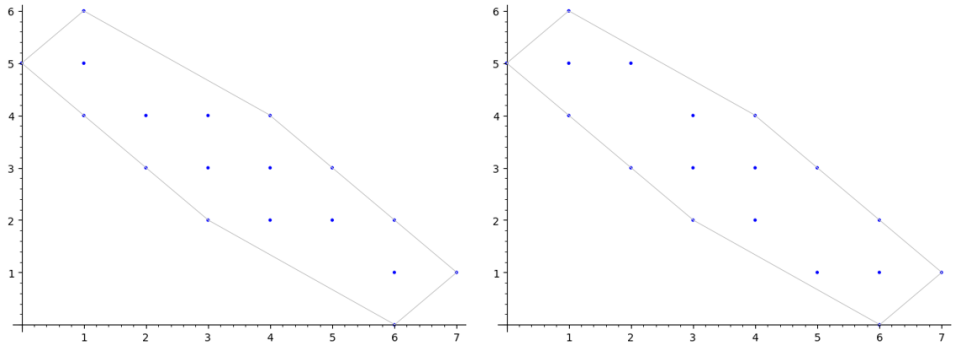

Figure 9.1: The supports of the taut and the Alexander polynomials of the veering triangulation `oLLLLLPwQQcccefgijlmkklnnnlnewbnetafobnkj_12001112122200` are different, but they have the same convex hull. (a) $\operatorname{supp}(\Theta_{\mathcal{V}})$. (b) $\operatorname{supp}(\Delta_M)$.

Let $(h_1, \ldots, h_r)$ be a basis of H. If a Laurent polynomial $P \in \mathbb{Z}[H]$ satisfies

$$P(h_1, \ldots, h_r) = P(h_1^{-1}, \ldots, h_r^{-1})$$

up to a unit in $\mathbb{Z}[H]$ we say that it is *palindromic*. For instance, the Alexander polynomial is palindromic [59, Corollary 4.5]. We used this fact in the proof of Proposition 9.2.1.

If P is palindromic then its Newton polytope $N(P)$ can be translated in $H_1(M;\mathbb{R})$ so that it is symmetric with respect to the origin. By $N^c(P)$ we denote the centralised Newton polytope of P. We then define the *dual polytope* of P by

$$N^*(P) = \{\eta \in H^1(M;\mathbb{R}) \mid \eta(h) \leq 1 \text{ for every } h \in N^c(P)\}.$$

When $\mathcal{V}$ is layered there is a norm on $H^1(M;\mathbb{R})$ whose unit norm ball is equal to $N^*(\Theta_{\mathcal{V}})$ scaled down by a factor of two [41, Section 6]. There is also a norm on $H^1(M;\mathbb{R})$ whose unit norm ball is equal to $N^*(\Delta_M)$ scaled down by a factor of two [42, Section 4]. Proposition 9.3.1 gives a sufficient condition for when these two norms agree. Example 9.4.1 shows that these norms can agree even when the assumption of Proposition 9.3.1 is not satisfied.

Chapter 10

Dehn filling veering triangulations

Let M be a 3-manifold equipped with a veering triangulation $\mathcal{V}$. Suppose that the truncated model of M has b boundary components $T_1, \ldots, T_b$. Let γ_j be a Dehn filling slope on T_j, that is a free homotopy class of an essential simple closed curve on T_j. By

$$N = M(\gamma_1, \ldots, \gamma_b) \tag{10.1}$$

we denote the 3-manifold obtained from M by Dehn filling T_j along γ_j. We call N a *Dehn filling* of M. We allow $\gamma_j = 0$ which corresponds to not filling T_j at all. In other words, we do not assume that N is closed.

From this chapter onwards we will be dealing with both M and N. Because of that we change the notation (4.1) and set

$$\begin{aligned} H_M &= H_1(M;\mathbb{Z})\,/_{\text{torsion}} \\ H_N &= H_1(N;\mathbb{Z})\,/_{\text{torsion}}. \end{aligned}$$

We denote the ranks of H_M, H_N by $b_1(M)$, $b_1(N)$, respectively. The inclusion of M into N induces an epimorphism $i_* : H_M \to H_N$. We are interested in the image of the taut polynomial of $\mathcal{V}$ under this epimorphism. We call the polynomial $i_*(\Theta_\mathcal{V})$ the *specialisation of the taut polynomial under a Dehn filling*.

We treat $i_*(\Theta_\mathcal{V}) \in \mathbb{Z}[H_N]$ as an invariant of a Dehn filling of a veering triangulation. There is another natural invariant corresponding to this Dehn filling. Namely, instead of computing

$$i_*(\Theta_\mathcal{V}) = i_*\left(\gcd\left(\text{minors of } D^\uparrow\right)\right)$$

we can compute

$$\Theta_{\mathcal{V}}^{i_*} = \gcd\left(i_*\left(\text{minors of } D^{\uparrow}\right)\right).$$

The latter is the zeroth Fitting invariant of the module obtained from the taut module by the extension of scalars through i_*. Both these polynomials are elements of $\mathbb{Z}[H_N]$. Clearly, $i_*(\Theta_{\mathcal{V}})$ divides $\Theta_{\mathcal{V}}^{i_*}$, but the equality does not always hold. The precise relation between $i_*(\Theta_{\mathcal{V}})$ and $\Theta_{\mathcal{V}}^{i_*}$ can be found using the *torsion of the veering chain complex* defined in Section 15.2. In this thesis we consider only $i_*(\Theta_{\mathcal{V}})$, because — as shown in [38, Proposition 7.2] — it is a generalisation of the Teichmüller polynomial which we study in Chapter 12.

In Section 4.2.3 we considered the free abelian quotient of $H_1(M;\mathbb{Z})$ determined by a collection C of dual cycles. Let us denote it by H_M^C. There is a corresponding epimorphism $\varrho_C : H_M \to H_M^C$. Note that i_* is just a special example of ϱ_C. Therefore in Section 10.1, which constitutes the computational part of this chapter, we are more general and consider the specialisation $\varrho_C(\Theta_{\mathcal{V}})$ of the taut polynomial under the epimorphism ϱ_C.

In Section 10.2 we use the results of Turaev [59, Section 4] to derive formulas relating $i_*(\Delta_M)$, the specialisation of the Alexander polynomial of M under a Dehn filling, and the Alexander polynomial Δ_N of the Dehn-filled manifold. These formulas are needed in the proof of Theorem 10.3.1 in which we compare $i_*(\Theta_{\mathcal{V}})$ with Δ_N.

10.1 Algorithm `Specialisation`

Let $\mathcal{V}$ be a veering triangulation. Let C be a finite collection of dual cycles of $\mathcal{V}$. It determines the epimorphism $\varrho_C : H_M \to H_M^C$. In this section we give an algorithm to compute $\varrho_C(P)$ given $P \in \mathbb{Z}[H_M]$.

Algorithm 4. `Specialisation`
Computing the specialisation of $P \in \mathbb{Z}[H_M]$ under the epimorphism determined by a collection of dual cycles

Input:

- A veering triangulation $\mathcal{V}$ of a 3-manifold M
- $P \in \mathbb{Z}[H_M]$ expressed in terms of the basis fixed by `FacePairings`$(\mathcal{V}, [\,])$
- A finite list C of dual cycles of $\mathcal{V}$

Output: The specialisation $\varrho_C(P)$ of P

1: $n :=$ the number of tetrahedra of $\mathcal{V}$

continued on the next page

Algorithm `Specialisation` continued

2: $U, r :=$ `FacePairings`$(\mathcal{V}, [\,]$, return type = "matrix")
3: $A_1 :=$ the matrix obtained from U^{-1} by deletings its first $n+1-r$ columns
4: $U', s :=$ `FacePairings`$(\mathcal{V}, C$, return type = "matrix")
5: $A_2 :=$ the matrix obtained from U' by deletings its first $n+1-s$ rows
6: exp := `Exponents`(P)
7: coeff := `Coefficients`(P)
8: newExp := [ ]
9: **for** v in exp **do**
10: append newExp with $A_2A_1(v)$
11: **end for**
12: spec := $\sum_{i=1}^{\text{length(coeff)}} \text{coeff}[i] \cdot u^{\text{newExp}[i]}$ # $u = (u_1, \ldots, u_s)$ and $u^v = u_1^{v_1} \cdots u_s^{v_s}$
13: **return** spec

Proposition 10.1.1. *Let $\mathcal{V}$ be a veering triangulation of a 3-manifold M. Let $P \in \mathbb{Z}[H_M]$ be expressed in terms of the basis fixed by* `FacePairings`$(\mathcal{V}, [\,])$*. Let C be a list of dual cycles of $\mathcal{V}$. Then* `Specialisation`$(\mathcal{V}, P, C)$ *is equal to $\rho_C(P)$.*

Proof. The whole proof follows from the discussion on page 40. Let n be the number of tetrahedra in the veering triangulation $\mathcal{V}$. Let Γ be the dual graph of $\mathcal{V}$. The pair (U, r) on line 2 of the algorithm is such that r equals the rank of H_M and the last r columns of the inverse $U^{-1} \in \mathrm{GL}(n+1, \mathbb{Z})$ give the expressions for the basis elements of H_M as simplicial 1-cycles in Γ_Υ, the graph obtained from Γ by contracting a spanning tree Υ to a point. The pair (U', s) on line 4 of the algorithm is such that s equals the rank of H_M^C and the last s rows of the matrix $U' \in \mathrm{GL}(n+1, \mathbb{Z})$ encode the H_M^C-pairings of the faces dual to the edges of Γ_Υ.

Let A_1 be the matrix obtained from U^{-1} by deleting its first $n+1-r$ columns. Let A_2 be the matrix obtained from U' by deleting its first $n+1-s$ rows. Then the matrix $A = A_2 \cdot A_1$ represents the epimorphism $\varrho_C : H_M \to H_M^C$ written in terms of the bases of H_M, H_M^C fixed by the algorithm `FacePairings`. Note that we use the fact that the algorithm `FacePairings` is deterministic; see Remark 4.2.5.

Each monomial $a_h \cdot h$ in P can be encoded by a pair (a_h, v) where $a_h \in \mathbb{Z}$, $v \in \mathbb{Z}^r$. Then the pair $(a_h, A_2A_1(v))$ encodes the corresponding monomial $a_h \cdot \varrho_C(h)$ appearing in $\varrho_C(P)$. Therefore the polynomial spec on line 12 of the algorithm is equal to $\varrho_C(P)$. □

Note that it only make sense to apply the algorithm `Specialisation` to an element of $\mathbb{Z}[H_M]$ which, as a Laurent polynomial, is expressed in terms of the basis

fixed by the algorithm `FacePairings`.

To compute $i_*(\Theta_{\mathcal{V}})$, where $i_* : H_M \to H_N$ is determined by the Dehn filling $N = M(\gamma_1, \ldots, \gamma_b)$ of M, we need to express the Dehn filling slopes $\gamma_1, \ldots, \gamma_b$ (or their multiples) as dual cycles. In Section 12.2 we explain how to do this in the case when γ_j's are parallel to the boundary components of a surface carried by $\mathcal{V}$.

10.2 The image of the Alexander polynomial under a Dehn filling

The main theoretical result of this thesis is a comparison between the specialisation $i_*(\Theta_{\mathcal{V}})$ of the taut polynomial of $\mathcal{V}$ under a Dehn filling and the Alexander polynomial of the Dehn filled manifold N. Our first step is to compare $i_*(\Delta_M)$ with Δ_N. This was previously studied by Turaev. By first recursively applying the formulas given in Corollary 4.2 of [59] and then using Corollary 4.1 of [59] we obtain the following lemma.

Lemma 10.2.1. *Let M be a compact, orientable, connected 3-manifold with nonempty boundary consisting of tori. Let N be any Dehn filling of M such that $b_1(N)$ is positive. Denote by $\ell_1, \ldots, \ell_k$ the core curves of the filling solid tori in N and by $i_* : H_M \to H_N$ the epimorphism induced by the inclusion of M into N. Assume that for every $j \in \{1, \ldots, k\}$ the class $[\ell_j] \in H_N$ is nontrivial.*

I. $b_1(M) \geq 2$ and

(a) $b_1(N) \geq 2$. Then

$$i_*(\Delta_M) = \Delta_N \cdot \prod_{j=1}^{k} ([\ell_j] - 1).$$

(b) $b_1(N) = 1$. Let h denote the generator of H_N.

- *If $\partial N \neq \emptyset$ then*

$$i_*(\Delta_M) = (h-1)^{-1} \cdot \Delta_N \cdot \prod_{j=1}^{k} ([\ell_j] - 1).$$

- *If N is closed then*

$$i_*(\Delta_M) = (h-1)^{-2} \cdot \Delta_N \cdot \prod_{j=1}^{k} ([\ell_j] - 1).$$

II. $b_1(M) = 1$. Let h denote the generator of $H_N \cong H_M$.

(a) If $\partial N \neq \emptyset$ then

$$i_*(\Delta_M) = \Delta_N.$$

(b) If N is closed set $\ell = \ell_1$, and then

$$i_*(\Delta_M) = (h-1)^{-1}([\ell]-1)\cdot\Delta_N. \qquad \square$$

10.3 The specialisation of the taut polynomial under a Dehn filling

Recall that in Proposition 9.3.1 we expressed the relation between the taut polynomial of $\mathcal{V}$ and the Alexander polynomial of M using the factor $\sigma : H_M \to \{-1, 1\}$ of the edge-orientation homomorphism of $\mathcal{V}$. After Dehn filling we need a homomorphism from H_N. Its existence depends on edge-orientability of the veering triangulation of the intermediate free abelian cover M^N of M determined by H_N as in Section 8.3. Alternatively, we can view M^N as a free abelian cover of M obtained from the maximal free abelian cover N^{ab} of N by removing the preimages of the filling solid tori under $N^{ab} \to N$. This is illustrated in the following commutative diagram.

$$\begin{array}{ccccc} M^{ab} & \longrightarrow & M^N & \longrightarrow & M \\ & & \downarrow & & \downarrow{\scriptstyle i} \\ & & N^{ab} & \longrightarrow & N. \end{array} \tag{10.2}$$

Let us denote the induced veering triangulation of M^N by $\mathcal{V}^N$. By Lemma 8.3.1, if $\mathcal{V}^N$ is edge-orientable, then the edge-orientation homomorphism of $\mathcal{V}$ factors through H_N. We denote this factor by $\sigma_N : H_N \to \{-1, 1\}$.

Theorem 10.3.1. *Let $\mathcal{V}$ be a veering triangulation of a 3-manifold M. Let N be a Dehn filling of M such that $s = b_1(N)$ is positive. Denote by $\ell_1, \ldots, \ell_k$ the core curves of the filling solid tori in N and by $i_* : H_M \to H_N$ the epimorphism induced by the inclusion of M into N. Assume that the veering triangulation $\mathcal{V}^N$ is edge-orientable and that for every $j \in \{1, \ldots, k\}$ the class $[\ell_j] \in H_N$ is nontrivial. Let $\sigma_N : H_N \to \{-1, 1\}$ be the homomorphism through which the edge-orientation homomorphism of $\mathcal{V}$ factors.*

I. $b_1(M) \geq 2$ and

(a) $s \geq 2$. *Then*

$$i_*(\Theta_{\mathcal{V}})(h_1, \ldots, h_s) = \Delta_N(\sigma_N(h_1) \cdot h_1, \ldots, \sigma_N(h_s) \cdot h_s) \cdot \prod_{j=1}^{k}([\ell_j] - \sigma_N([\ell_j])).$$

(b) $s = 1$. *Let* h *denote the generator of* H_N.

- *If* $\partial N \neq \emptyset$ *then*

$$i_*(\Theta_{\mathcal{V}})(h) = (h - \sigma_N(h))^{-1} \cdot \Delta_N(\sigma_N(h) \cdot h) \prod_{j=1}^{k}([\ell_j] - \sigma_N([\ell_j])).$$

- *If* N *is closed then*

$$i_*(\Theta_{\mathcal{V}})(h) = (h - \sigma_N(h))^{-2} \cdot \Delta_N(\sigma_N(h) \cdot h) \cdot \prod_{j=1}^{k}([\ell_j] - \sigma_N([\ell_j])).$$

II. $b_1(M) = 1$. *Let* h *denote the generator of* $H_N \cong H_M$.

(a) If $\partial N \neq \emptyset$ *then*

$$i_*(\Theta_{\mathcal{V}})(h) = \Delta_N(\sigma_N(h) \cdot h).$$

(b) If N *is closed set* $\ell = \ell_1$, *and then*

$$i_*(\Theta_{\mathcal{V}})(h) = (h - \sigma_N(h))^{-1}([\ell] - \sigma_N([\ell])) \cdot \Delta_N(\sigma_N(h) \cdot h).$$

In particular with the above assumptions we have

$$i_*(\Theta_{\mathcal{V}})(h_1, h_2, \ldots, h_s) = \Delta_N(\pm h_1, \ldots, \pm h_s)$$

if and only if one of the following four conditions holds

- $N = M$, *or*
- $b_1(N) = 1$, $\partial N \neq \emptyset$, $k = 1$, *and* $[\ell_1]$ *generates* H_N, *or*
- $b_1(N) = 1$, N *is closed,* $k = 2$ *and* $[\ell_1] = [\ell_2]$ *generates* H_N, *or*
- $b_1(M) = 1$, N *is closed and* $[\ell_1]$ *generates* H_N. □

Proof. Set $r = b_1(M)$ and let $(h'_1, \ldots, h'_r)$ be a basis of H_M. First note that if $\mathcal{V}^N$ is edge-orientable, then $\mathcal{V}^{ab}$ is edge-orientable as well. Therefore there is a homomorphism $\sigma : H_M \to \{-1, 1\}$ through which the edge-orientation homomorphism of $\mathcal{V}$

factors. By Proposition 9.3.1, if $\mathcal{V}^{ab}$ is edge-orientable then

$$\Theta_{\mathcal{V}}(h'_1, \dots, h'_r) = \Delta_M(\sigma(h'_1) \cdot h'_1, \dots, \sigma(h'_r) \cdot h'_r).$$

Since $\mathcal{V}^N$ is edge-orientable, the kernel of i_* is contained in the kernel of σ and $\sigma(h) = \sigma_N(i_*(h))$ for every $h \in H_M$. Therefore

$$i_*(\Theta_{\mathcal{V}})(h_1, \dots, h_s) = i_*(\Delta_M)(\sigma_N(h_1) \cdot h_1, \dots, \sigma_N(h_s) \cdot h_s),$$

where $s = b_1(N)$ and $(h_1, \dots, h_s)$ is a basis of H_N. Now the claim follows from Lemma 10.2.1. □

10.3.1 Edge-orientability of $\mathcal{V}^N$

We already noted in the proof of Corollary 9.3.2 that the veering triangulation $\mathcal{V}^{ab}$ of the *maximal* free abelian cover of M can fail to be edge-orientable only if the torsion subgroup of $H_1(M; \mathbb{Z})$ is of even order. Edge-orientability of $\mathcal{V}^N$ additionally depends on Dehn filling slopes $\gamma_1, \dots, \gamma_b$. That is, $\mathcal{V}^N$ is edge-orientable if and only if $\mathcal{V}^{ab}$ is edge-orientable and moreover $\sigma(\gamma_j) = 1$ for every $j \in \{1, \dots, b\}$. (Here we identify γ_j with the image of its homology class in $H_1(T_j; \mathbb{Z})$ under $H_1(T_j; \mathbb{Z}) \to H_M$.) Using the language of Section 8.3, Dehn filling slopes have to be untwisted.

Suppose that $\mathcal{V}^{ab}$ is edge orientable. If the preimage of every torus boundary component of M under the covering map $\mathcal{V}^{or} \to \mathcal{V}$ is disconnected then *any* Dehn filling N of M determines an edge-orientable veering triangulation $\mathcal{V}^N$. More generally, denote by $\mathcal{I}$ the subset of $\{1, \dots, b\}$ of indices of the boundary tori of M with a connected preimage under $\mathcal{V}^{or} \to \mathcal{V}$. For $j \in \mathcal{I}$ let (a_j, b_j) be a basis of $H_1(T_j; \mathbb{Z})$ such that $\sigma(a_j) = -1$ and $\sigma(b_j) = 1$. Then the triangulation $\mathcal{V}^N$ is edge-orientable if and only if the algebraic intersection of γ_j with b_j is even for every $j \in \mathcal{I}$.

Remark. There are 87047 veering triangulations in the Veering Census [26]. 62536 (71.8%) of them are not edge-orientable. Out of 62536 not edge-orientable veering triangulations there are 49637 (79.4%) whose edge-orientable double cover $\mathcal{V}^{or}$ has the same number of cusps as $\mathcal{V}$. There are only 5854 (9.4%) whose edge-orientable double cover $\mathcal{V}^{or}$ has twice as many cusps as $\mathcal{V}$.

Chapter 11

Veering triangulations and the Thurston norm

In this chapter we outline the connection between veering triangulations and the Thurston norm. Our main goal is to give an algorithm to find the vertices spanning the face $\mathtt{F}_{\mathcal{V}}$ of the Thurston norm ball determined by a veering triangulation $\mathcal{V}$. Given a basis of $H_1(M;\mathbb{R})$ we always pick the dual basis of $H_2(M,\partial M;\mathbb{R}) \cong H^1(M;\mathbb{R})$. This is important for two reasons. First, in the layered case it makes it easy to establish for which fibrations lying in the cone $\mathbb{R}_+ \cdot \mathtt{F}_{\mathcal{V}}$ the invariant laminations of the monodromy are orientable; see Corollary 12.6.4. Second, motivated by the results of McMullen in the fibred case [41, Section 6], we wish to compare $\mathbb{R}_+ \cdot \mathtt{F}_{\mathcal{V}}$ with the cones on the faces of the dual polytope of the taut polynomial of $\mathcal{V}$; see Example 12.4.1.

11.1 The Thurston norm

Let N be a compact, oriented 3-manifold. Thurston showed that we can equip $H_2(N,\partial N;\mathbb{R})$ with a semi-norm defined as follows.

Every integral class $\xi \in H_2(N,\partial N;\mathbb{Z})$ can be represented by an embedded surface $S \subset N$ [55, Lemma 1]. If S is connected set

$$\chi_-(S) = \max\{0, -\chi(S)\},$$

where $\chi(S)$ denotes the Euler characteristic of S. When S is disconnected, with connected components $S_1, S_2, \ldots, S_k$, let

$$\chi_-(S) = \sum_{i=1}^{k} \chi_-(S_i).$$

The semi-norm $\|\cdot\|_{\mathrm{Th}}$ is first defined on $H_2(M, \partial M; \mathbb{Z})$ by the formula

$$\|\xi\|_{\mathrm{Th}} = \inf \{\chi_-(S) \mid S \text{ is an embedded surface in } M \text{ representing } \xi\}.$$

An embedded surface S which represents ξ and satisfies $\chi(S) = -\|S\|_{\mathrm{Th}}$ is called a *taut representative* of ξ.

$\|\cdot\|_{\mathrm{Th}}$ is extended to $H_2(N, \partial N; \mathbb{Q})$ by requiring linearity on each ray through the origin in $H_2(N, \partial N; \mathbb{R})$ and then to $H_2(N, \partial N; \mathbb{R})$ by requiring continuity. $\|\cdot\|_{\mathrm{Th}}$ is a norm if we assume that every surface representing a nonzero class in $H_2(N, \partial N; \mathbb{Z})$ has negative Euler characteristic [55, Theorem 1].

The unit norm ball $B_{\mathrm{Th}}(N)$ with respect to $\|\cdot\|_{\mathrm{Th}}$ is a finite-sided polytope with vertices in $H_2(N, \partial N; \mathbb{Q})$ [55, Theorem 2]. Thurston observed that if S is the fibre of a fibration of N over the circle then the homology class $[S]$ lies in the interior of the cone $\mathbb{R}_+ \cdot \mathtt{F}$ on some top-dimensional face $\mathtt{F}$ of $B_{\mathrm{Th}}(N)$. Moreover, in this case *every* integral primitive class $[S']$ from the interior of $\mathbb{R}_+ \cdot \mathtt{F}$ determines a fibration of N over the circle [55, Theorem 3]. The taut representative of $[S']$ is the fibre of that fibration.

Top-dimensional faces of $B_{\mathrm{Th}}(N)$ with the above property are called *fibred faces* of the Thurston norm ball in $H_2(N, \partial N; \mathbb{R})$ or fibred faces of N. The collection of fibred faces for a given N might be empty, but if we know that there exists some fibring $S \to N \to S^1$ and the dimension of $H_2(N, \partial N; \mathbb{R})$ is at least two, then N fibers in infinitely many distinct ways.

Landry, Minsky and Taylor showed that a veering triangulation $\mathcal{V}$ of M determines a (potentially empty, not necessarily top-dimensional, not necessarily fibred) face of $B_{\mathrm{Th}}(M)$ [38, Theorem 5.12]. In the next section we explain what precisely does it mean and give an algorithm to find this face.

Remark. If M admits a finite veering triangulation then its truncated model is compact, hence we can consider the Thurston norm on $H_2(M, \partial M; \mathbb{R})$.

11.1.1 The Poincaré-Lefschetz duality

Recall that the Poincaré-Lefschetz duality identifies $H_2(N, \partial N; \mathbb{R})$ with $H^1(N; \mathbb{R})$ [29, Theorem 3.43]. For the sake of consistency, it could be desirable either to stick to second relative homology classes, and their algebraic intersection with first homology classes, or to first cohomology classes, and their evaluation on first homology classes. We, however, choose clarity over consistency and consider $H_2(N, \partial N; \mathbb{R})$ when we have surfaces in mind, and $H^1(N; \mathbb{R})$ in more algebraic contexts.

11.2 The face of the Thurston norm ball determined by a veering triangulation

Let $\mathcal{V}$ be a veering triangulation of a 3-manifold M. We consider the *cone of surfaces carried by* $\mathcal{V}$

$$\texttt{carried}(\mathcal{V}) \subset \mathbb{R}^F$$

and the *cone of homology classes of surfaces carried by* $\mathcal{V}$

$$\texttt{hom}(\mathcal{V}) = \{[S] \mid S \text{ is carried by } \mathcal{V}\} \subset H_2(M, \partial M; \mathbb{R}).$$

It turns out that if a veering triangulation carries a taut representative of a class lying in the cone on the interior of a (not necessarily top-dimensional) face of the Thurston norm ball, then it carries taut representatives of all classes lying in that cone.

Theorem 11.2.1 (Theorems 5.12 and 5.15 of [38])**.** *Let $\mathcal{V}$ be a layered or measurable veering triangulation of M. Then*

$$\texttt{hom}(\mathcal{V}) = \mathbb{R}_+ \cdot \texttt{F},$$

for some (not necessarily top-dimensional) face F *of the Thurston norm ball in $H_2(M, \partial M; \mathbb{R})$. Moreover,* F *is fibred if and only if $\mathcal{V}$ is layered.* □

In other words, if $\mathcal{V}$ is layered or measurable then by projecting the cone $\texttt{carried}(\mathcal{V})$ into $H_2(M, \partial M; \mathbb{R})$ we obtain a cone on a face of the Thurston norm ball. We will denote this face by $\texttt{F}_\mathcal{V}$ and call it the *face of the Thurston norm ball determined by* $\mathcal{V}$.

Remark. We say that a nonmeasurable veering triangulation determines an *empty face* of the Thurston norm ball.

11.3 Algorithm `VeeringFace`

Given a veering triangulation $\mathcal{V}$ of M the algorithm `FacePairings` (Alg. 1) fixes a spanning tree Υ of the dual graph of $\mathcal{V}$ and, using this, a basis $(h_1, \ldots, h_r)$ of H_M. Let n be the number of tetrahedra of $\mathcal{V}$. Let U be as in line 6 of the algorithm `FacePairings`, when applied to $\mathcal{V}$ and an empty list of dual cycles. Denote by φ_2 the matrix obtained from U by deleting its first $n+1-r$ rows. Let $\varphi_1 = \mathrm{I}_{n+1} \oplus 0_{n+1,n-1}$, where I_{n+1} denotes the identity matrix and $0_{n+1,n-1}$ denotes the zero matrix with $n+1$ rows and $n-1$ columns. Remarks 4.2.2 and 4.2.4 imply the following lemma.

Lemma 11.3.1. *Suppose that* $F = \{f_1, \ldots, f_{2n}\}$ *and* $F_\Upsilon = \{f_1, \ldots, f_{n+1}\}$. *With the notation as above*

$$\varphi : \mathbb{Z}^F \xrightarrow{\varphi_1} \mathbb{Z}^{F_\Upsilon} \xrightarrow{\varphi_2} H_M$$

is a homomorphism which projects a dual cycle c *to its class* $[c]$ *in* H_M, *expressed in terms of the basis* $(h_1, \ldots, h_r)$ *fixed by the algorithm* `FacePairings`. □

Now we are interested in the projection

$$\varphi^* : \mathbb{Z}^F \xrightarrow{\varphi_1^*} \mathbb{Z}^{F_\Upsilon} \xrightarrow{\varphi_2^*} H_2(M, \partial M; \mathbb{Z})$$

which maps a relative 2-cycle S to its class $[S]$ in $H_2(M, \partial M; \mathbb{Z})$, expressed in terms of the dual basis $(h_1^*, \ldots, h_r^*)$ of $H_2(M, \partial M; \mathbb{Z}) \cong H^1(M; \mathbb{Z})$.

Let B_Υ be as in Subsection 4.2.3. The matrix U satisfies

$$S = U B_\Upsilon V,$$

where S is the Smith normal form of B_Υ. The algorithm `FacePairings` relies on the observation that $H_1(M; \mathbb{Z}) \cong \operatorname{coker} B_\Upsilon$. To find the basis of $H_2(M, \partial M; \mathbb{Z})$ which is dual to $(h_1, \ldots, h_r)$ we use the fact that

$$H_2(M, \partial M; \mathbb{Z}) \cong \ker B_\Upsilon^{\mathrm{tr}}.$$

Since

$$S^{\mathrm{tr}} = V^{\mathrm{tr}} B_\Upsilon^{\mathrm{tr}} U^{\mathrm{tr}}$$

is the Smith normal form of B_Υ^{tr}, we obtain that the matrix φ_2^* is obtained from $(U^{\mathrm{tr}})^{-1}$ by deleting its first $n + 1 - r$ rows.

Note that faces dual to tree edges (*tree faces*) contribute nontrivially to the homology class of the 2-cycle which contains them. In order to find the matrix φ_1^* we need to express each tree face as a linear combination of non-tree faces. This is similar to what we did in Proposition 5.2.3, except now the linear dependencies are induced by the "usual" boundary map $\partial_3^{rel} : \mathbb{Z}^T \to \mathbb{Z}^F$ on the triangulation.

Recall from Remark 4.2.2 that a non-tree edge $f \in F_\Upsilon$ determines the non-tree cycle $\zeta(f) \in \mathbb{Z}^F$. The triangles of $\mathcal{V}$ are oriented by their coorientation and the right hand rule. Hence the rows of the matrix φ_1^* are given by $\{\zeta(f) \mid f \in F_\Upsilon\}$.

Lemma 11.3.2. *With the notation as above*

$$\varphi^* : \mathbb{Z}^F \xrightarrow{\varphi_1^*} \mathbb{Z}^{F_\Upsilon} \xrightarrow{\varphi_2^*} H_2(M, \partial M; \mathbb{Z})$$

is a homomorphism which maps a relative 2-cycle $S \in \mathbb{Z}^F$ to its homology class $[S] \in H_2(M, \partial M; \mathbb{Z})$, expressed in terms of the basis $(h_1^*, \ldots, h_r^*)$ of $H_2(M, \partial M; \mathbb{Z})$ which is dual to the basis $(h_1, \ldots, h_r)$ fixed by the algorithm `FacePairings`. □

By tensoring the free $\mathbb{Z}$-modules $\mathbb{Z}^F$, $\mathbb{Z}^{F_\Upsilon}$, H_M and $H_2(M, \partial M; \mathbb{Z})$ with $\mathbb{R}$ we may view φ, φ^* as projections

$$\varphi : \mathbb{R}^F \xrightarrow{\varphi_1} \mathbb{R}^{F_\Upsilon} \xrightarrow{\varphi_2} H_1(M; \mathbb{R})$$
$$\varphi^* : \mathbb{R}^F \xrightarrow{\varphi_1^*} \mathbb{R}^{F_\Upsilon} \xrightarrow{\varphi_2^*} H_2(M, \partial M; \mathbb{R}).$$

We give the algorithm `VeeringFace` which takes as an input a veering triangulation $\mathcal{V}$ and outputs the vertices spanning the face $\mathtt{F}_\mathcal{V}$. In the pseudocode we use the algorithm `NonTreeCycles` which given an ideal triangulation fixes a spanning tree of its dual graph (using a deterministic algorithm `SpanningTree` as in the algorithm `FacePairings`) and then outputs the list of non-tree cycles; recall Definition 4.2.3. This is a standard algorithm in graph theory for which we do not give pseudocode.

In Chapter 13 we follow the algorithm `VeeringFace` to find the face determined by the veering triangulation `eLMkbcdddedde_2100` of the 6_2^2 link complement.

Algorithm 5. `VeeringFace`
Finding the face of the Thurston norm ball determined by a veering triangulation

Input: A veering triangulation $\mathcal{V}$ of M, with the set T of tetrahedra, the set F of triangular faces and the set E of edges

Output: A list of vertices spanning the face $\mathtt{F}_\mathcal{V}$ of the Thurston norm ball in $H_2(M, \partial M; \mathbb{R})$ determined by $\mathcal{V}$

$B :=$ the branch equations matrix of $(\mathcal{T}, \alpha)$
change the parent of B to the ring of matrices with real entries
TautCone $:= \left(\ker B^{\mathrm{tr}} \cap \mathbb{R}^F_{\geq 0}\right)$
TautRays := the pritimive integral vectors on the extremal rays of TautCone
if length(TautRays) == 0 **then** # $\mathcal{V}$ is nonmeasurable
    return TautRays
else
    $\varphi_1^* :=$ Matrix(`NonTreeCycles`($\mathcal{V}$)) # $(n+1) \times 2n$ matrix, $n = |T|$
    $U, r :=$ `FacePairings`($\mathcal{V}$, [ ], return type = "matrix")
    $\varphi_2^* :=$ the matrix built from the last r rows of $(U^{\mathrm{tr}})^{-1}$ # $r \times (n+1)$ matrix
    TautRaysInHomology := $[\varphi_2^*\varphi_1^*(v)$ for v in TautRays$]$
    HomCone := the cone spanned by TautRaysInHomology

continued on the next page

Algorithm `VeeringFace` continued

13: HomRays := the primitive integral vectors on the extremal rays of HomCone
14: φ_2 := the matrix built from the last r rows of U
15: ClassOfDualGraph := $\sum_{j=1}^{n+1} \varphi_2(j)$
16: Vertices = [ ]
17: **for** v in HomRays **do**
18: TwiceNorm := $\langle v, \text{Class ofDualGraph} \rangle$
19: append Vertices with $\frac{2}{\text{TwiceNorm}} \cdot v$
20: **end for**
21: **return** Vertices
22: **end if**

Proposition 11.3.3. *Let $\mathcal{V}$ be a veering triangulation of M. If $\mathcal{V}$ is nonmeasurable then the list* `VeeringFace`$(\mathcal{V})$ *is empty. Otherwise* `VeeringFace`$(\mathcal{V})$ *consists of vertices of the face $\mathtt{F}_{\mathcal{V}}$ of the Thurston norm unit ball in $H_2(M, \partial M; \mathbb{R})$, expressed in terms of the basis which is dual to the integral basis of $H_1(M; \mathbb{R})$ fixed by the algorithm* `FacePairings`.

Proof. Let B be the branch equations matrix of $\mathcal{V}$, viewed as a matrix with real entries. The set TautCone on line 3 gives the cone `carried`$(\mathcal{V})$. If it contains any nonzero vector, it has finitely many extremal rays which are rational. The list TautRays on line 4 consists of primitive integral vectors on these extremal rays. If TautCone contains only the zero vector then $\mathcal{V}$ is nonmeasurable and the output of `VeeringFace` is the empty list.

By Lemma 11.3.2 and Theorem 11.2.1 the elements of the list TautRaysIn-Homology on line 11 span the cone $\mathbb{R}_+ \cdot \mathtt{F}_{\mathcal{V}}$. In order to find the vertices of $\mathtt{F}_{\mathcal{V}}$ we need to compute the Thurston norm in $\mathbb{R}_+ \cdot \mathtt{F}_{\mathcal{V}}$. This is, however, relatively simple using the relative Euler class $e_{\mathcal{V}} \in H^2(M, \partial M; \mathbb{R})$ associated to $\mathcal{V}$. As explained in [38, Section 5], given $[S] \in \mathbb{R}_+ \cdot \mathtt{F}_{\mathcal{V}}$

$$\|[S]\|_{\text{Th}} = -e_{\mathcal{V}}([S]) = \frac{1}{2}\langle [S], [\Gamma] \rangle, \tag{11.1}$$

where $[\Gamma]$ denotes the class of the dual graph Γ in $H_1(M; \mathbb{R})$ and $\langle \cdot, \cdot \rangle$ denotes the algebraic intersection number. By Lemma 11.3.1, the class $[\Gamma]$ is equal to the sum of H_M-pairings of $f \in F$. We compute it on line 15.

The list HomRays on line 13 consists of the primitive integral vectors on the extremal rays of $\mathbb{R}_+ \cdot \mathtt{F}_{\mathcal{V}}$. By (11.1) for every element v of HomRays the dot product

$\langle v, [\Gamma] \rangle$ is equal to twice the Thurston norm of v. Hence

$$\frac{2}{\langle v, [\Gamma] \rangle} \cdot v$$

gives the vertex of $\mathtt{F}_{\mathcal{V}}$ lying on the extremal ray of $\mathbb{R}_+ \cdot \mathtt{F}_{\mathcal{V}}$ containing v. Therefore the list Vertices on line 20 gives the full list of vertices spanning $\mathtt{F}_{\mathcal{V}}$. □

Remark. Theorem 11.2.1 has a further generalisation to Dehn fillings of M, assuming that on each filled boundary torus the Dehn filling slope intersects ladderpoles at least 6 times [35, Main Theorem].

Chapter 12

The Teichmüller polynomial

In this chapter we discuss yet another polynomial invariant of 3-manifolds, the *Teichmüller polynomial*. It was defined by McMullen in [41, Section 3] and is associated to a fibred face of the Thurston norm ball.

Similarly as in the previous chapters, we are interested in both computational and theoretical results. Relying on the results of Landry, Minsky and Taylor [38, Section 7], we give an algorithm to compute the Teichmüller polynomial of any fibred face of any hyperbolic 3-manifold. Then we use Theorem 10.3.1 to obtain a relation between the Teichmüller polynomial of a fibred face in $H^1(N;\mathbb{R})$ and the Alexander polynomial of N. We interpret this relation in terms of orientability of invariant laminations in the fibres.

12.1 The taut polynomial and the Teichmüller polynomial

Let N be a compact, oriented, hyperbolic 3-manifold which is fibred over the circle. Let $\mathtt{F}$ be a fibred face of the Thurston norm ball in $H^1(N;\mathbb{R})$. An integral primitive class from the interior of the cone $\mathbb{R}_+ \cdot \mathtt{F}$ determines a fibration

$$S \to N \to S^1$$

of N over the circle [55, Theorem 3]. N can be expressed as the mapping torus

$$N = (S \times [0,1]) \Big/ \{(x,1) \sim (\psi(x),0)\}$$

of a pseudo-Anosov homeomorphism $\psi : S \to S$ [56, Proposition 2.6]. This homeomorphism is called the *monodromy* of the fibration $S \to N \to S^1$.

As discussed in Section 3.2, the monodromy ψ determines a pair of 1-

dimensional laminations in S which are invariant under ψ. In this chapter by $\mathscr{L}$ we denote the mapping torus of the stable lamination of ψ.

Fried showed that two fibrations lying over the same fibred face $\mathtt{F}$ determine isotopic suspension flows on N [22, Theorem 14.11]. Hence up to isotopy there is a unique flow Ψ on N associated to $\mathtt{F}$. This allows us to denote the set $\{\ell_1, \ldots, \ell_k\}$ of the singular orbits of Ψ by $\mathrm{sing}(\mathtt{F})$.

Definition 12.1.1. We say that a fibred face $\mathtt{F} \subset H^1(N;\mathbb{R})$ is *fully-punctured* if $\mathrm{sing}(\mathtt{F}) = \emptyset$.

It follows from Fried's theorem that the lamination $\mathscr{L}$ is canonically associated to $\mathtt{F}$; see also [41, Corollary 3.2]. McMullen used this fact to define the *Teichmüller polynomial* $\Theta_{\mathtt{F}}$ of $\mathtt{F}$ as the zeroth Fitting invariant of the *module of transversals* to the lamination induced by $\mathscr{L}$ in the maximal free abelian cover of N [41, Section 3]. The main feature of this polynomial is that it encodes information on the stretch factors of monodromies of all fibrations lying in the fibred cone $\mathbb{R}_+ \cdot \mathtt{F}$ [41, Theorem 5.1].

If we pick a fibration lying over $\mathtt{F}$ then following Agol's algorithm [2, Section 4] yields a *layered* veering triangulation $\mathcal{V}$ of $M = N - \mathrm{sing}(\mathtt{F})$ encoding the suspension flow associated to $\mathtt{F}$. Landry, Minsky and Taylor observed that we can compute the Teichmüller polynomial of $\mathtt{F}$ using the taut polynomial of $\mathcal{V}$.

Theorem 12.1.2 (Proposition 7.2 of [38])**.** *Let N be a compact, oriented, hyperbolic 3-manifold which is fibred over the circle. Let $\mathtt{F}$ be a fibred face of the Thurston norm ball in $H^1(N;\mathbb{R})$. Denote by $\mathcal{V}$ the veering triangulation of $M = N - \mathrm{sing}(\mathtt{F})$ associated to $\mathtt{F}$. Let $i_* : H_M \to H_N$ be the epimorphism induced by the inclusion of M into N. Then*

$$\Theta_{\mathtt{F}} = i_*(\Theta_{\mathcal{V}}).$$ □

Hence the output of the algorithm `TautPolynomial` (Alg. 2) applied to a layered veering triangulation is the Teichmüller polynomial of a fully-punctured fibred face. Furthermore, the algorithm `Specialisation` (Alg. 4) can be used to compute the Teichmüller polynomial of any fibred face. We additionally need an algorithm to find a collection of dual cycles which are homologous to the boundary components of a given fibre (or, more generally, a carried surface). We give such an algorithm in Section 12.2. Using this, in Section 12.3 we give an algorithm to compute the Teichmüller polynomial.

Theorem 12.1.2 also allows us to interpret Theorem 10.3.1 as a theorem which relates the Teichmüller polynomial with the Alexander polynomial. The details of that relationship are given in Corollary 12.5.3. In Section 12.6 we explain that the formulas from Corollary 12.5.3 are controlled by orientable fibred classes.

12.2 Algorithm `BoundaryCycles`

Let $(\mathcal{T}, \alpha)$ be a transverse taut triangulation of M. Suppose that the truncated model of M has b boundary components $T_1, \ldots, T_b$. Let $n = |T|$ and let $w = (w_1, \ldots, w_{2n})$ be a nonzero, nonnegative, integral solution to the system of branch equations of $(\mathcal{T}, \alpha)$. This solution determines a surface S^w carried by $(\mathcal{T}, \alpha)$ expressed as a relative simplicial 2-cycle (2.4).

The goal of this section is to present an algorithm which given $(\mathcal{T}, \alpha)$ and w as above outputs a collection C of dual cycles which are homotopic to the boundary components of S^w. Such a collection can then be used as an input for the algorithm `Specialisation` (Alg. 4). Note that given a boundary torus T_j of M the intersection $\partial S^w \cap T_j$ might be disconnected. In this case the obtained cycle in Γ is homotopic to a *multiple* of a Dehn filling slope on T_j. Finding multiples of Dehn filling slopes is sufficient for our purpose, that is finding the projection $H_M \to H_M^C$, because H_M^C is by definition torsion-free; see (4.2).

The boundary components of the surface S^w are carried by the boundary track (defined in Section 2.3). The tuple w endows each boundary track $\beta_1, \ldots, \beta_k$, $\beta_{k+1}, \ldots, \beta_b$ with a nonnegative integral transverse measure which encodes the boundary components $\partial S^w \cap T_j$ for $1 \leq j \leq b$.

The general idea to find a dual cycle c_j homologous to $\partial S^w \cap T_j$ is as follows.

1. Perturb $\partial S^w \cap T_j$ slightly, so that it becomes transverse to the boundary track.
2. Push the (perturbed) $\partial S^w \cap T_j$ away from the boundary of M into the dual graph Γ.

First we define an auxiliary object, the *dual boundary graph* Γ^β.

Definition 12.2.1. Let $(\mathcal{T}, \alpha)$ be a (truncated) transverse taut ideal triangulation of a 3-manifold M. The *dual boundary graph* Γ^β is the oriented graph contained in ∂M which is dual to the boundary track β of $(\mathcal{T}, \alpha)$. The orientation on the edges of Γ^β is determined by α.

If $b \geq 1$ then the dual boundary graph is disconnected, with connected components $\Gamma_1^\beta, \ldots, \Gamma_b^\beta$ such that Γ_j^β is dual to the boundary track β_j. If an edge of Γ^β is dual to a branch of β lying in $f \in F$, then we label it with f. Hence for every $f \in F$ there are three edges of Γ^β labelled with f.

Example 12.2.2. The dual boundary graph for the veering triangulation `cPcbbbiht_12` of the figure-eight knot complement is presented in Figure 12.1.

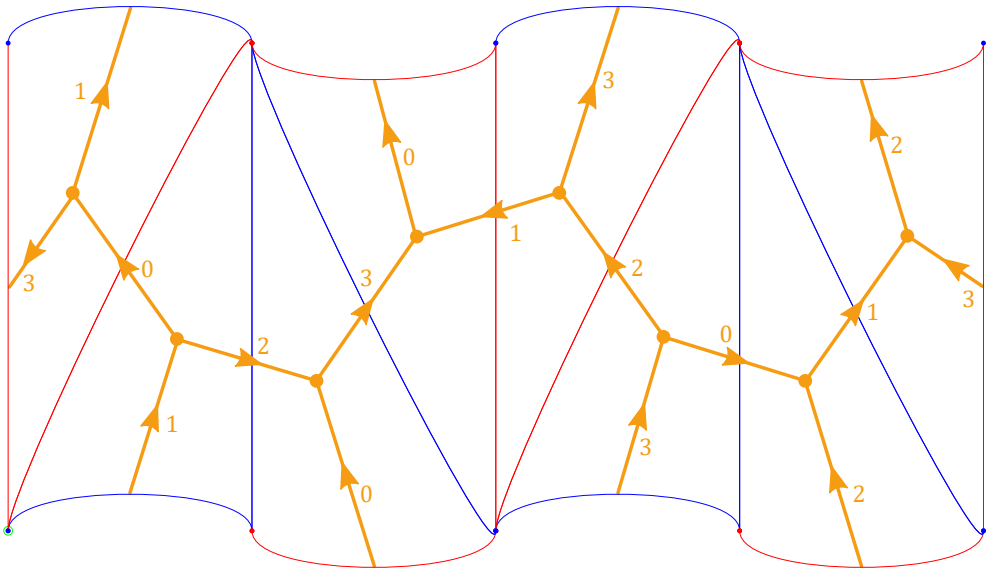

Figure 12.1: The boundary track β of the veering triangulation `cPcbbbiht_12` of the figure-eight knot complement and its dual graph Γ^β (in orange). The orientation on the edges of Γ^β is determined by the coorientation on their dual branches of β. Edges of Γ^β are labelled with indices of triangles that they pass through. The picture of the boundary track is taken from [26]. The dual boundary graph has been added by the author.

The dual boundary graph is a combinatorial tool that we use to encode paths which are transverse to the boundary track. Moreover, every cycle in the dual boundary graph can be homotoped inside M to a cycle in the dual graph.

Lemma 12.2.3. *Let $(\mathcal{T}, \alpha)$ be a transverse taut triangulation of a 3-manifold M. Denote by Γ, Γ^β its oriented dual graph and its oriented dual boundary graph, respectively. Let c^β be a cycle in Γ^β. Suppose it passes consecutively through the edges of Γ^β labelled with $f_{i_1}, \dots, f_{i_l}$, where $1 \leq i_j \leq 2n$.*

We set

$$s_{i_j} = \begin{cases} +1 & \text{if } c \text{ passes through an edge labelled with } f_{i_j} \text{ upwards} \\ -1 & \text{if } c \text{ passes through an edge labelled with } f_{i_j} \text{ downwards.} \end{cases}$$

Let c be the cycle $(s_{i_1} f_{i_1}, \dots, s_{i_l} f_{i_l})$ in the dual graph Γ. If we embed Γ^β and Γ in M in the natural way, then c^β and c are homotopic.

Proof. A homotopy between c^β and c can be obtained by pushing each edge of the cycle c^β towards the middle of the triangle through which it passes; see Figure 12.2. □

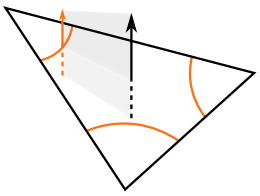

Figure 12.2: Homotoping a dual boundary cycle to a dual cycle. The black arrow is an edge of Γ dual to f. The orange arrow is an edge of Γ^β labelled with f.

Fix an integer j between 1 and b. The curve $\partial S^w \cap T_j$ is contained in the boundary track β_j. Let ϵ be a branch of β_j. Let s^- and s^+ be the initial and the terminal switches of ϵ, respectively. We replace each subarc of $\partial S^w \cap T_j$ contained in ϵ by the following 1-chain c_ϵ in Γ^β_j

$$c_\epsilon = -\begin{pmatrix}\text{outgoing branches}\\ \text{of } s^- \text{ above } \epsilon\end{pmatrix} + \begin{pmatrix}\text{incoming branches}\\ \text{of } s^+ \text{ above } \epsilon\end{pmatrix}.$$

This is schematically depicted in Figure 12.3.

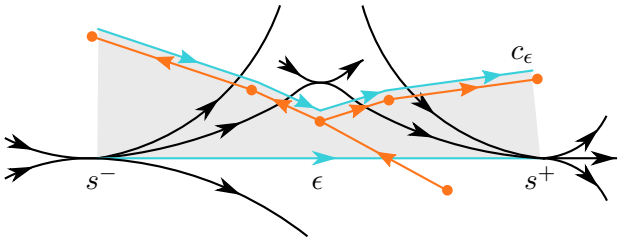

Figure 12.3: A local picture of the boundary track β (in black) and the dual boundary graph Γ^β (in orange). We push the branch ϵ of β (light blue) upwards to the 1-chain c_ϵ in Γ^β (also light blue).

Let us denote the transverse measure on ϵ determined by $w = (w_1, \ldots, w_{2n})$ by $w(\epsilon)$. The curve $\partial S^w \cap T_j$ passes through ϵ $w(\epsilon)$ times. Since chain groups are abelian, the 1-cycle in Γ^β homotopic to $\partial S^w \cap T_j$ is given by

$$c_j^\beta = \sum_{\epsilon \subset \beta_j} w(\epsilon) c_\epsilon,$$

where the sum is over all branches ϵ of β_j. By Lemma 12.2.3 we can homotope the cycles c_j^β in Γ^β to cycles c_j in Γ.

The procedure explained in this section is summed up in the algorithm `Boundary Cycles` below. In the algorithm we use the notion of *upward* and *downward*

edges. They are defined as follows. A vertex v of an ideal triangle $f \in F$ gives a branch ϵ_v of β. We say that an edge e of f is the *downward* edge for v in f if its intersection with ∂M is the initial switch of ϵ_v. An edge e of f is the *upward* edge for v in f if its intersection with ∂M is the terminal switch of ϵ_v. The names reflect the fact that when we homotope the branch ϵ_v to a 1-chain in Γ^β we go downwards above the initial switch of ϵ_v and upwards above the terminal switch of ϵ_v; see Figure 12.3.

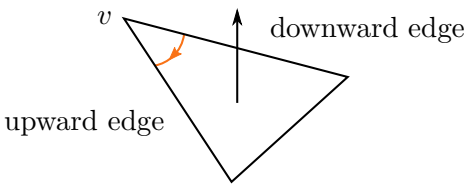

Figure 12.4: Downward and upward edges for an ideal vertex v of a triangle.

Algorithm 6. `BoundaryCycles`
Expressing boundary components of a surface carried by a transverse taut triangulation $(\mathcal{T}, \alpha)$ as dual cycles

Input:

- A transverse taut triangulation $(\mathcal{T}, \alpha)$ with n tetrahedra and b ideal vertices, $\mathcal{T} = (T, F, E)$
- A nonzero tuple $w \in \mathbb{Z}^{2n}$ of integral nonnegative weights on elements of F

Output:

- A list of b vectors from $\mathbb{Z}^{2n}$, each encoding a dual cycle c_j homotopic to $\partial S^w \cap T_j$, for $1 \leq j \leq b$

```
1:  Boundaries := the list of b zero vectors from Z^{2n}
2:  for f in F do
3:      for vertex v of f do
4:          j := the index of v as an ideal vertex of T
5:          e_1, e_2 : = the downward and upward edges of v in f
6:          for f' above f on the same side of e_1 do
7:              subtract w(f) from the entry f' of Boundaries[j]
8:          end for
9:          for f' above f on the same side of e_2 do
10:             add w(f) to the entry f' of Boundaries[j]
```

continued on the next page

Algorithm `BoundaryCycles` continued

11: **end for**
12: **end for**
13: **end for**
14: **return** Boundaries

Remark. Algorithm `BoundaryCycles` is due to Saul Schleimer and Henry Segerman. We include it here, with permission, for completeness.

12.3 Algorithm `TeichmüllerPolynomial`

Let S be an oriented, closed or punctured, surface of finite genus. Let $\psi : S \to S$ be a pseudo-Anosov homeomorphism. Denote by N the mapping torus of ψ. The unit norm ball $B_{\mathrm{Th}}(N)$ of the Thurston norm on $H_2(N, \partial N; \mathbb{R})$ admits a fibred face $\mathtt{F}$ such that $[S] \in \mathbb{R}_+ \cdot \mathtt{F}$. We give an algorithm which given ψ computes the Teichmüller polynomial of $\mathtt{F}$.

By `Veering` we denote an algorithm which given a pseudo-Anosov homeomorphism $\psi : S \to S$ outputs

- the veering triangulation $\mathcal{V}$ of the mapping torus of $\mathring{\psi} : \mathring{S} \to \mathring{S}$, where $\mathring{S}$ is obtained from S by puncturing it at the singularities of ψ and $\mathring{\psi}$ is the restriction of ψ to $\mathring{S}$,
- a nonnegative solution $w = (w_1, \ldots, w_{2n})$ to the system of branch equations of $\mathcal{V}$ such that the carried surface $S^w = \sum_{i=1}^{2n} w_i f_i$ is homologous to the fibre $\mathring{S}$.

Algorithm `Veering` is explained in [2, Section 4]. It has been implemented by Mark Bell in `flipper` [5].

Algorithm 7. `TeichmüllerPolynomial`
Computing the Teichmüller polynomial of a fibred face of the Thurston norm ball

Input: A pseudo-Anosov homeomorphism $\psi : S \to S$
Output: The Teichmüller polynomial of the face $\mathtt{F}$ in $H_2(N, \partial N; \mathbb{R})$, where N is the mapping torus of ψ and $[S] \in \mathbb{R}_+ \cdot \mathtt{F}$

1: $(\mathcal{V}, w) :=$ `Veering`(ψ)
2: $C :=$ `BoundaryCycles`$(\mathcal{V}, w)$
3: if the j-th torus cusp is not filled in N, remove $C[j]$ from the list C
4: $\Theta :=$ `Specialisation`$(\mathcal{V},$ `TautPolynomial`$(\mathcal{V}), C)$
5: **return** Θ

Proposition 12.3.1. *Let $\psi : S \to S$ be a pseudo-Anosov homeomorphism. Denote by N its mapping torus. Let $\mathtt{F}$ be the fibred face of the Thurston norm ball in $H_2(N, \partial N; \mathbb{Z})$ such that $[S] \in \mathbb{R}_+ \cdot \mathtt{F}$. Then* `TeichmüllerPolynomial`$(\psi)$ *is equal to the Teichmüller polynomial $\Theta_{\mathtt{F}}$ of $\mathtt{F}$.*

Proof. Let $\mathring{S}$ denote the surface obtained from S by puncturing it at the singularities of the invariant foliations of ψ. The pair $(\mathcal{V}, w)$ on line 1 consists of the veering triangulation of $M = N - \mathrm{sing}(\mathtt{F})$ associated to $\mathtt{F}$, and a nonnegative solution to its system of branch equations which puts $\mathring{S}$ in a fixed carried position. Then the list C constructed in line 2 consists of dual cycles homologous to the boundary components of $\mathring{S} = S^w$. If a boundary torus T of the underlying manifold of $\mathcal{V}$ is not filled in N, we remove the dual cycle encoding $S^w \cap T$ from the list C. After this, C satisfies $H_N = H_M^C$, where the meaning of the superscript C is as in (4.2).

Let $i_* : H_M \to H_N$ be the epimorphism determined by the inclusion of M into N. Since $i_* = \varrho_C$, by Proposition 10.1.1 the polynomial Θ on line 4 is equal to $i_*(\Theta_{\mathcal{V}})$ and hence, by Theorem 12.1.2, to $\Theta_{\mathtt{F}}$. □

12.4 Comparison with McMullen's computations

Note that if N is fibred over the circle with fibre S and monodromy ψ then

$$H_1(N; \mathbb{Z}) = \Big(H_1(S; \mathbb{Z}) \Big/ \{\gamma = \psi_*(\gamma)\} \Big) \oplus \mathbb{Z}. \tag{12.1}$$

Let $H_1(S; \mathbb{Z})^\psi$ denote $H_1(S; \mathbb{Z}) \Big/ \{\gamma = \psi_*(\gamma)\}$ and let H_S^ψ denote its the torsion-free part. We have

$$H_N = H_S^\psi \oplus \mathbb{Z}.$$

We say that a basis $(u_1, \ldots, u_{r-1}, u)$ of H_N such that $u_i \in H_S^\Psi$ for $i = 1, \ldots, r-1$ and $\langle [S], u \rangle = 1$ is *suited to a fibration* $S \to N \to S^1$.

In [41, Section 3] McMullen gave an algorithm to compute the Teichmüller polynomial of a fibred face $\mathtt{F}$ which relies on fixing a particular fibration lying in $\mathbb{R}_+ \cdot \mathtt{F}$ and choosing a basis for H_N which is suited to that fibration. He proved that with this choice of basis it is possible to find the fibred cone $\mathbb{R}_+ \cdot \mathtt{F}$ having just $\Theta_{\mathtt{F}}$. By Theorem 6.1 of [41] the cone $\mathbb{R}_+ \cdot \mathtt{F}$ is equal to the cone on some top-dimensional face of the dual polytope $N^*(\Theta_{\mathtt{F}})$ of the Teichmüller polynomial of $\mathtt{F}$. But since the basis is suited to a fibration from $\mathbb{R}_+ \cdot \mathtt{F}$, we know which face of $N^*(\Theta_{\mathtt{F}})$ is the "correct" one, as the cone $\mathbb{R}_+ \cdot \mathtt{F}$ must contain $(0, 0, \ldots, 0, 1) \in H^1(M; \mathbb{R})$.

In contrast, we choose our basis for H_N somewhat randomly. So while finding $N^*(\Theta_{\mathtt{F}})$ is easy, we do not know a priori which face of $N^*(\Theta_{\mathtt{F}})$ gives the fibred cone.

That is why in order to find $\mathbb{R}_+ \cdot \mathtt{F}$ we need to follow the computation explained in Section 11.3.

One might ask if Thereom 6.1 of [41] can be extended to the taut polynomials of measurable veering triangulations. That is, is the cone of homology classes of surfaces carried by a measurable veering triangulation $\mathcal{V}$ equal to the cone on some face of the dual polytope $N^*(\Theta_\mathcal{V})$ of $\Theta_\mathcal{V}$? Unfortunately, the answer to that question is generally negative.

Example 12.4.1. Let $\mathcal{V} =$ `iLLLQPcbeegefhhhhhhahahha_01110221`. This is a measurable veering triangulation of the manifold $M =$ t12032. We have

$$\Delta_M = 2a + b + 2 + b^{-1} + 2a^{-1}$$
$$\Theta_\mathcal{V} = b + 2 + b^{-1}.$$

The Newton polytope of $\Theta_\mathcal{V}$ is a vertical segment in the 2-dimensional plane $H_1(M;\mathbb{R})$. The dual set $N^*(\Theta_\mathcal{V})$ is given by $-1 \leq b^* \leq 1$, so it is not even compact.

If we pick the dual basis (a^*, b^*) of $H_2(M, \partial M; \mathbb{R})$, the cone of homology classes of surfaces carried by $\mathcal{V}$ is spanned by the rays passing through $(1,-1), (1,1)$. Note that it is equal to the cone on a face of the polytope $N^*(\Delta_M)$. But this is also not true in general, even in the fibred case [14, Section 6].

12.5 The Teichmüller polynomial and the Alexander polynomial

In this section we prove lemmas that allow us to interpret Theorem 10.3.1 as an extension to Theorem 7.1 of [41]. We summarise the findings in Corollary 12.5.3.

Recall that given a fibred face $\mathtt{F}$ of the Thurston norm ball in $H_2(N, \partial N; \mathbb{R})$ there is

- a unique (up to isotopy) 2-dimensional stable lamination $\mathscr{L}$ in N associated to $\mathtt{F}$ [41, Corollary 3.2],
- a unique veering triangulation $\mathcal{V}$ of $M = N - \mathrm{sing}(\mathtt{F})$ carrying fibres from $\mathbb{R}_+ \cdot \mathtt{F}$ punctured at the singularities of the monodromies [45, Proposition 2.7].

Note that $\mathscr{L} \subset M$. Consistently with the diagram (10.2) we denote the laminations in M^N, M^{ab} induced by $\mathscr{L} \subset M$ by $\mathscr{L}^N$, $\mathscr{L}^{ab}$, respectively. The lamination $\mathscr{L}^N$ can also be seen inside N^{ab}. By Lemma 8.1.8, $\mathscr{L}$ is transversely orientable if and only if $\mathcal{V}$ is edge-orientable. This property passes to covers of M.

Corollary 12.5.1. *Let* $\mathtt{F}$ *be a fibred face of the Thurston norm ball in* $H^1(N;\mathbb{R})$. *Let* $M = N - \mathrm{sing}(\mathtt{F})$. *Let* $\mathscr{L}$, $\mathcal{V}$ *be the stable lamination and the veering triangulation associated to* $\mathtt{F}$, *respectively. Then the lamination* $\mathscr{L}^N$ *in* N^{ab} *is transversely orientable if and only if* $\mathcal{V}^N$ *is edge-orientable.* □

It follows that if the lamination $\mathscr{L}^N \subset N^{ab}$ is transversely orientable then the edge-orientation homomorphism of $\mathcal{V}$ factors through $\sigma_N : H_N \to \{-1, 1\}$; see Lemma 8.3.1.

Recall that by $\mathrm{sing}(\mathtt{F}) = \{\ell_1, \dots, \ell_k\}$ we denote the singular orbits of the flow canonically associated to $\mathtt{F}$. In the language of Theorem 10.3.1 they correspond to the core curves of the filling solid tori in N. In Theorem 10.3.1 we needed to assume that their classes in $H_N = H_1(N;\mathbb{Z})/_{\mathrm{torsion}}$ are nontrivial. In the fibred setting we know that the classes $[\ell_j]$ have a nonzero algebraic intersection with every $[S] \in \mathrm{int}(\mathbb{R}_+ \cdot \mathtt{F}) \cap H_2(N, \partial N; \mathbb{Z})$. Therefore we get the following lemma.

Lemma 12.5.2. *Let* $\mathtt{F}$ *be a fibred face of the Thurston norm ball in* $H^1(N;\mathbb{R})$. *Let* $\mathrm{sing}(\mathtt{F}) = \{\ell_1, \dots, \ell_k\}$ *be the singular orbits of the flow associated to* $\mathtt{F}$. *Then for every* $j \in \{1, 2, \dots, k\}$ *the class* $[\ell_j]$ *in* H_N *is nontrivial.* □

Using Theorem 12.1.2, Corollary 12.5.1, Lemma 12.5.2 and Theorem 10.3.1 we derive formulas relating the Teichmüller polynomial of $\mathtt{F}$ and the Alexander polynomial of N.

Corollary 12.5.3. *Let* N *be a compact, oriented, hyperbolic 3-manifold with a fibred face* $\mathtt{F} \subset H^1(N;\mathbb{R})$ *of the Thurston norm ball. Let* $\mathrm{sing}(\mathtt{F}) = \{\ell_1, \dots, \ell_k\}$. *Denote by* $\mathscr{L}$ *the 2-dimensional lamination in* N *associated to* $\mathtt{F}$. *Assume that the lamination in* N^{ab} *induced by* $\mathscr{L}$ *is transversely orientable. Set* $s = b_1(N)$ *and* $M = N - \mathrm{sing}(\mathtt{F})$.

I. $b_1(M) \geq 2$ *and*

(a) $s \geq 2$. *Then*

$$\Theta_{\mathtt{F}}(h_1, \dots, h_s) = \Delta_N(\sigma_N(h_1) \cdot h_1, \dots, \sigma_N(h_s) \cdot h_s) \cdot \prod_{j=1}^{k} ([\ell_j] - \sigma_N([\ell_j])).$$

(b) $s = 1$. *Let* h *denote the generator of* H_N.

- *If* $\partial N \neq \emptyset$ *then*

$$\Theta_{\mathtt{F}}(h) = (h - \sigma_N(h))^{-1} \cdot \Delta_N(\sigma_N(h) \cdot h) \prod_{j=1}^{k} ([\ell_j] - \sigma_N([\ell_j])).$$

- *If N is closed then*

$$\Theta_{\mathtt{F}}(h) = (h - \sigma_N(h))^{-2} \cdot \Delta_N(\sigma_N(h) \cdot h) \cdot \prod_{j=1}^{k} ([\ell_j] - \sigma_N([\ell_j])).$$

II. $b_1(M) = 1$. Let h denote the generator of $H_N \cong H_M$.

(a) If $\partial N \neq \emptyset$ then

$$\Theta_{\mathtt{F}}(h) = \Delta_N(\sigma_N(h) \cdot h).$$

(b) If N is closed set $\ell = \ell_1$, and then

$$\Theta_{\mathtt{F}}(h) = (h - \sigma_N(h))^{-1}([\ell] - \sigma_N([\ell])) \cdot \Delta_N(\sigma_N(h) \cdot h). \qquad \square$$

12.6 Orientability of invariant laminations in the fibre

In this section we discuss how to interpret the close relation between the Teichmüller polynomial and the Alexander polynomial obtained in Corollary 12.5.3. First we point out that it implies that the Teichmüller polynomials of distict fibred faces of the same manifold are often almost the same.

Corollary 12.6.1. *Let N be a compact, oriented, hyperbolic 3-manifold which is fibred over the circle. Let $\mathtt{F}_1$, $\mathtt{F}_2$ be two fibred faces of the Thurston norm ball in $H^1(N;\mathbb{R})$. For $i = 1, 2$ denote by $\mathscr{L}_i$ the lamination associated to $\mathtt{F}_i$ and by Θ_i the Teichmüller polynomial of $\mathtt{F}_i$. If the induced laminations $\mathscr{L}_1^N, \mathscr{L}_2^N$ in N^{ab} are transversely orientable then*

$$\Theta_1(h_1, \ldots, h_s) = P(h_1, \ldots, h_s) \cdot \Theta_2(\pm h_1, \ldots, \pm h_s)$$

where P is a product of factors of the form $(h \pm 1)$ and $(h \pm 1)^{-1}$, $h \in H_N$. $\square$

Below we explain why this corollary is not surprising. Every nonzero cohomology class $\eta \in H^1(N;\mathbb{Z})$ determines an infinite cyclic cover $N^\eta \to N$. We denote the specialisation of $P \in \mathbb{Z}[H_N]$ under the associated homomorphism $H_N \to \mathbb{Z}$ by P^η. If

$$P = \sum_{h \in H_N} a_h \cdot h,$$

then

$$P^\eta(z) = \sum_{h \in H_N} a_h \cdot z^{\eta(h)}.$$

An integral cohomology class $\eta \in H^1(N;\mathbb{Z})$ from the interior of a cone over a fibred face $\mathtt{F}$ determines a fibration of N over the circle. Let ψ denote the monodromy of this fibration. McMullen showed that the largest real root of $\Theta^\eta_{\mathtt{F}}(z)$ is equal to the stretch factor of ψ [41, Theorem 5.1]. On the other hand, the largest in the absolute value real root of $\Delta^\eta_N(z)$ is equal to the homological stretch factor of ψ [44, Assertion 4]. By Theorem 3.2.2 these two numbers are equal if and only if the 1-dimensional laminations in S which are invariant under ψ are orientable. In particular, it is clear that when the lamination $\mathscr{L}$ associated to a fibred face $\mathtt{F}$ is transversely orientable, then the Teichmüller polynomial of $\mathtt{F}$ and the Alexander polynomial of N have to be very tightly related; for all cohomology classes $\eta \in \mathrm{int}(\mathbb{R}_+ \cdot \mathtt{F}) \cap H^1(N;\mathbb{Z})$ the largest real roots of their specialisations at η have to be equal up to the sign.

When the lamination $\mathscr{L}$ is not transversely orientable it is still possible that its intersection with a given fibre is an orientable 1-dimensional lamination. In this case the monodromy of the fibration reverses the orientation of the invariant laminations in the fibre.

Definition 12.6.2. Let $\mathtt{F}$ be a fibred face of the Thurston norm ball in $H^1(N;\mathbb{R})$. Let $\mathscr{L}$ be the stable lamination of the suspension flow associated to $\mathtt{F}$. Let $\eta \in \mathrm{int}(\mathbb{R}_+ \cdot \mathtt{F}) \cap H^1(N;\mathbb{Z})$. Denote by S the unique taut representative of the Poincaré-Lefschetz dual of η. We say that the fibred class η is *orientable* if the 1-dimensional lamination $S \cap \mathscr{L}$ in S is orientable.

Proposition 12.6.3. *Let $\mathtt{F}$ be a fibred face of the Thurston norm ball in $H^1(N;\mathbb{R})$. Let $\mathscr{L}$ be the lamination associated to $\mathtt{F}$. If $\mathscr{L}$ is not transversely orientable, but the induced lamination $\mathscr{L}^N \subset N^{ab}$ is transversely orientable, then a primitive class $\eta \in \mathrm{int}(\mathbb{R}_+ \cdot \mathtt{F}) \cap H^1(N;\mathbb{Z})$ is orientable if and only if for every $h \in H_N$*

$$\eta(h) = \begin{cases} \textit{odd} & \textit{if } \sigma_N(h) = -1 \\ \textit{even} & \textit{if } \sigma_N(h) = 1 \end{cases}. \tag{12.2}$$

Proof. Let S be the taut representative of the Poincaré-Lefschetz dual of η. Recall from (12.4) that η determines a splitting $H_N = H_S^\psi \oplus \mathbb{Z}$. Since we assume that $\mathscr{L}$ is not transversely orientable, η is orientable if and only if $H_S^\psi = \ker \sigma_N$.

Let $u \in H_N$ be the (Hom-)dual of η. A proof that the condition (12.2) is sufficient and necessary follows from the observation that $\eta(h) = k$ if and only if $h = h' + k \cdot u$ for some $h' \in H_S^\psi$, $k \in \mathbb{Z}$, and hence $\sigma_N(h) = \sigma_N(h') \cdot \sigma_N(u)^k$. □

To obtain an easy criterion for checking whether a given fibred class is orientable we express the condition (12.2) in terms of a fixed basis of H_N.

Corollary 12.6.4. *Let* $\mathtt{F}$ *be a fibred face of the Thurston norm ball in* $H^1(N;\mathbb{R})$. *Let* $(h_1,\dots,h_s)$ *be a basis of* H_N *and let* $(h_1^*,\dots,h_s^*)$ *be the dual basis of* $H^1(N;\mathbb{Z})$. *Denote by* $\mathscr{L}$ *the stable lamination associated to* $\mathtt{F}$.

If $\mathscr{L}$ *is not transversely orientable, but the induced lamination* $\mathscr{L}^N \subset N^{ab}$ *is transversely orientable then a primitive class*

$$\eta = a_1 h_1^* + \ldots + a_r h_r^* \in \mathrm{int}(\mathbb{R}_+ \cdot \mathtt{F}) \cap H^1(N;\mathbb{Z})$$

is orientable if and only if for every $j = 1,\dots,s$

$$a_j = \begin{cases} \textit{odd} & \textit{if } \sigma_N(h_j) = -1 \\ \textit{even} & \textit{if } \sigma_N(h_j) = 1. \end{cases} \tag{12.3}$$

In particular, with the above assumptions on $\mathscr{L}$ *there are orientable fibred classes in* $\mathbb{R}_+ \cdot \mathtt{F}$. □

Therefore the close relation between $\Theta_{\mathtt{F}}$ and Δ_N obtained in Corollary 12.5.3 is just a reflection of the fact that when the assumptions of Corollary 12.5.3 are satisfied then there are orientable fibred classes in $\mathbb{R}_+ \cdot \mathtt{F}$. By Theorem 3.2.2 specialising $\Theta_{\mathtt{F}}$ and Δ_N on such an orientable class η must yield polynomials whose largest in the absolute value real roots are equal up to a sign. Using the formulas given in Corollary 12.5.3 one can directly check that if $\mathscr{L}$ is not transversely orientable, but $\mathscr{L}^N$ is, then indeed $\Delta_N^\eta(-z)$ divides $\Theta_{\mathtt{F}}^\eta(z)$ if and only if the condition (12.3) is satisfied.

Note that the factors $([\ell_j] \pm 1)$ which appear in $\Theta_{\mathtt{F}}$, but not in Δ_N, when $\mathtt{F}$ is not fully-punctured specialise to polynomials whose only roots are roots of unity. Hence these extra factors do not carry any information on the stretch factor.

In Section 15.1 we discuss a possibility to extend the interpretation of Theorem 10.3.1 to the nonfibred setting by passing to *layered surgery parents* of nonlayered veering triangulations.

Using the splitting (12.1) determined by a fibration we can show that when the lamination $\mathscr{L}^N$ in the maximal free abelian cover N^{ab} is not transversely orientable, then no fibred class in the corresponding fibred cone is orientable.

Proposition 12.6.5. *Let* $\mathtt{F}$ *be a fibred face of the Thurston norm ball in* $H^1(N;\mathbb{R})$*. Let* $\mathscr{L}$ *be the stable lamination associated to* $\mathtt{F}$*. If the induced lamination* $\mathscr{L}^N$ *in* N^{ab} *is not transversely orientable, then there is no orientable fibred class in the interior of* $\mathbb{R}_+ \cdot \mathtt{F}$*.*

Proof. Let $M = N - \mathrm{sing}(\mathtt{F})$ and let $\mathcal{V}$ be the veering triangulation of M determined by $\mathtt{F}$. Let $i^* : H^1(N;\mathbb{R}) \to H^1(M;\mathbb{R})$ be the homomorphism induced by the inclusion of M into N. Let $\eta \in \mathrm{int}(\mathbb{R}_+ \cdot \mathtt{F}) \cap H^1(N;\mathbb{Z})$. Let S be the fibre of a fibration of M determined by $i^*\eta \in H^1(M;\mathbb{Z})$, and let ψ denote the monodromy of this fibration. As in (12.1) we get a splitting

$$H_1(M;\mathbb{Z}) = H_1(S;\mathbb{Z})^\psi \oplus \mathbb{Z}.$$

Observe that the edge-orientation homomorphism ω of $\mathcal{V}$ always factors through $\overline{\omega} : H_1(M;\mathbb{Z}) \to \{-1,1\}$. The class η is orientable if and only if $i^*\eta$ is orientable, that is if and only if $H_1(S;\mathbb{Z})^\psi \leq \ker \overline{\omega}$.

First suppose that $\mathtt{F}$ is fully-punctured. By Corollaries 9.3.2 and 12.5.1, if $\mathscr{L}^N = \mathscr{L}^{ab}$ is not transversely orientable, then there is a torsion element in $H_1(S;\mathbb{Z})^\psi$ with a nontrivial image under $\overline{\omega}$.

If $\mathtt{F}$ is not fully-punctured then the lamination $\mathscr{L}^N$ in N^{ab} is not transversely orientable either because $\mathscr{L}^{ab}$ in M^{ab} is not transversely orientable, or because at least one of the Dehn filling slopes that recover N from M has a nontrivial image under $\overline{\omega}$. In either case we obtain an element of $H_1(S;\mathbb{Z})^\psi$ with a nontrivial image under $\overline{\omega}$. □

Proposition 12.6.5 and Theorem 3.2.2 imply that if the lamination $\mathscr{L}^N$ in N^{ab} is not transversely orientable, then the largest in the absolute value real roots of Δ_N^η and $\Theta_{\mathtt{F}}^\eta$ are different for every fibred class $\eta \in \mathbb{R}_+ \cdot \mathtt{F}$.

Chapter 13

Example: the face of the Thurston norm ball determined by `eLMkbcddddedde_2100`

Let M be the complement of the 6_2^2 link complement, that is the manifold m203 in the SnapPea census. We consider the veering triangulation $\mathcal{V} =$ `eLMkbcddddedde_2100` of M presented in Figure 13.1.

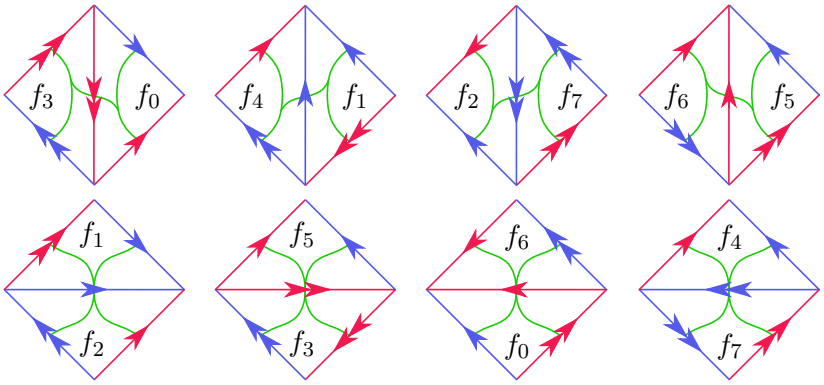

Figure 13.1: The veering triangulation `eLMkbcddddedde_2100` of the manifold m203.

In Section 13.1 we follow the algorithm `VeeringFace` to find the face `F` of the Thurston norm ball in $H_2(M, \partial M; \mathbb{R})$ determined by $\mathcal{V}$. The face `F` is fibred because $\mathcal{V}$ is layered; see Theorem 11.2.1.

Note that in the face f_7 two half-branches of the upper track of $\mathcal{V}$ form the core curve of the Möbius band. Thus $\mathcal{V}$ is not edge-orientable. Since $H_1(M; \mathbb{Z}) = \mathbb{Z} \oplus \mathbb{Z}$, by Corollary 12.6.4 the triangulation $\mathcal{V}^{ab}$ induced in the maximal free abelian cover

of M is edge-orientable. Therefore $\Theta_{\mathcal{V}} = \Theta_{\mathtt{F}}$ is closely related to Δ_M. Using Corollary 12.6.4 we can easily find orientable fibred classes in $\mathbb{R}_+ \cdot \mathtt{F}$.

In Section 13.2 we analyse two fibrations of m203 lying in $\mathbb{R}_+ \cdot \mathtt{F}$. One of them satisfies the assumption of Corollary 12.6.4 and the other does not. We directly check orientability of the stable laminations of their monodromies by finding representatives of the fibres in a fixed carried position.

13.1 The face of the Thurston norm ball determined by $\mathcal{V}$

The first step to find the face of the Thurston norm ball determined by $\mathcal{V}$ is to find the cone $\texttt{carried}(\mathcal{V}) \subset \mathbb{R}^F$ of surfaces carried by $\mathcal{V}$. Using `taut_polytope.taut_rays` from [48] we find the primitive integral vectors on the extremal rays of $\texttt{carried}(\mathcal{V})$.

$$\begin{array}{llll}
[(0,0,1,0,1,0,2,0), & (2,3,0,0,2,0,0,1), & (1,1,0,0,1,0,1,0), & (1,2,0,0,0,1,0,0),\\
(2,0,0,1,2,0,3,0), & (3,0,0,4,0,3,0,2), & (1,0,0,1,1,0,0,1), & (1,0,0,1,0,1,1,0),\\
(0,0,2,1,0,2,3,0), & (0,0,3,2,3,0,0,4), & (0,0,1,1,0,1,0,1), & (0,1,1,0,1,0,0,1),\\
(0,1,1,0,0,1,1,0), & (0,3,2,0,0,2,0,1)] & &
\end{array}$$

We use Lemmas 11.3.1 and 11.3.2 to compute the projections

$$\varphi : \mathbb{R}^F \to H_1(M;\mathbb{R})$$
$$\varphi^* : \mathbb{R}^F \to H_2(M, \partial M;\mathbb{R}).$$

We pick a spanning tree $\Upsilon = \{f_0, f_5, f_6\}$ of the dual graph of $\mathcal{V}$. We consider the Smith normal form $S = UB_\Upsilon V$ of B_Υ. The last $r = 2$ rows of S are zero and

$$U = \begin{array}{c} \begin{matrix} f_1 & f_2 & f_3 & f_4 & f_7 \end{matrix} \\ \begin{bmatrix} 3 & 0 & -2 & 0 & 0 \\ -4 & -1 & 2 & 0 & 0 \\ 2 & 1 & -1 & 0 & 0 \\ 4 & 1 & -2 & 1 & 0 \\ -3 & 0 & 2 & 0 & 1 \end{bmatrix} \end{array}, \quad \left(U^{\mathrm{tr}}\right)^{-1} = \begin{array}{c} \begin{matrix} f_1 & f_2 & f_3 & f_4 & f_7 \end{matrix} \\ \begin{bmatrix} -1 & 0 & -2 & 0 & 1 \\ -2 & 1 & -3 & 1 & 0 \\ -2 & 2 & -3 & 0 & 0 \\ 0 & 0 & 0 & 1 & 0 \\ 0 & 0 & 0 & 0 & 1 \end{bmatrix} \end{array}.$$

By Lemma 11.3.1

$$\varphi = \begin{array}{c} \begin{matrix} f_0 & f_1 & f_2 & f_3 & f_4 & f_5 & f_6 & f_7 \end{matrix} \\ \begin{bmatrix} 0 & 4 & 1 & -2 & 1 & 0 & 0 & 0 \\ 0 & -3 & 0 & 2 & 0 & 0 & 0 & 1 \end{bmatrix} \end{array},$$

hence $[\Gamma] = (4, 0)$. The matrix $\varphi_1^* : \mathbb{R}^F \to \mathbb{R}^{F_\Upsilon}$ whose rows are non-tree cycles is equal to

$$\varphi_1^* = \begin{array}{c} \\ f_1 \\ f_2 \\ f_3 \\ f_4 \\ f_7 \end{array} \begin{array}{c} \begin{matrix} f_0 & f_1 & f_2 & f_3 & f_4 & f_5 & f_6 & f_7 \end{matrix} \\ \begin{bmatrix} 1 & 1 & 0 & 0 & 0 & 1 & -1 & 0 \\ 1 & 0 & 1 & 0 & 0 & 0 & 0 & 0 \\ -1 & 0 & 0 & 1 & 0 & -1 & 1 & 0 \\ 0 & 0 & 0 & 0 & 1 & 1 & 0 & 0 \\ 0 & 0 & 0 & 0 & 0 & 0 & 1 & 1 \end{bmatrix} \end{array}.$$

Thus, by Lemma 11.3.2, the projection $\mathbb{R}^F \to H_2(M, \partial M; \mathbb{R})$ is given by

$$\varphi^* = \begin{array}{c} \begin{matrix} f_0 & f_1 & f_2 & f_3 & f_4 & f_5 & f_6 & f_7 \end{matrix} \\ \begin{bmatrix} 0 & 0 & 0 & 0 & 1 & 1 & 0 & 0 \\ 0 & 0 & 0 & 0 & 0 & 0 & 1 & 1 \end{bmatrix} \end{array}.$$

By computing the images of the primitive integral vectors on the extremal rays of $\texttt{carried}(\mathcal{V})$ under φ^* we find that the cone $\mathbb{R}_+ \cdot \mathtt{F}$ is spanned by the rays in directions $(1, 0)$ and $(1, 2)$. Since

$$\|(1,0)\|_{\mathrm{Th}} = \frac{1}{2}\langle (4,0), (1,0) \rangle = 2,$$
$$\|(1,2)\|_{\mathrm{Th}} = \frac{1}{2}\langle (4,0), (1,2) \rangle = 2,$$

the face $\mathtt{F}$ determined by $\mathcal{V}$ is spanned by vertices $\left(\frac{1}{2}, 0\right)$ and $\left(\frac{1}{2}, 1\right)$. We present the face $\mathtt{F}$ and the cone on $\mathtt{F}$ in Figure 13.2.

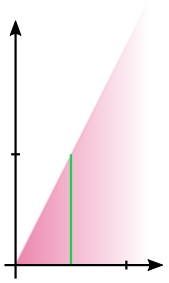

Figure 13.2: Green: the fibred face $\mathtt{F}$ of the Thurston norm unit ball in $H_2(M, \partial M; \mathbb{R})$ determined by $\mathcal{V}$. Pink: the fibred cone $\mathbb{R}_+ \cdot \mathtt{F}$.

13.2 Fibrations determined by the classes $(1, 1)$ and $(2, 1)$

Since the face $\mathtt{F}$ is fibred, by Theorem 12.1.2 the taut polynomial of $\mathcal{V}$ is equal to the Teichmüller polynomial of $\mathtt{F}$. The Alexander polynomial of M and the Teichmüller polynomial of $\mathtt{F}$ are as follows.

$$\Delta_M(a, b) = a^2 b + a^2 - ab + b^2 + b$$
$$\Theta_{\mathtt{F}}(a, b) = -a^2 b + a^2 + ab + b^2 - b = \Delta_M(a, -b).$$

In Figure 13.3 we show that the cone of homology classes of surfaces carried by $\mathcal{V}$ is equal to the cone on a face of the dual polytope of $\Theta_{\mathtt{F}}$ [41, Theorem 6.1].

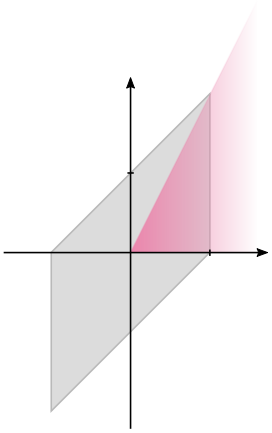

Figure 13.3: The dual polytope of the taut polynomial of $\mathcal{V} =$ `eLMkbcdddddedde_2100`. The cone of homology classes of surfaces carried by $\mathcal{V}$ is shaded in pink.

Since $\sigma(a) = 1$ and $\sigma(b) = -1$, by Corollary 12.6.4 the primitive orientable fibred classes in $\mathbb{R}_+ \cdot \mathtt{F}$ are of the form $(2k, l)$ where $k, l \in \mathbb{Z}$ and $\gcd(2, l) = \gcd(k, l) = 1$.

13.2.1 $\eta = (1,1) \in \mathbb{R}_+ \cdot \mathtt{F}$

This class does not satisfy the condition (12.3). We verify that the stable lamination in the fibre determined by η is indeed nonorientable.

The specialisations of the Alexander polynomial of M and the Teichmüller polynomial of $\mathtt{F}$ at η are as follows.

$$\Delta_M^\eta(z) = z^3 + z^2 - z^2 + z^2 + z = z(z^2 + z + 1)$$
$$\Theta_{\mathtt{F}}^\eta(z) = -z^3 + z^2 + z^2 + z^2 - z = -z(z^2 - 3z + 1).$$

The only real root of $\Delta_M^\eta(z)$ is 0. Real roots of $\Theta_{\mathtt{F}}^\eta(z)$ are 0 and $\frac{3\pm\sqrt{5}}{2}$. Therefore the stretch factor of the monodromy of the fibration determined by η is equal to $\frac{3+\sqrt{5}}{2} \approx 2.62$. The invariant laminations of the monodromy are nonorientable by Theorem 3.2.2.

We can also check this directly. The relative 2-cycle $S = f_1 + f_2 + f_4 + f_7$ is a carried representative of $(1,1)$. We present it in Figure 13.4. This surface is a four times punctured sphere and the stable train track in S is nonorientable.

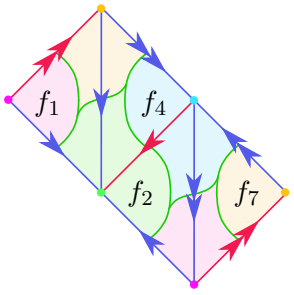

Figure 13.4: The 2-cycle $f_1 + f_2 + f_4 + f_7$ represents $(1,1) \in \mathbb{R}_+ \cdot \mathtt{F}$. Each complementary region of the stable train track is shaded with a different colour.

13.2.2 $\eta = (2,1) \in \mathbb{R}_+ \cdot \mathtt{F}$

This class satisfies the condition (12.3). We verify that the stable lamination in the fibre determined by η is indeed orientable.

The specialisations of the Alexander polynomial of M and the Teichmüller polynomial of $\mathtt{F}$ at η are as follows.

$$\Delta_M^\eta(z) = z^5 + z^4 - z^3 + z^2 + z = z(z^4 + z^3 - z^2 + z + 1)$$
$$\Theta_{\mathtt{F}}^\eta(z) = -z^5 + z^4 + z^3 + z^2 - z = \Delta_M^\eta(-z).$$

The real roots of $\Delta_M^\eta(z)$ are 0 and $\frac{-1-\sqrt{13}\pm\sqrt{2(\sqrt{13}-1)}}{4}$. Real roots of $\Theta_{\mathtt{F}}^\eta(z)$ are 0 and

$\frac{1+\sqrt{13}\pm\sqrt{2(\sqrt{13}-1)}}{4}$. Therefore the stretch factor of the monodromy of the fibration determined by η is equal to $\frac{1+\sqrt{13}+\sqrt{2(\sqrt{13}-1)}}{4} \approx 1.72$. The invariant laminations of the monodromy are orientable by Theorem 3.2.2.

We can also check this directly. The relative 2-cycle $S = 2f_0 + 3f_1 + 2f_4 + f_7$ is a carried representative of $(2, 1)$. We present it in Figure 13.5. S is a genus 2 surface with 2 punctures and the stable train track in S is orientable.

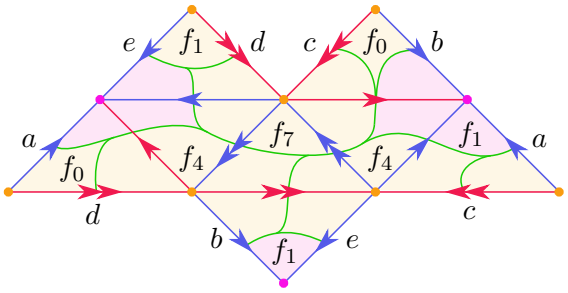

Figure 13.5: The 2-cycle $2f_0+3f_1+2f_4+f_7$ represents $(2, 1) \in \mathbb{R}_+\mathbf{F}$. Each complementary region of the stable train track is shaded with a different colour. Letters a, b, c, d, e indicate side identifications.

Chapter 14

Example: the Teichmüller polynomial of a not fully-punctured fibred face

A majority of computations of multivariable Teichmüller polynomials previously known in the literature concern only fully-punctured fibred faces. Such Teichmüller polynomials can be computed using the algorithm `TautPolynomial` (Alg. 2). Table 14.1 compares the outputs of this algorithm with computations of other authors.

Table 14.1: Teichmüller polynomials of fully-punctured fibred faces previously known in the literature compared to the outputs of `TautPolynomial` on the associated veering triangulations.

Example 1	
Source of the example	McMullen [41, Subsection 11.I]
Polynomial in the source	$1 - u - ut - ut^{-1} + u^2$
Veering triangulation $\mathcal{V}$	`eLMkbcddddedde_2100`
`TautPolynomial`$(\mathcal{V})$	$a^2b - a^2 - ab - b^2 + b$
Change of basis	$t \mapsto ab^{-1}$, $u \mapsto a$
Example 2	
Source of the example	McMullen [41, Subsection 11.II]
Polynomial in the source	$t^{-2} - ut - u - ut^{-1} - ut^{-2} - ut^{-3} + u^2$
Veering triangulation $\mathcal{V}$	`ivvPQQcfghghfhgfaddddaaaa_20000222`
`TautPolynomial`$(\mathcal{V})$	$ab^4 - a^2b^2 + ab^3 + ab^2 + ab - b^2 + a$
Change of basis	$t \mapsto b^{-1}$, $u \mapsto ab$

Example 3	
Source of the example	Lanneau & Valdez [39, Subsection 7.2]
Polynomial in the source	$u^2 - ut_At_B - ut_B - u - ut_A^{-1} + t_B$
Veering triangulation $\mathcal{V}$	`gvLQQcdeffefffaafa_201102`
`TautPolynomial`($\mathcal{V}$)	$a^2bc^2 - abc - ac^2 - ab - ac + 1$
Change of basis	$t_A \mapsto bc^{-1}$, $t_B \mapsto b^{-1}c^2$, $u \mapsto ac^2$

In this chapter we compute the Teichmüller polynomials of not fully-punctured fibred faces. This is a rather involved computation, relying on multiple algorithms given in this thesis (`FacePairings`, `TautPolynomial`, `BoundaryCycles` and `Specialisation`). We use Python modules which implement these algorithms [48] and present the computation in the form which mimics a command line Sage session [53].

14.1 Filling the 8_2^4 link complement along boundary components of a fibre

Let M be the 8_2^4 link complement, that is the manifold t12047 from the SnapPea census. It has 4 torus cusps and $H_1(M;\mathbb{Z}) = H_M = \mathbb{Z}\oplus\mathbb{Z}\oplus\mathbb{Z}\oplus\mathbb{Z}$. This manifold admits a layered veering triangulation `ivvPQQcfhghgfghfaaaaaaaaa_01122000`, which we denote by $\mathcal{V}$. Let `F` be the fibred face of the Thurston norm ball in $H^1(M;\mathbb{R})$ determined by $\mathcal{V}$.

We will fix an integral class from the interior of the fibred cone $\mathbb{R}_+ \cdot$ `F`. It determines Dehn filling slopes on the boundary tori of M which are parallel to the boundary components of the fibre. We will compute the specialisations of the taut polynomial of $\mathcal{V}$ under Dehn filling one, two, three, and four boundary components of M along these slopes. By Theorem 12.1.2 they are equal to the Teichmüller polynomials of the fibred faces of the Dehn-filled manifolds. We will also compute the specialisations of the Alexander polynomial of M under these Dehn fillings to experimentally verify the claim of Theorem 10.3.1.

First we compute $\Theta_{\mathcal{V}}$ and Δ_M.

```
sage: import snappy
sage: import regina
sage: import taut_polynomial
sage: t12047='ivvPQQcfhghgfghfaaaaaaaaa_01122000'
sage: taut_polynomial.taut_polynomial_via_tree(t12047)
```

```
a*b*c*d - a*c*d - b*c*d - b*c - a*d - a - b + 1
sage: taut_polynomial.taut_polynomial_via_tree(t12047,mode='
    alexander')
a*b*c*d - a*c*d - b*c*d + b*c + a*d - a - b + 1
```

Since $H_1(M;\mathbb{Z})$ is torsion-free, using Corollary 9.3.2 we could have predicted that $\Theta_{\mathcal{V}}$ and Δ_M differ only by sign changes in variables. But the above computation tells us which basis elements are twisted. This in turn allows us to use Corollary 12.6.4 to find orientable fibred classes in $\mathbb{R}_+ \cdot \mathtt{F}$.

We obtained $\Theta_{\mathcal{V}}(a,b,c,d) = \Delta_M(a,b,-c,-d)$. Therefore primitive orientable fibred classes in $\mathbb{R}_+ \cdot \mathtt{F}$ are of the form $(2k, 2l, m, n)$ with $\gcd(k,l,m,n) = \gcd(2,m) = \gcd(2,n) = 1$.

14.1.1 Dehn filling determined by $\eta = (2,2,1,1)$

First we verify that $\eta = (2,2,1,1)$ is contained in the interior of $\mathbb{R}_+ \cdot \mathtt{F}$.

```
sage: import taut_polytope
sage: cone_in_homology=taut_polytope.cone_in_homology(t12047)
sage: Cone(cone_in_homology).interior_contains((2,2,1,1))
True
```

Let S be the taut representative of the Poincaré-Lefschetz dual of η. To compute the specialisations of $\Theta_{\mathcal{V}}$ and Δ_M under Dehn filling M along the slopes parallel to the boundary components of S we need to find a weight vector which puts S in a fixed carried position.

```
sage: taut_cone=taut_polytope.taut_rays(t12047)
sage: P=taut_polytope.projection_to_homology(t12047)
sage: projected_taut_rays=[P*v for v in taut_cone]
sage: projected_taut_rays
[(1, 0, 1, -1),
 (0, 1, 0, 0),
 (1, 1, 0, -1),
 (1, 1, -1, 0),
 (0, 0, 1, 0),
 (0, 0, 0, 1),
 (1, 0, 0, 0),
 (1, 1, 1, -1),
 (1, 1, 0, 0),
 (1, 1, 0, 0),
 (1, 1, 0, 0),
 (1, 1, 1, -1),
 (1, 1, 0, 0),
 (1, 1, -1, 1),
 (1, 1, 0, 0),
```

```
 (0, 1, -1, 1),
 (1, 1, 0, 0),
 (1, 1, -1, 1),
 (1, 1, 0, 0),
 (1, 1, 0, 0)]
#we express (2,2,1,1) as a nonnegative linear combination of
    projected_taut_rays
sage: class2211=projected_taut_rays[4]+projected_taut_rays[5]+2*
    projected_taut_rays[8]
sage: class2211
(2, 2, 1, 1)
#now we use linearity of the projection to find a relative
    simplicial 2-cycle representing the fibre
sage: surface2211=taut_cone[4]+taut_cone[5]+2*taut_cone[8]
sage: surface2211
(0, 0, 3, 2, 0, 1, 3, 2, 0, 1, 0, 0, 0, 0, 0, 0)
```

Now that we have the fibre represented as a nonnegative relative 2-cycle, we can express its boundary components as dual cycles.

```
sage: import taut
sage: tri,angle=taut.isosig_to_tri_angle(t12047)
sage: import transverse_taut
sage: coorientations = transverse_taut.is_transverse_taut(t12047,
    return_type = "tet_vert_coorientations")
sage: import taut_carried
sage: bc2211=taut_carried.boundary_cycles_from_surface(tri,angle,
    surface2211,coorientations)
sage: bc2211
[[0, 0, 0, 0, -3, 3, 0, -1, 0, -1, 0, -1, -1, 0, 4, -4],
 [0, 1, 0, 1, 1, 0, 0, 0, 2, -2, -1, 0, 2, 0, 0, 0],
 [0, 0, 0, 0, 2, -2, 0, 1, 1, 0, 2, 1, -1, 0, 0, 0],
 [0, -1, 0, -1, 0, -1, 0, 0, -3, 3, -1, 0, 0, 0, -4, 4]]
```

Let N denote the closed Dehn filling of M determined by η. Corollary 12.6.4 implies that $\eta = (2, 2, 1, 1)$ is an orientable fibred class. In particular, the boundary components of S are untwisted and hence $\mathcal{V}^N$ is edge-orientable; see Subsection 10.3.1. By Theorem 10.3.1, the specialisations of the taut polynomial of $\mathcal{V}$ and of the Alexander polynomial of M determined by η differ only by sign changes in variables. We now verify this experimentally.

Since we are particularly interested in multivariable Teichmüller polynomials of not fully-punctured fibred faces, and $b_1(N) = 1$, we also consider the intermediate (not closed) Dehn fillings of M.

```
#filling the first cusp
sage: taut_polynomial.taut_polynomial_image(t12047,[bc2211[0]])
```

```
a*b^4 - b^2*c^3 - a*c^4 - b*c^4 - a*b^3 - b^4 - a*b^2*c + c^4
sage: taut_polynomial.taut_polynomial_image(t12047,[bc2211[0]],mode
    ='alexander')
a*b^4 + b^2*c^3 - a*c^4 - b*c^4 - a*b^3 - b^4 + a*b^2*c + c^4
#the specialisations differ by (a,b,c)->(a,b,-c)

#filling the first two cusps
sage: taut_polynomial.taut_polynomial_image(t12047,[bc2211[0],
    bc2211[1]])
a^14*b^8 - a^12*b^8 - a^9*b^5 - a^8*b^5 - a^6*b^3 - a^5*b^3 - a^2 +
     1
sage: taut_polynomial.taut_polynomial_image(t12047,[bc2211[0],
    bc2211[1]],mode='alexander')
a^14*b^8 - a^12*b^8 - a^9*b^5 + a^8*b^5 + a^6*b^3 - a^5*b^3 - a^2 +
     1
#the specialisations differ by (a,b)->(-a,-b)

#filling the first three cusps
sage: taut_polynomial.taut_polynomial_image(t12047,[bc2211[0],
    bc2211[1],bc2211[2]])
a^6 - 2*a^4 - 2*a^3 - 2*a^2 + 1
sage: taut_polynomial.taut_polynomial_image(t12047,[bc2211[0],
    bc2211[1],bc2211[2]],mode='alexander')
a^6 - 2*a^4 + 2*a^3 - 2*a^2 + 1
#the specialisations differ by a->-a

#filling all cusps -- we are already at rank 1, so nothing changes
sage: taut_polynomial.taut_polynomial_image(t12047,bc2211)
a^6 - 2*a^4 - 2*a^3 - 2*a^2 + 1
sage: taut_polynomial.taut_polynomial_image(t12047,bc2211,mode='
    alexander')
a^6 - 2*a^4 + 2*a^3 - 2*a^2 + 1
```

14.1.2 Dehn filling determined by $\eta = (1, 1, 0, 0)$

In this subsection we follow the same steps as in Subsection 14.1.1, this time to compute the specialisations of the taut polynomial of $\mathcal{V}$ and of the Alexander polynomial of M under Dehn fillings determined be the fibred class $\eta = (1, 1, 0, 0)$. By Corollary 12.6.4, this class is not orientable and we will see that specialisations differ by more than sign changes in variables.

```
#we check whether (1,1,0,0) is in the interior of the fibred cone
sage: Cone(cone_in_homology).interior_contains((1,1,0,0))
True
#we express (1,1,0,0) as a nonnegative linear combination of
    projected_taut_rays
```

```
sage: class1100=projected_taut_rays[19]
sage: class1100
(1, 1, 0, 0)
#we use linearity of the projection to find a relative simplicial
    2-cycle representing the fibre
sage: surface1100=taut_cone[19]
sage: surface1100
(0, 0, 0, 0, 0, 0, 0, 0, 0, 0, 1, 0, 1, 0, 1, 1)
#the Euler characteristic of the fibre is -2 and hence it is a four
     times punctured sphere; in particular all boundary components
    are twisted

#we express boundary components of the fibre as dual cycles
sage: bc1100=taut_carried.boundary_cycles_from_surface(tri,angle,
    surface1100,coorientations)
sage: bc1100
[[0, 1, 1, 0, 0, 0, 0, -1, 0, 0, 0, -1, 0, 0, 0, 0],
 [1, 0, 0, 1, 0, 0, -1, 0, 0, 0, 0, 0, 0, -1, 0, 0],
 [-1, 0, -1, 0, 0, 0, 0, 1, 0, 0, 0, 0, 0, 1, 0, 0],
 [0, -1, 0, -1, 0, 0, 1, 0, 0, 0, 0, 1, 0, 0, 0, 0]]

#filling the first cusp
sage: taut_polynomial.taut_polynomial_image(t12047, [bc1100[0]])
a*b^2*c - 2*a*b*c - b^2*c - a^2 - 2*a*b + a
sage: taut_polynomial.taut_polynomial_image(t12047, [bc1100[0]],
    mode='alexander')
a*b^2*c - b^2*c - a^2 + a
#specialisations differ by more than sign changes in variables
    because the capped off boundary component of the fibre is
    twisted

#filling the first two cusps
sage: taut_polynomial.taut_polynomial_image(t12047, [bc1100[0],
    bc1100[1]])
a*b^2 - a^2 - 4*a*b - b^2 + a
sage: taut_polynomial.taut_polynomial_image(t12047, [bc1100[0],
    bc1100[1]],mode='alexander')
a*b^2 - a^2 - b^2 + a

#filling the first three cusps
sage: taut_polynomial.taut_polynomial_image(t12047, [bc1100[0],
    bc1100[1],bc1100[2]])
a^2 - 6*a + 1
sage: taut_polynomial.taut_polynomial_image(t12047, [bc1100[0],
    bc1100[1],bc1100[2]],mode='alexander')
a^2 - 2*a + 1
```

```
#filling all cusps
sage: taut_polynomial.taut_polynomial_image(t12047, bc1100)
a^2 - 6*a + 1
sage: taut_polynomial.taut_polynomial_image(t12047, bc1100,mode='
    alexander')
a^2 - 2*a + 1
```

Chapter 15

Future research directions

In this chapter we return to denoting the torsion-free part of $H_1(M;\mathbb{Z})$ by H.

As shown in this thesis, the taut polynomial is very closely related to the Alexander polynomial. Even the algebraic setup for the computation is very similar. The vast literature on the Alexander polynomial can therefore be an abundant source of research ideas concerning the taut polynomial.

There is, however, one very important remark to make. By Proposition 9.3.1, if $\mathcal{V}^{ab}$ is edge-orientable then the properties of the taut polynomial of $\mathcal{V}$ can be directly derived from the properties of the Alexander polynomial of the underlying manifold M. Therefore the most interesting taut polynomials are the ones associated to veering triangulations whose maximal free abelian cover is *not* edge-orientable. Comparing the taut polynomial of such veering triangulations with the Alexander polynomial is outside the scope of this thesis; we only observed in Subsection 9.3.1 that ($\Theta_{\mathcal{V}}$ mod 2) and (Δ_M mod 2) always have a common factor.

Virtually every question that has ever been asked with regard to the Alexander polynomial can be restated in the context of the taut polynomial. In this chapter we do not aim to mention many of them. Instead, we concentrate on describing two research projects that relate to the content of this thesis the most.

15.1 Layered surgery parents of nonlayered veering triangulations

Every pseudo-Anosov flow restricts to a suspension flow in the complement of finitely many closed orbits [7, Theorem 1]. The original pseudo-Anosov flow on N determines a veering triangulation $\mathcal{V}$ of $M = N - \mathrm{sing}(\Psi)$. The restricted suspension flow determines a layered veering triangulation $\mathring{\mathcal{V}}$ of $\mathring{M} = M - \Lambda$, where Λ denotes the set of orbits that we drill out to pass to a suspension. We call $\mathring{\mathcal{V}}$ a *layered surgery*

parent of $\mathcal{V}$. Observe that $\mathring{\mathcal{V}}$ is edge-orientable if and only if $\mathcal{V}$ is.

If the conjecture that every veering triangulation comes from a pseudo-Anosov flow is true then every veering triangulation admits a layered surgery parent. In Section 12.6 we interpreted Theorem 10.3.1 in the fibred setting in terms of orientability of the laminations in the fibre that are invariant under the monodromy of a fibration. Layered surgery parents of nonlayered veering triangulations could be used to extend the interpretation of Theorem 10.3.1 to the nonfibred setting.

Proposition 15.1.1. *Let $\mathcal{V}$ be a veering triangulation of a 3-manifold M with $b_1(M) > 1$. Suppose that $\mathcal{V}$ comes from a pseudo-Anosov flow. Let $\mathring{M}$ be a 3-manifold which admits a layered surgery parent $\mathring{\mathcal{V}}$ of $\mathcal{V}$. Then $\mathring{M} = M - \Lambda$ for some collection of curves $\Lambda = \{\ell_1, \dots, \ell_k\} \subset M$. Let $\mathring{H}$ be the torsion-free part of $H_1(\mathring{M}; \mathbb{Z})$ and let $i_* : \mathring{H} \to H$ be induced by the inclusion of $\mathring{M}$ into M. If $\mathcal{V}^{ab}$ is edge-orientable and the classes $[\ell_j] \in H$ are nontrivial then*

$$i_*(\Theta_{\mathring{\mathcal{V}}}) = \Theta_{\mathcal{V}} \cdot \prod_{j=1}^{k} \left([\ell_j] - \sigma([\ell_j])\right). \tag{15.1}$$

Proof. If $\mathcal{V}^{ab}$ is edge-orientable, then so is $\mathring{\mathcal{V}}^{ab}$. In this case there is a homomorphism $\mathring{\sigma} : \mathring{H} \to \{-1, 1\}$ satisfying $\mathring{\sigma} = \sigma \circ i_*$. By Proposition 9.3.1 we have

$$\Theta_{\mathring{\mathcal{V}}}(g_1, \dots, g_r) = \Delta_{\mathring{M}}(\mathring{\sigma}(g_1) \cdot g_1, \dots, \mathring{\sigma}(g_r) \cdot g_r).$$

Since $\mathring{\sigma} = \sigma \circ i_*$ we have

$$i_*(\Theta_{\mathring{\mathcal{V}}})(h_1, \dots, h_s) = i_*(\Delta_{\mathring{M}})(\sigma(h_1) \cdot h_1, \dots, \sigma(h_s) \cdot h_s).$$

On the other hand, by Lemma 10.2.1

$$i_*(\Delta_{\mathring{M}})(\sigma(h_1)\cdot h_1, \dots, \sigma(h_s)\cdot h_s) = \Delta_M(\sigma(h_1)\cdot h_1, \dots, \sigma(h_s)\cdot h_s) \cdot \prod_{j=1}^{k} \left([\ell_j] - \sigma([\ell_j])\right).$$

Using Proposition 9.3.1 again we obtain $\Delta_M(\sigma(h_1)\cdot h_1, \dots, \sigma(h_s)\cdot h_s) = \Theta_{\mathcal{V}}(h_1, \dots, h_s)$. Substituting it into the formula for $i_*(\Delta_{\mathring{M}})(\sigma(h_1) \cdot h_1, \dots, \sigma(h_s) \cdot h_s)$ above gives the desired equality. □

Therefore if it is possible to find a layered surgery parent by drilling out only orbits which are nontrivial in H, the close relation between $\Theta_{\mathcal{V}}$ and Δ_M is inherited from the relation between $\Theta_{\mathring{\mathcal{V}}}$ and $\Delta_{\mathring{M}}$ discussed in Section 12.6.

Note that the assumption $b_1(M) > 1$ can be dropped. We assumed this only for simplicity, as without it the formula relating $i_*(\Delta_{\mathring{M}})$ with Δ_M might be slightly different; see Lemma 10.2.1.

The above proposition is an instance of deriving properties of the taut polynomial from analogous properties of the Alexander polynomial in the case when $\mathcal{V}^{ab}$ is edge-orientable. It is natural to ask whether the formula (15.1) holds regardless of the assumption on edge-orientability of $\mathcal{V}^{ab}$. In the next section we discuss a potential approach to answer this question.

15.2 The torsion of the veering chain complex

Let M be a 3-manifold with zero Euler characteristic. We can associate to M a chain complex

$$0 \to C_3(M^{ab};\mathbb{Z}) \to C_2(M^{ab};\mathbb{Z}) \to C_1(M^{ab};\mathbb{Z}) \to C_0(M^{ab};\mathbb{Z}) \to 0.$$

Let $\mathcal{Q}[H]$ denote the field of fractions of the group ring $\mathbb{Z}[H]$. Since every chain group above admits a $\mathbb{Z}[H]$-module structure, after tensoring them with $\mathcal{Q}[H]$ we obtain a chain complex over $\mathcal{Q}[H]$. Let us denote it by $\mathcal{C}(M)$. If $\mathcal{C}(M)$ is acyclic, we may compute its *torsion* $\mathscr{T}_M$ as defined in [58, Definition 1.2]. Similarly to all polynomial invariants discussed in this thesis, it is well-defined only up to multiplying by $\pm h$, $h \in H$. By convention, if $\mathcal{C}(M)$ is not acyclic we set $\mathscr{T}_M = 0$.

The connection between $\mathscr{T}_M$ and the Alexander polynomial Δ_M was studied by Turaev in [59]. He proved that these invariants differ at most by factors $(u-1)$, $(u-1)^2$ or (u^2-1) [59, Theorem A].

Now suppose that M admits a veering triangulation $\mathcal{V} = ((T,F,E),\alpha,\nu)$. Let t be a tetrahedron of $\mathcal{V}$. Let f_1, f_2 be the bottom faces of the tetrahedron $1\cdot t$ of $\mathcal{V}^{ab}$. A top face of $1\cdot t$ is adjacent (in $1\cdot t$) along its upper large edge either to f_1 or to f_2. In the first case we denote it by f_1', in the latter — by f_2'. By Lemma 5.2.1 the presentation (5.1) for the taut module of $\mathcal{V}$ can be extended to the *veering chain complex*

$$0 \longrightarrow \mathbb{Z}[H]^T \xrightarrow{C^\uparrow} \mathbb{Z}[H]^F \xrightarrow{D^\uparrow} \mathbb{Z}[H]^E \longrightarrow 0, \tag{15.2}$$

where

$$C^\uparrow(1\cdot t) = f_1 + f_1' - f_2 - f_2'.$$

Remark. We call (15.2) the "veering chain complex" and not the "taut chain complex", because this construction works only if the triangulation is veering; see Remark 5.2.2.

By tensoring (15.2) with $\mathcal{Q}[H]$ we obtain a chain complex $\mathcal{C}(\mathcal{V})$ over a field. We call the torsion $\mathscr{T}_\mathcal{V}$ of $\mathcal{C}(\mathcal{V})$ the *(veering) torsion* of $\mathcal{V}$. It is easy to see that $\mathcal{C}(\mathcal{V})$ is acyclic if and only if $\Theta_\mathcal{V} \neq 0$. Therefore if $\Theta_\mathcal{V} = 0$ we set $\mathscr{T}_\mathcal{V} = 0$. Otherwise we can compute $\mathscr{T}_\mathcal{V}$ using the following scheme. Pick any maximal minor $d_1 \neq 0$ of $D^\uparrow$. Suppose that this minor is determined by faces $\{f_1, \dots, f_n\}$ of $\mathcal{V}$. Let d_2 denote the minor of $C^\uparrow$ determined by $F - \{f_1, \dots, f_n\}$. Then

$$\mathscr{T}_\mathcal{V} = \frac{d_1}{d_2} \in \mathcal{Q}[H].$$

Remark 15.2.1. Computation of the veering torsion can be simplified by reducing the chain complex (15.2) modulo a spanning tree Υ of the dual graph of $\mathcal{V}$ to obtain

$$0 \longrightarrow \mathbb{Z}[H] \xrightarrow{C^\uparrow_\Upsilon} \mathbb{Z}[H]^{F_\Upsilon} \xrightarrow{D^\uparrow_\Upsilon} \mathbb{Z}[H]^E \longrightarrow 0.$$

The homomorhism $D^\uparrow_\Upsilon$ is defined on page 47. The entry of $C^\uparrow_\Upsilon$ corresponding to a non-tree edge f is equal to $[\zeta(f)] - \omega(\zeta(f))$, where $[\zeta(f)]$ is the class in H of the non-tree cycle associated to f (Definition 4.2.3) and $\omega(\zeta(f))$ records whether it is twisted or untwisted.

When M admits a veering triangulation (hence is orientable and $\partial M \neq \emptyset$), the relation between $\mathscr{T}_M$ and Δ_M depends only on $b_1(M)$ [59, Theorem A]. Namely

$$\mathscr{T}_M = \begin{cases} \frac{\Delta_M}{u-1} & \text{if } b_1(M) = 1 \\ \Delta_M & \text{if } b_1(M) > 1. \end{cases}$$

The relation between $\mathscr{T}_\mathcal{V}$ and $\Theta_\mathcal{V}$ must depend on $b_1(M)$, edge-orientability of $\mathcal{V}$ and edge-orientability of $\mathcal{V}^{ab}$. We expect that

$$\mathscr{T}_\mathcal{V} = \begin{cases} \frac{\Theta_\mathcal{V}}{u-1} & \text{if } b_1(M) = 1 \text{ and } \mathcal{V} \text{ is e.o.} \\ \frac{\Theta_\mathcal{V}}{u+1} & \text{if } b_1(M) = 1, \mathcal{V} \text{ is not e.o and } \mathcal{V}^{ab} \text{ is e.o.} \\ \Theta_\mathcal{V} & \text{if } b_1(M) > 1 \text{ or } \mathcal{V}^{ab} \text{ is not e.o.} \end{cases} \tag{15.3}$$

Turaev found the formulas relating the Alexander polynomial of a 3-manifold with toroidal boundary components to the Alexander polynomial of its Dehn filling [59, Corollary 4.2] using the connection of Δ_M with $\mathscr{T}_M$ and multiplicativity of the torsion [58, Theorem 1.5]. We hope that this approach will work in the case of the taut polynomial to prove (15.1) for triangulations whose maximal free abelian cover is not edge-orientable.

More generally, finding the formula relating the taut polynomial $\Theta_{\mathcal{V}}$ and the veering torsion $\mathscr{T}_{\mathcal{V}}$ could allow us to use some of the algebraic machinery from [59] to study the properties of the taut polynomial. Furthermore, (15.3) suggests an algorithm to compute the taut polynomial of $\mathcal{V}$ which would not require calculating multiple minors and their greatest common divisor. By Remark 15.2.1, if $\Theta_{\mathcal{V}} \neq 0$ it would be enough to compute one nonzero minor of $D^{\uparrow}_{\Upsilon}$, and divide it by a polynomial of the form $[\zeta(f)] - \omega(\zeta(f))$. Recall that $[\zeta(f)]$ is already computed by the algorithm `FacePairings`; see Remark 4.2.2.

Finally, observe that $(\mathscr{T}_{\mathcal{V}} \bmod 2) = (\mathscr{T}_M \bmod 2)$. Hence if (15.3) holds, then $(\Theta_{\mathcal{V}} \bmod 2)$ and $(\Delta_M \bmod 2)$ are either equal, or they differ by $(u+1)$; the latter occuring only when $b_1(M) = 1$ and $\mathcal{V}^{ab}$ is not edge-orientable. This would be a strengthening of the observation that we made in Subsection 9.3.1.

Bibliography

[1] S. Adams-Florou. Oriented cover. *The Manifold Atlas Project*, 2014. `http://www.map.mpim-bonn.mpg.de/Oriented_cover#Hatcher2002l`.

[2] I. Agol. Ideal triangulations of pseudo-Anosov mapping tori. In W. Li, L. Bartolini, J. Johnson, F. Luo, R. Myers, and J. H. Rubinstein, editors, *Topology and Geometry in Dimension Three: Triangulations, Invariants, and Geometric Structures*, volume 560 of *Contemporary Mathematics*, pages 1–19. American Mathematical Society, 2011.

[3] H. Baik, C. Wu, K. Kim, and T. Jo. An algorithm to compute the Teichmüller polynomial from matrices. *Geometriae Dedicata*, 204:175–189, 2020.

[4] G. Band and P. Boyland. The Burau estimate for the entropy of a braid. *Algebr. Geom. Topol.*, 7:1345–1378, 2007.

[5] M. Bell. `flipper` (computer software). `pypi.python.org/pypi/flipper`, 2013–2020.

[6] R. Billet and L. Lechti. Teichmüller polynomials of fibered alternating links. *Osaka J. Math.*, 56(4):787–806, 2019.

[7] M. Brunella. Surfaces of section for expansive flows on three-manifolds. *J. Math. Soc. Japan*, 47(3):491–501, 1995.

[8] B. A. Burton. The Pachner graph and the simplification of 3-sphere triangulations. In *Proceedings of the Twenty-Seventh Annual Symposium on Computational Geometry*, pages 153–162. Association for Computing Machinery, 2011.

[9] D. Calegari. *Foliations and the geometry of 3-manifolds*. Oxford mathematical monographs. Clarendon Press, Oxford, 2007.

[10] C. Camacho and A. L. Neto. *Geometric Theory of Foliations*. Springer Science+ Business Media, 1985.

[11] J. W. Cannon and W. P. Thurston. Group invariant Peano curves. *Geometry & Topology*, 11:1315–1355, 2007.

[12] R. Crowell and R. Fox. *Introduction to Knot Theory*, volume 57 of *Graduate Texts in Mathematics*. Springer-Verlag New York, 1963.

[13] M. Culler, N. Dunfield, and J. R. Weeks. SnapPy. A computer program for studying the geometry and topology of 3-manifolds. `http://snappy.computop.org/`.

[14] N. R. Dunfield. Alexander and Thurston norms of fibered 3-manifolds. *Pacific Journal of Mathematics*, 200(1):43–58, 2001.

[15] B. Farb and D. Margalit. *A Primer on Mapping Class Groups*, volume 49 of *Princeton Mathematical Series*. Princeton Univ. Press, 2011.

[16] S. R. Fenley. Foliations with good geometry. *Journal of the American Mathematical Society*, 12:619–676, 1999.

[17] S. R. Fenley. Foliations, topology and geometry of 3-manifolds: $\mathbb{R}$-covered foliations and transverse pseudo-Anosov flows. *Comment. Math. Helv.*, 77:415–490, 2002.

[18] S. R. Fenley. Ideal boundaries of pseudo-Anosov flows and uniform convergence groups with connections and applications to large scale geometry. *Geometry & Topology*, 16:1–110, 2012.

[19] S. R. Fenley. Quasigeodesic pseudo-Anosov flows in hyperbolic 3-manifolds and connections with large scale geometry. *Advances in Mathematics*, 303:192–278, 2016.

[20] S. R. Fenley and L. Mosher. Quasigeodesic flows in hyperbolic 3-manifolds. *Topology*, 40(3):503–537, 2001.

[21] W. Floyd and U. Oertel. Incompressible surfaces via branched surfaces. *Topology*, 23(1):117–125, 1984.

[22] D. Fried. Fibrations over S^1 with Pseudo-Anosov Monodromy. In A. Fathi, F. Laudenbach, and V. Poénaru, editors, *Thurston's work on surfaces*, chapter 14, pages 215–230. Princeton University Press, 2012.

[23] D. Futer and F. Guéritaud. Explicit angle structures for veering triangulations. *Algebr. Geom. Topol.*, 13(1):205–235, 2013.

[24] D. Futer, S. Taylor, and W. Worden. Random veering triangulations are not geometric. `arXiv:1808.05586 [math.GT]`.

[25] D. Gabai and U. Oertel. Essential laminations in 3-manifolds. *Annals of Mathematics*, 130(1):41–73, 1989.

[26] A. Giannopolous, S. Schleimer, and H. Segerman. A census of veering structures. `https://math.okstate.edu/people/segerman/veering.html`.

[27] F. Guéritaud. Veering triangulations and Cannon-Thurston maps. *Journal of Topology*, 9(3):957–983, 2016.

[28] U. Hamenstädt. Geometry of the mapping class groups I: Boundary amenability. *Inventiones mathematicae*, 175:545–609, 2009.

[29] A. Hatcher. *Algebraic topology*. Published for noncommercial use on the author's webpage, 2001. `https://pi.math.cornell.edu/~hatcher/AT/AT.pdf`.

[30] C. D. Hodgson, A. Issa, and H. Segerman. Non-geometric veering triangulations. *Experimental Mathematics*, 25(1):17–45, 2016.

[31] C. D. Hodgson, J. H. Rubinstein, H. Segerman, and S. Tillmann. Veering triangulations admit strict angle structures. *Geometry & Topology*, 15(4):2073–2089, 2011.

[32] M. Lackenby. Taut ideal triangulations of 3-manifolds. *Geometry & Topology*, 4(1):369–395, 2000.

[33] M. Lackenby. Word hyperbolic Dehn surgery. *Inventiones mathematicae*, 140:243–282, 2000.

[34] M. Landry. Stable loops and almost transverse surfaces. `arXiv:1903.08709 [math.GT]`.

[35] M. Landry. Veering triangulations and the Thurston norm: homology to isotopy. `arXiv:2006.16328 [math.GT]`.

[36] M. Landry. Taut branched surfaces from veering triangulations. *Algebraic & Geometric Topology*, 18(2):1089–1114, 2018.

[37] M. Landry, Y. N. Minsky, and S. J. Taylor. Flows, growth rates, and the veering polynomial. In preparation.

[38] M. Landry, Y. N. Minsky, and S. J. Taylor. A polynomial invariant for veering triangulations. `arXiv:2008.04836 [math.GT]`.

[39] E. Lanneau and F. Valdez. Computing the Teichmüller polynomial. *Journal of the European Mathematical Society*, 19(12):3867–3910, 2017.

[40] W. B. R. Lickorish. *An Introduction to Knot Theory.* Graduate Texts in Mathematics. Springer-Verlag New York, 1997.

[41] C. T. McMullen. Polynomial invariants for fibered 3-manifolds and Teichmüller geodesics for foliations. *Ann. Scient. Éc. Norm. Sup.*, 33(4):519–560, 2000.

[42] C. T. McMullen. The Alexander polynomial of a 3-manifold and the Thurston norm on cohomology. *Annales scientifiques de l'École Normale Supérieure*, Ser. 4, 35(2):153–171, 2002.

[43] J. W. Milnor. A duality theorem for Reidemeister torsion. *Annals of Mathematics*, 76(1):137–147, 1962.

[44] J. W. Milnor. Infinite cyclic coverings. In *Conference on the Topology of Manifolds (Michigan State Univ.)*, pages 115–133, 1968.

[45] Y. N. Minsky and S. J. Taylor. Fibered faces, veering triangulations, and the arc complex. *Geom. Funct. Anal.*, 27(6):1450–1496, 2017.

[46] D. Northcott. *Finite Free Resolutions.* Cambridge Tracts in Mathematics. Cambridge University Press, 1976.

[47] U. Oertel. Measured Laminations in 3-Manifolds. *Transactions of the American Mathematical Society*, 305(2):531–573, 1988.

[48] A. Parlak, S. Schleimer, and H. Segerman. GitHub Veering repository. Regina-Python and sage code for working with transverse taut and veering ideal triangulations. `https://github.com/henryseg/Veering`.

[49] R. Penner and J. Harer. *Combinatorics of train tracks.* Number 125 in Annals of Mathematics Studies. Princeton University Press, 1992.

[50] J. S. Purcelli. *Hyperbolic Knot Theory.* Graduate Studies in Mathematics. American Mathematical Society, 2020.

[51] S. Schleimer and H. Segerman. From veering triangulations to link spaces and back again. arXiv:1911.00006 [math.GT].

[52] S. Schleimer and H. Segerman. From veering triangulations to pseudo-Anosov flows. In preparation.

[53] The Sage Developers. *SageMath, the Sage Mathematics Software System (Version 9.1)*, 2020. `https://www.sagemath.org`.

[54] W. P. Thurston. The geometry and topology of three–manifolds. Notes from Princeton University, 1980.

[55] W. P. Thurston. A norm for the homology of 3-manifolds. *Memoirs of the American Mathematical Society*, 59(339):100–130, 1986.

[56] W. P. Thurston. Hyperbolic structures on 3-manifolds, II: Surface groups and 3-manifolds which fiber over the circle. arXiv:math/9801045 [math.GT], 1998.

[57] L. Traldi. The determinantal ideals of link modules. *Pacific J. Math*, 101(1):215–222, 1982.

[58] V. Turaev. *Introduction to Combinatorial Torsions*. Lectures in Mathematics ETH Zürich. Birkhauser Basel, 2001.

[59] V. G. Turaev. The Alexander polynomial of a three-dimensional manifold. *Math. USSR Sbornik*, 26(3):313–329, 1975.

[60] W. Worden. Experimental statistics of veering triangulations. *Experimental Mathematics*, 29(1):101–122, 2020.